Fall 2009

Glycan targeted gene delivery to the dendritic cell SIGN receptor

B Kevin Anderson
University of Iowa

GLYCAN TARGETED GENE DELIVERY TO THE DENDRITIC CELL SIGN RECEPTOR

by

B. Kevin Anderson

An Abstract

Of a thesis submitted in partial fulfillment
of the requirements for the Doctor of
Philosophy degree in Pharmacy (Medicinal and Natural Products Chemistry)
in the Graduate College of
The University of Iowa

December 2009

Thesis Supervisor: Professor Kevin G. Rice

ABSTRACT

The 21st century has been called the age of genomic medicine, yet gene therapy for medicinal use remains a theory. One reason that there are no safe and effective treatments for human disease is the lack of a vehicle capable of delivering genetic material to a specific target. In nature we observe gene pathology by viral vectors, which deliver their own genetic material to specific host cells efficient at spreading the viral blueprint throughout the organism.

The aim of my research into gene therapy has been to develop a synthetic vector with the delivery capability of viral vectors found in nature. This includes the ability to protect genetic cargo from modification and degradation *in vivo*, target to a desired cell type within a specific tissue, facilitating absorption into the cell, and delivery to the nucleus, where expression of genetic material occurs.

The goal of this thesis project was to synthesize a novel vector which would selectively target the dendritic cell SIGN receptor, mirroring the method of pathogens such as HIV, which target this receptor and subsequently the immune system, resulting in chronic infection.

The vector we designed contains two major components, the high mannose N-glycan $Man_9GlcNAc_2Asn$, and a peptide composed of nine amino acids: four lysine spacing residues, four lysines derivatized with acridine on the epsilon amine of their side chains, and a cysteine for conjugation to the glycan. This compound, the Man_9-AcrLys Glycopeptide, was engineered to intercalate into plasmid DNA via the acridine functional groups and to bind the DC-SIGN receptor through the glycan's mannose residues.

The vehicle was tested *in vitro* in CHO cells bearing a recombinant DC-SIGN receptor in the context of luciferase reporter gene delivery. We found that under equal treatment conditions, DC-SIGN (+) CHO cells expressed more luciferase and were 100-fold more luminescent than control DC-SIGN (-) CHO cells.

My delivery method was further analyzed in a cell-sorting FACS experiment. I covalently labeled pGL3 reporter plasmid with a fluorophore, and transfected the CHO cells under typical transfection conditions. The experimental results confirmed preferential DC-SIGN mediated gene delivery.

Abstract Approved:_____

Kevin G. Rice, Thesis Supervisor

_____

Title and Department

_____

Date

GLYCAN TARGETED GENE DELIVERY TO THE DENDRITIC CELL SIGN RECEPTOR

by

B. Kevin Anderson

A thesis submitted in partial fulfillment
of the requirements for the Doctor of
Philosophy degree in Pharmacy (Medicinal and Natural Products Chemistry)
in the Graduate College of
The University of Iowa

December 2009

Thesis Supervisor: Professor Kevin G. Rice

Graduate College
The University of Iowa
Iowa City, Iowa

CERTIFICATE OF APPROVAL

_____

PH.D. THESIS

_____

This is to certify that the Ph.D. thesis of

B. Kevin Anderson

has been approved by the Examining Committee
for the thesis requirement for the Doctor of Philosophy
degree in Pharmacy (Medicinal and Natural Products Chemistry) at the
December 2009 graduation.

Thesis Committee: _____
Kevin G. Rice, Thesis Supervisor

_____
Jonathan A. Doorn

_____
Michael W. Duffel

_____
Ernesto J. Fuentes

_____
Robert J. Kerns

ACKNOWLEDGMENTS

Thank you, Dr. Rice, for your exceptional leadership and guidance throughout my graduate career. From the time of my first correspondence with the University of Iowa until the end, you made sure that I and the rest of my colleagues had a graduate experience which met and exceeded expectations.

I would also like to thank the Medicinal and Natural Products Chemistry faculty who served on my committee, Dr. Jonathan Doorn, Dr. Michael Duffel, and Dr. Robert Kerns. Without your educational and challenging courses, and your experimental knowledge and experience, I would not have learned fundamental principles of Medicinal Chemistry nor made the advances which I realized on my thesis project. I would like to individually thank my extra-departmental committee member, Dr. Ernesto Fuentes. Your experience was very valuable and your advice was timely and came at a critical period when my research project was well into maturity.

Finally I would like to thank my colleagues and my family members who supported my educational endeavor. My parents, Milton and Vinette Anderson, who instilled in me the value of education and the importance of doing my best, and my siblings, Michelle and Richard Anderson, who provided role models for their younger brother. Richard, without having you obtain your PhD 7 years before me, it would have been much more difficult for me. Thank you.

ABSTRACT

The 21st century has been called the age of genomic medicine, yet gene therapy for medicinal use remains a theory. One reason that there are no safe and effective treatments for human disease is the lack of a vehicle capable of delivering genetic material to a specific target. In nature we observe gene pathology by viral vectors, which deliver their own genetic material to specific host cells efficient at spreading the viral blueprint throughout the organism.

The aim of my research into gene therapy has been to develop a synthetic vector with the delivery capability of viral vectors found in nature. This includes the ability to protect genetic cargo from modification and degradation *in vivo*, target to a desired cell type within a specific tissue, facilitating absorption into the cell, and delivery to the nucleus, where expression of genetic material occurs.

The goal of this thesis project was to synthesize a novel vector which would selectively target the dendritic cell SIGN receptor, mirroring the method of pathogens such as HIV, which target this receptor and subsequently the immune system, resulting in chronic infection.

The vector we designed contains two major components, the high mannose N-glycan $Man_9GlcNAc_2Asn$, and a peptide composed of nine amino acids: four lysine spacing residues, four lysines derivatized with acridine on the epsilon amine of their side chains, and a cysteine for conjugation to the glycan. This compound, the Man_9-AcrLys Glycopeptide, was engineered to intercalate into plasmid DNA via the acridine functional groups and to bind the DC-SIGN receptor through the glycan's mannose residues.

The vehicle was tested *in vitro* in CHO cells bearing a recombinant DC-SIGN receptor in the context of luciferase reporter gene delivery. We found that under equal treatment conditions, DC-SIGN (+) CHO cells expressed more luciferase and were 100-fold more luminescent than control DC-SIGN (-) CHO cells.

My delivery method was further analyzed in a cell-sorting FACS experiment. I covalently labeled pGL3 reporter plasmid with a fluorophore, and transfected the CHO cells under typical transfection conditions. The experimental results confirmed preferential DC-SIGN mediated gene delivery.

TABLE OF CONTENTS

LIST OF TABLES

Table

LIST OF FIGURES

Figure

LIST OF SCHEMES

Scheme

LIST OF EQUATIONS

Equation

LIST OF ABBREVIATIONS

ACN . .....acetonitrile

ASGP-R….. .....asialoglycoprotein receptor

CD…. .....cluster of differentiation

CDI…..... 1,1'carbonyldiimidazole

CHO…. .....chinese hamster ovary

COS .....CVI (simian) in Origin with SV40 genetic material

CRD. ..... carbohydrate recognition domain

DC…. .....dendritic cell

DCC . .....dicyclohyexyl carbodiimide

DHB……. .....dihydroxy benzoic acid

DMEM…. ..... dulbecco's modified eagle medium

DMF .....dimethyl formamide

DMSO. ..... dimethyl sulfoxide

DNA. ..... deoxyribonucleic acid

DOTMA ..... 1,2-di-O-octadecenyl-3-trimethylammonium propane

EDTA. .....ethylenediaminetetraacetic acid

EGTA. .....ethylene glycol tetraacetic acid

ESI…..... electrospray ionization

FACS…..... fluorescence activated cell sorting

GP…….. ..... glycoprotein

HBM . .....hepes buffered mannitol

HIV…. .....human immunodeficiency virus

HPLC….. .....high performance liquid chromatography

ICAM. ..... intracellular adhesion molecule

IL…..... interleukin

KLH…. ..... keyhole limpet hemocyanin

LAM .....lipoarabinomannan

LFA ..... lymphocyte function associated integrin

LPG….. ..... lipophosphoglycan

LPS…..... lipopolysaccharide

MALDI-TOF….....matrix assisted laser desorption ionization-time of flight

MES. .....2-(N-morpholino)ethanesulfonic acid

MS…..…..mass spectrometry

NHS….....N-hydroxy succinimide

NMR….. ..... nuclear magnetic resonance

N:P….. .....nitrogen:phosphorous

PAGE…….. .....polyacrylamide gel electrophoresis

PBS….. ..... phosphate buffered saline

PEI…….....poly(ethylenimine)

PSA….. .....phenol sulfuric assay

RT….. .....room temperature

SBA ..... soybean agglutinin

SIGN….. .....specific intracellular adhesion molecule-3 grabbing non-integrin

SEA ..... soluble egg antigen

SDS . ..... sodium dodecyl-sulfate

SEAP…..... secreted human embryonic alkaline phosphatase

TFA….. ..... trifluoroacetic acid

UV/VIS….. ..... ultraviolet visible

CHAPTER 1

LITERATURE REVIEW

Introduction

DNA vaccination is an experimental therapeutic method where a subject is dosed with DNA which is expressed in the host as foreign, antigenic protein. This protein should elicit humoral and cell-mediated immunity against the antigen.[1] DNA vaccines could potentially be as effective as live attenuated vaccines, with a much higher degree of safety.

Dendritic cells are the primary antigen presenting cells in the immune system, and are therefore an ideal target for gene delivery.[2] The challenge lies in designing a vector to selectively target DCs. My hypothesis was that I could selectively target the dendritic cell SIGN receptor and stimulate gene expression to a significant level above control. This is demonstrated by the application of the Man_9-AcrLys Bioconjugate. This non-viral gene delivery vector is composed of two principal components: a peptide containing cysteine, lysine and lysine derivatized with an ε-amino acridine, and the high mannose N-glycan $Man_9GlcNAc_2Asn$.

Acridine has a 140 year history of scientific usage, as an antiviral, antimicrobial, anti-inflammatory and antiprion agent, among other medicinal purposes.[3] It contains a vivid chromophore, and is also used in various labeling applications.[4] Although some studies suggest that the therapeutic action of acridinylated compounds is due to direct interaction with biologically active protein,[5] most attribute their activity to DNA binding, cell cycle arrest and the resulting cytotoxicity.[6] The first portion of this review will be devoted to examining the discovery, chemical and physical properties of acridine, and the chemical synthesis of acridine, with an emphasis on 9-chloroacridine, the starting material for the compounds described in the experimental sections of this thesis. The

interaction of select acridine containing compounds with nucleic acids will also be discussed.

Dendritic cells are generally accepted as the most potent antigen presenting cells in the immune system,[2] and as such would be a logical target for a synthetic DNA vector bearing a therapeutic gene. The vector designed in this thesis was targeted to the DC-SIGN receptor on dendritic cells. The structure, function and role of the DC-SIGN receptor in normal and abnormal physiology is also examined in this review. Special emphasis will be placed on oligosaccharide targeting to the DC-SIGN receptor, as the high mannose glycan $Man_9GlcNAc_2$ was incorporated into our vector design.

Isolation and Synthesis of Acridine

Carl Graebe and Heinrich Caro announced their discovery of a new compound in the anthracene fraction of coal tar in 1870.[7] They named the molecule 'Acridin' because of its 'acrid smell and irritating action on the skin and mucous membrane' (Figure 1-1).[8]

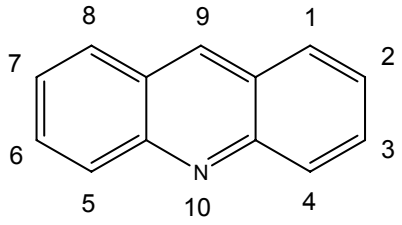

Figure 1-1 *Acridine Structure, Nomenclature and Numbering.* Carl Graebe proposed the given numbering system for acridine in 1893.[9] Ten systems were proposed over the next 50 years. Graebe's numbering system is most widely employed at present.

Acridine was isolated from the anthracene fraction of coal tar by extraction with dilute sulfuric acid and addition of potassium dichromate to precipitate acridine bichromate, which is decomposed with ammonia.

Acridine is a pale yellow solid which melts at 111°C and boils at 346°C. It is weakly basic, with a pKa of 5.60[10,11]. Acridine is poorly soluble in water but dissolves readily in most organic solvents. In an ethanol solution, it absorbs UV light at λ_{ex} 360 nm, and it emits violet-colored light at λ_{em} 417 nm, with lower maxima at 400, 435 and 460 nm.[12]

One of the earliest syntheses of acridine was completed in 1884 by August Bernthsen.[13] The reaction was achieved by heating a mixture of a formic acid with diphenyl amine and 1.5 to 3 moles of zinc chloride to 200-270°C for 24 hr. in the absence of solvent (Scheme 1-1). The yield of the reaction is poor, however substituting acetic or benzoic acid for formic acid increases the yield of the corresponding 9-substituted acridines. The temperature, time of reaction, and quantity of zinc chloride used are important in obtaining optimum yields.

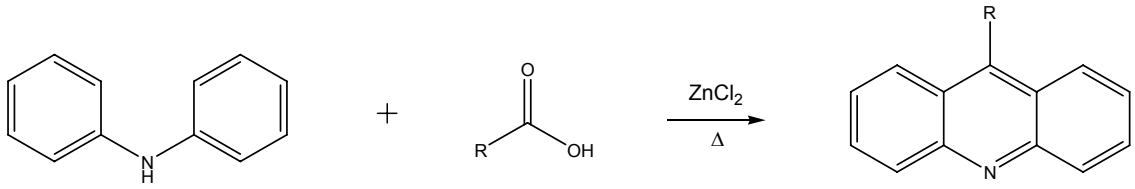

Scheme1-1. *The Bernthsen Reaction.* Unsubstituted acridine is made by this method when formic acid (R = H) is used.

Frank Popp proposed the use of polyphosphoric acid in place of zinc chloride for the cyclization of diphenyl amine.[14] This modification greatly reduced the reaction time and temperature necessary to obtain the desired product. Many acridines and benzacridines have been made through this method by varying the carboxylic acid and diphenylamine used (Table 1-1).[8] Di-substituted acridines are also made by Bernthsen's method (Scheme 1-2), and substitutents can be introduced at the 2, 3 or 4 position (Table 1-2).

Acridines Prepared by Bernthsen's Reaction and Popp's Modification[1]			
Acridine	Yield (%)	Acid or acid component	Ref
Unsubstituted	Very low	Formic acid	13
9-(4-Aminophenyl)-	24	4-Aminobenzoic acid[1]	14
9-Benzyl-	50	Phenylacetic acid	15
9-(4-Bromophenyl)-	?	4-Bromobenzoic acid	16
9-Butyl-	?	Valeric acid	17
9-isobutyl-	15	Isovaleric acid	18
9-tertButyl-	20	Trimethylacetic acid	18
9-(2-Carboxyphenyl)-	40-50	Phthalic anhydride	19
9-(4-Chlorophenyl)-	29	4-Chlorobenzoic acid	20
9-(2,4-Demethylphenyl)-	40	2,4-Dimethylbenzoic acid	21
9-(2,5-Dimethlylphenyl)-	46	2,5-Dimethylbenzoic acid	21
9-Ethyl-	?	Proprionic acid	22
9-(1-Ethylpropyl)	30	2-Ethylbutyric acid	18
9-Heptyl-	20	Octanoic acid	18
9-Heptadecyl-	?	Stearic acid	23
9-(4-Hydroxyphenyl)-	27	4-Hydroxybenzoic acid	24
9-Methyl-	55	Acetic Acid	13
9-(2-Methylphenyl)-	50	2-Methylbenzoic acid	21
9-[3-(*p*-Methylphenyl)-propyl]	30	4-(p-Methylphenyl)-butyric	18
-9-Pelargonic acid	31	Ethyl sebcyl chloride	25
9-Pentadecyl	?	Palmitic acid	22
9-Phenyl	48	Benzoic acid	13
9-(1-Phenylethyl)-	30	2-Phenylproprionic acid	18
-9-Proprionic acid	10	Succinic acid	23
9-Propyl	?	Butyric acid	22
9-isoPropyl-	20	isoButyric acid	18
9-(3-Pyridyl)-	10	Nicotinic acid	26
9-Undecyl-	20	Lauric acid	18
-9-Valeric acid	12	Ethyl adipyl chloride	25

[1]Polyphosphoric acid as the catalyst and solvent.[8]

Table 1-1. *Acridines Prepared by Bernthesen's Reaction and Popp's Modification*. Adapted from Acheson *et al.*, 1973.

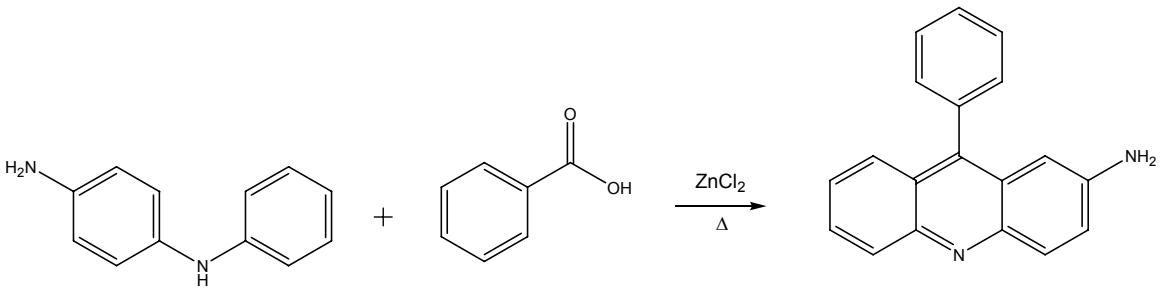

Scheme1-2. *2-Amino-9-phenyl-Acridine Prepared by the Bernthsen Reaction*.[8]

Disubstituted Acridines Prepared by Bernthsen's Reaction and Popp's Modification[1]				
Acridine	Yield (%)	Diphenylamine	Acid or Acid component	Ref
2-Amino-9-phenyl	8-10	4-Amino-	Benzoic acid[1]	27
2-Benzamido-9-phenyl-	?	4-Benzamido-	Benzoic acid	28
9-(2-Carboxyphenyl)-3-phenylamino-	?	3-Phenylamino-	Phthalic anhydride	29
2-Chloro-9-methyl-	71.5	2-Chloro-	Acetic acid	30
2,9-Dimethyl-	?	4-Methyl-	Acetic acid	31
3,9-Dimethyl-	45.5	3-Methyl-	Acetic acid	30
4,9-Dimethyl-	51.2	2-Methyl-	Acetic acid	30
3-Hydroxy-9-(4-hydroxy-phenyl)-	13	3-Hydroxy-	4-Hydroxybenzoic acid	32
2-Hydroxy-9-phenyl	Low	4-Hydroxy-	Benzoic acid	27
3-Hydroxy-9-phenyl	27-34	3-Hydroxy-	Benzoic acid	33
2-Methyl	Low	4-Methyl-	Formic acid	31
2-Methyl-9-phenyl	37	4-Methyl-	Benzoic acid	31
9-Methyl-3-phenyl amino	76	3-Phenylamino-	Acetic acid	29
9-Phenyl-3-phenyl-amino	76	3-Phenylamino	Benzoic acid	29
3-Phenylamino	"Good"	3-Phenylamino-	Formic acid	29

[1]Polyphosphoric acid as the catalyst and solvent. [8]

Table 1-2. *Disubstituted Acridines Prepared by Bernthsen's Reaction and Popp's Modification*. Adapted from Acheson *et al.*, 1973.

Recent methods for the synthesis of acridine include high temperature gas phase, flash vacuum pyrolitic, and acid halide catalyzed reactions (Scheme 1-3,4,5).

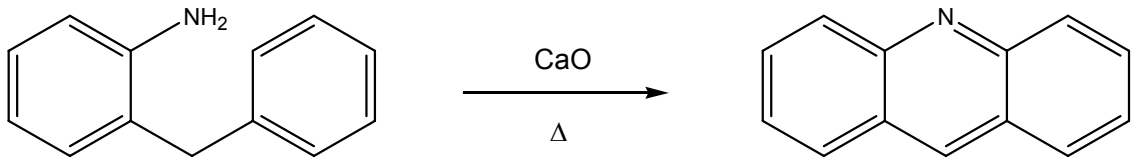

Scheme1-3. *High temperature gas phase conversion of 2-benzylaniline to acridine.*[34]

In 2004, Horaguchi et. al.[34] published a thermal cyclization reaction to produce acridine (Scheme 1-3). 2-Benzylaniline was placed in a quartz column, vaporized with a traveling furnace and introduced by nitrogen carrier gas to calcium oxide. The calcium oxide was heated to 600°C in a 40 minute reaction. The product was then collected in an ice-water cooled vessel, extracted with acetone, and chromatographed on a silica column. The conversion to acridine was quantitive and the yield was 75%.

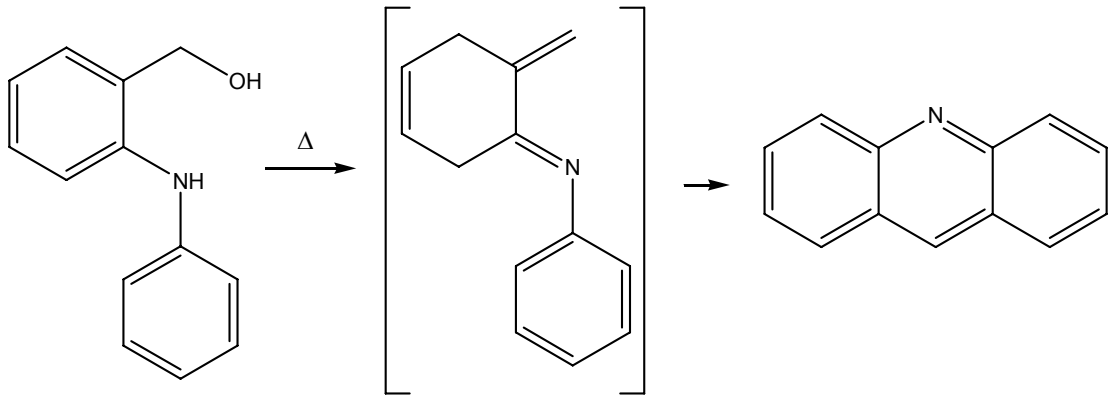

Scheme1-4. *Flash vacuum pyrolytic conversion of (2-Phenylamino-phenyl)-methanol to acridine.* [35]

In 1984 Hodgetts et. al.[35] published a flash vacuum pyrolytic method for the conversion of (2-phenylamino-phenyl)-methanol to acridine (Scheme 1-4). The starting material was passed over molecular sieves (3" boat containing 1/16") pellets at 450°C resulting in quantitative conversion to acridine. Typically, the intermediate azaxylylene intermediate requires a minimum temperature of 650°C for elimination of CO_2 and subsequent cyclization, however the SiO_2, Al_2O_3, and molecular sieve catalysts introduced in these reactions lower the necessary reaction temperature.

One of the more mild contemporary syntheses of acridine was published by Baum et. al.[36] in 1987. In this reaction, a 2.5-fold molar excess of $AlCl_3$ is added to diphenylamine-2-carboxaldehyde (Scheme 1-5). After neutralization with 1 N NaOH and extraction with ether, the product is concentrated and washed with petroleum ether. The reaction yielded 85% acridine.

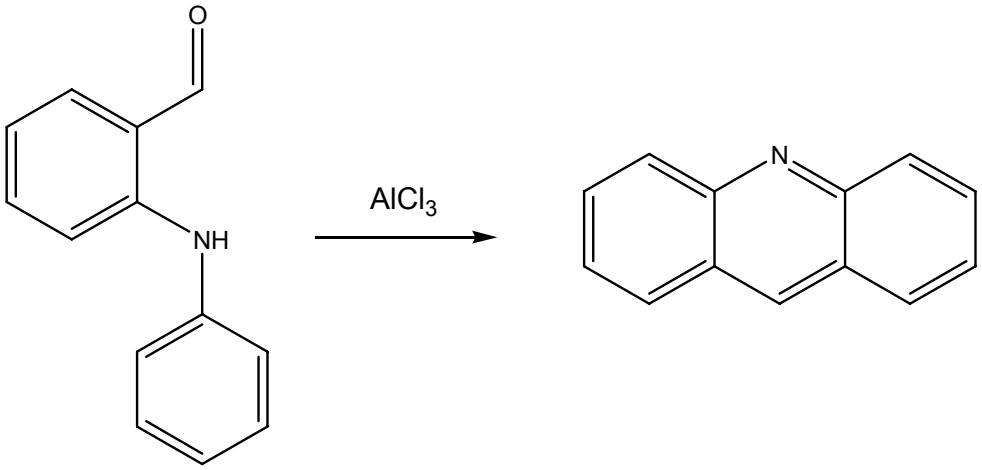

Scheme 1-5. *Aluminum chloride catalyzed formation of acridine.*[36]

Synthesis of 9-Chloroacridine

It is interesting to note that although acridine is the parent compound of many useful and widely differing properties, it is not very useful itself. [8] 9-Chloroacridine, the starting material used in the syntheses in this volume, is a more valuable compound due to the reactivity of the chlorine atom. The compound can be made on a large scale with a nearly quantitative yield from N-phenylanthranilic acid through the addition of an excess of phosphorous oxychloride. The mixture is first heated to 140°C for two hours, then the excess $POCl_3$ is removed by distillation under vacuum (Scheme 1-6). A mixture of chloroform/ammonia is added to the reaction, and the organic layer is extracted, dried with calcium chloride and filtered. The solvent is finally removed by distillation, and the 9-chloracridine is dried by heating.[37]

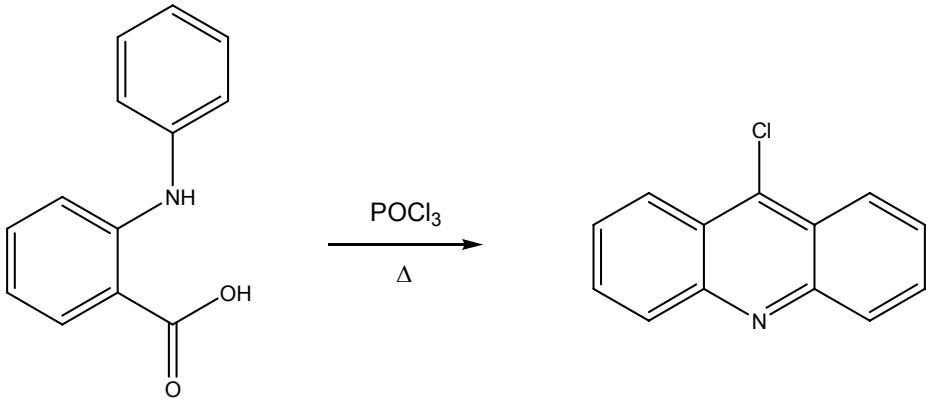

Scheme 1-6. *The synthesis of 9-chloroacridine from N-phenylanthranilic acid*

9-chloroacridine can also be made from 9-acridanone and thionyl chloride; (Scheme 1-7)[38] however, 9-acridanone is typically a more expensive starting material than N-phenylanthranilic acid and is typically made from the acid.[39] Also, thionyl chloride is slightly more toxic than phosphorous oxychloride.

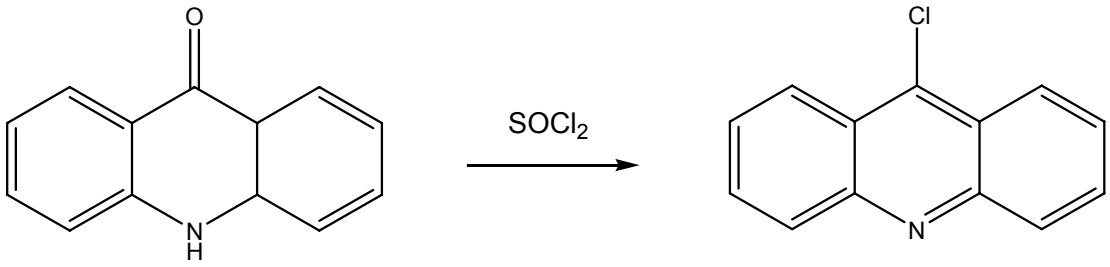

Scheme1-7. *Conversion of 9-acridanone to 9-chloroacridine*

The Interaction of Acridine With Nucleic Acid

The effect of acridine in biological systems is due in large part to its intercalation with nucleic acid. This interaction was first observed by Peacocke and Skerrett, who published a binding curve of proflavine to herring sperm DNA (Figure 1-2).[40]

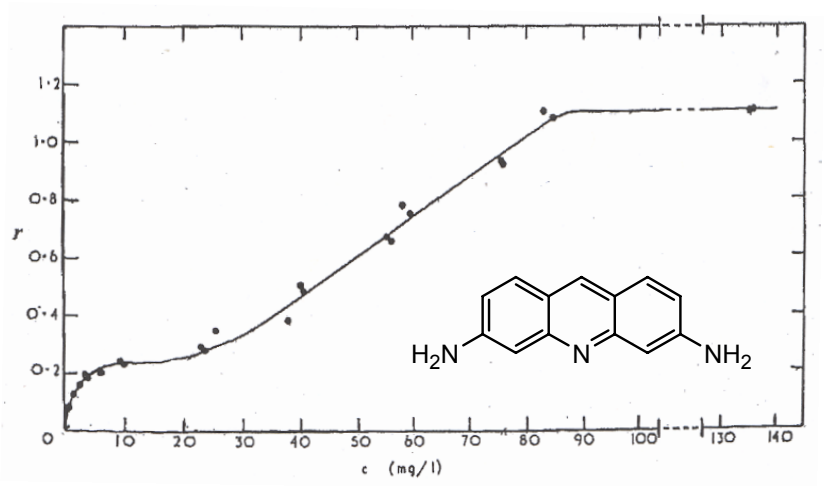

Figure 1-2. *The binding of proflavine to herring sperm DNA.* r = number of ligands bound per molecule; c = free ligand concentration Reproduced with the addition of proflavine from Peacocke *et al.*, 1956.

Analysis of the curve and the derived Scatchard plot revealed binding by two processes, (I), a high affinity process up to approximately 0.2 molecules proflavine per nucleotide,

and (II), a weaker mode up to r ≈ 1.0. Five years later, Leonard Lerman first identified binding by process (I) as intercalation. [41] He utilized x-ray crystallography as well as the dialysis and spectrophotometric methods of Peacocke and Skerret and was thus able to rule out simple aggregation as responsible for the binding phenomena and proposed a novel model for binding (Figure 1-3).

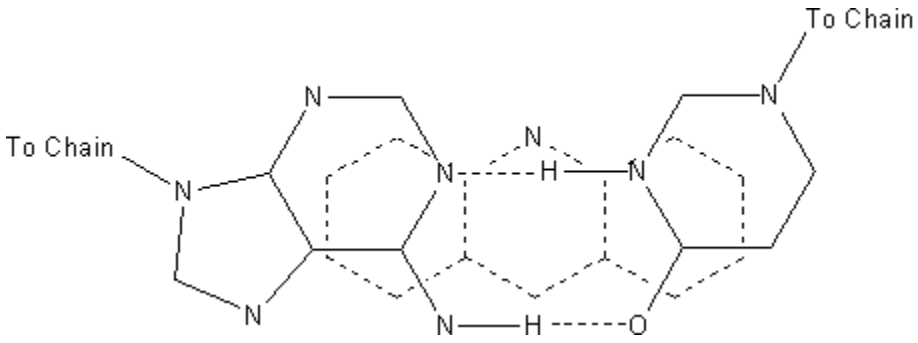

Figure 1-3. *Lerman's model for the interaction of acridine and DNA.*[42] Adapted from Pritchard *et al.*, 1973.

In 1966 N.J. Pritchard et. al. published a modified model which proposed that acridine bound DNA within a single strand, as opposed to across a base pair (Figure 1-4).[42] This was significant because it meant that acridine could bind single stranded and denatured nucleic acid species. He stated that the negatively charged oxygen atom on the phosphate group between two bases can swing to the inside of the chain, where it is adjacent to the positively charged ring nitrogen of the amino acridine. And further, if acridine is oriented as shown, a long side chain at the nine position should not cause steric hindrance to binding, as is seen in the case of acranil and atebrin, which do not bind less strongly to DNA than proflavine.

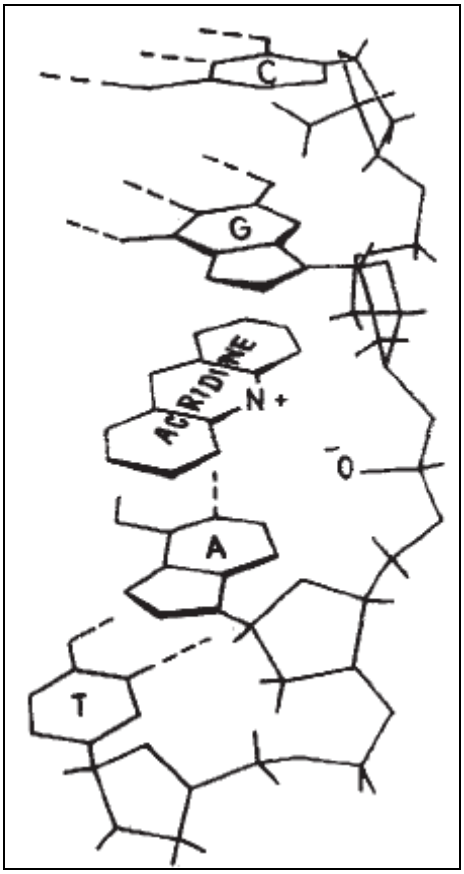

Figure 1-4. *Modified intercalation model for Acridine-DNA interaction.* [42] Reproduced from Pritchard *et al.*, 1973.

Although Lerman's physical intercalation model was slightly incorrect, his characterization of the acridine-DNA complex for proflavine and acridine was very good. He characterized the intercalation interaction as disrupting the normal double helix, casusing the DNA to become longer and/or stiffer, while retaining its 3.4 Å spacing along the helix with the base pairs remaining perpendicular to the axis. These observations formed the basis of the classical intercalation model. [41]

However, we know now that there are additional factors to consider when binding between an acridine compound and a nucleic acid occurs. First, acridine compounds bind differently when stacking between consecutive A-A, A-G, G-G, C-C or G-C bases.

Secondly, acridine compounds can contain multiple functional groups of varying polarity, size and hydrophobicity; this results in differing acridine-nucleic acid complex conformation. New details regarding the intercalation interaction were uncovered by the research of Cohen and Eisenberg in the late 1960's. [43] They analyzed the DNA-proflavine complex using sonicated calf thymus DNA. These short rod-like molecules could be analyzed more accurately than high-molecular weight DNA with tertiary structure. They derived equations which related change in the length of the double helix to change in solution viscosity and ligand-DNA sedimentation rates. Their study was the first quantitative hydrodynamic experiment to test and confirm the structural predictions of the classical intercalation model.[44] However, their experimental methods and techniques laid the foundation for a new, 'nonclassical' intercalation model. Saucier *et al*.[45] adopted the methods of Cohen and Eisenberg and found that daunorubicin and 9-methoxyellipticine gave the predicted increase in viscosity, while Ethidium bromide, quinacrine, and proflavine gave less than the theoretically predicted increase. Gabbay *et al*.[46] worked with a series of methylated phenanthroline analogs, and found that the viscosity of intercalated solutions varied with the number and position of methylated substituents (Figure 1-5). They found that (1) unsubstituted phenanthroline binds in a classical manner; (2) symmetrically substituted compounds bind in a classical manner but cause larger increases in length than unsubstituted compound due to the greater effective thickness of their intercalated methylated ring systems; (3) asymmetrically substituted compounds bind by intercalation but can cause lengthening and bending of the double helix, resulting in a smaller viscosity change than that predicted by the classical model.

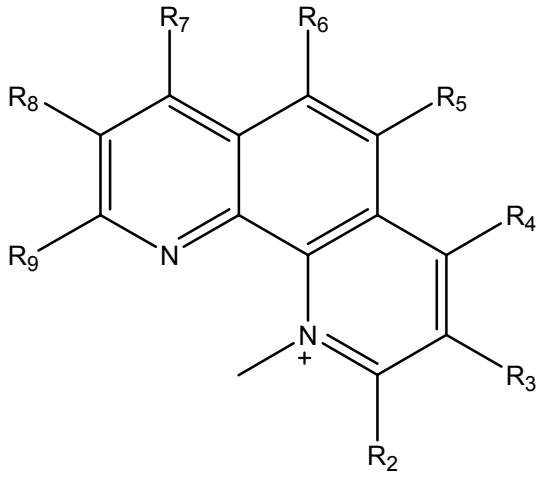

	R_2	R_3	R_4	R_5	R_6	R_7	R_8	R_9
1	H	H	H	H	H	H	H	H
2	CH_3	H	H	H	H	H	H	CH_3
3	H	H	H	CH_3	CH_3	H	H	H
4	CH_3	H	H	CH_3	CH_3	H	H	CH_3
5	H	CH_3	H	H	H	H	CH_3	H
6	H	CH_3	H	CH_3	CH_3	H	CH_3	H
7	H	H	CH_3	H	H	CH_3	H	H
8	H	H	C_6H_5	H	H	C_6H_5	H	H

Figure 1-5. *Phenanthraline analogs.* In 1973, Gabbay et al.[46] published the results of their investigation into the steric effects of methyl and phenyl functional groups on the intercalation of methylated phenanthroline in DNA. Adapted from Gabbay *et al*., 1973.

Sobell *et al*.[47] published an X-ray analysis of intercalating drugs crystallized with complimentary dinucleotide monophosphates, and this lent further support to the bending and stretching phenomena caused by intercalation of acridines with the necessary substituents (Figure 1-6). The new, nonclassical model was illustrated by Wilson *et al*. in 1981.

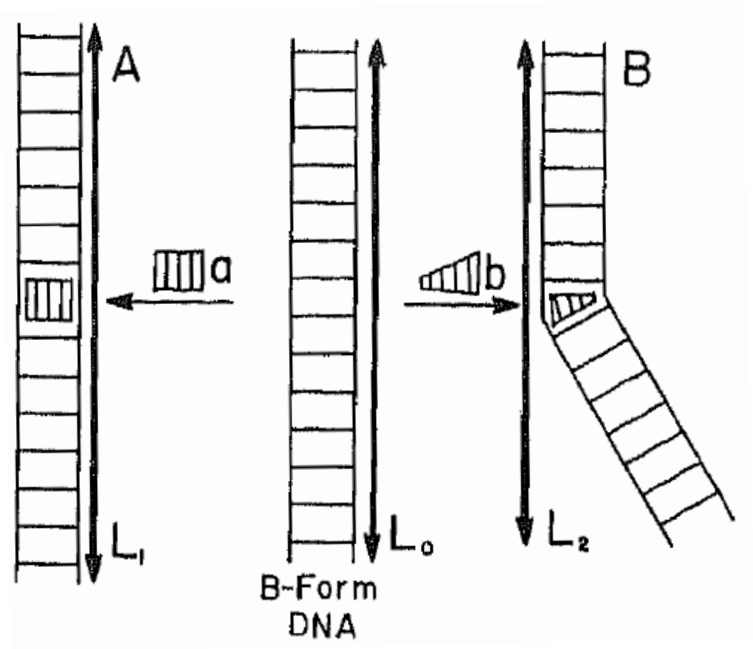

Figure 1-6. *The classical (A) and non-classical (B) intercalation models of DNA-ligand interaction.*[44] L_0 is a section of B-form DNA, L_1 is the same section after binding a simple, unsubstituted intercalator, L_2 represents the DNA after binding a non-classical intercalating molecule, such as a large aromatic ring system with an assymetrical distribution of bulky substituents. Reproduced from Wilson *et al.*, 1981.

Further experimentation has provided more detail to the non-classical model. It is now evident that intercalating molecules have an unwinding effect on superhelical DNA, and in fact, each molecule will cause a specific amount of unwinding, termed the unwinding angle. [41] The discovery of closed, superhelical DNA made this analysis more simple, and the unwinding angles of a variety of intercalators have been quantitatively determined. [44] Today it is well known that as the concentration of an intercalator in solution with a fixed amount of DNA is increased, naturally right-handed superhelical DNA will unwind until it is hydrodynamically equivalent to nicked circular DNA, and then wind into a left handed superhelical structure. The viscosity of the solution will also rise and decrease with the concentration of intercalator (Figure 1-7). [48,49]

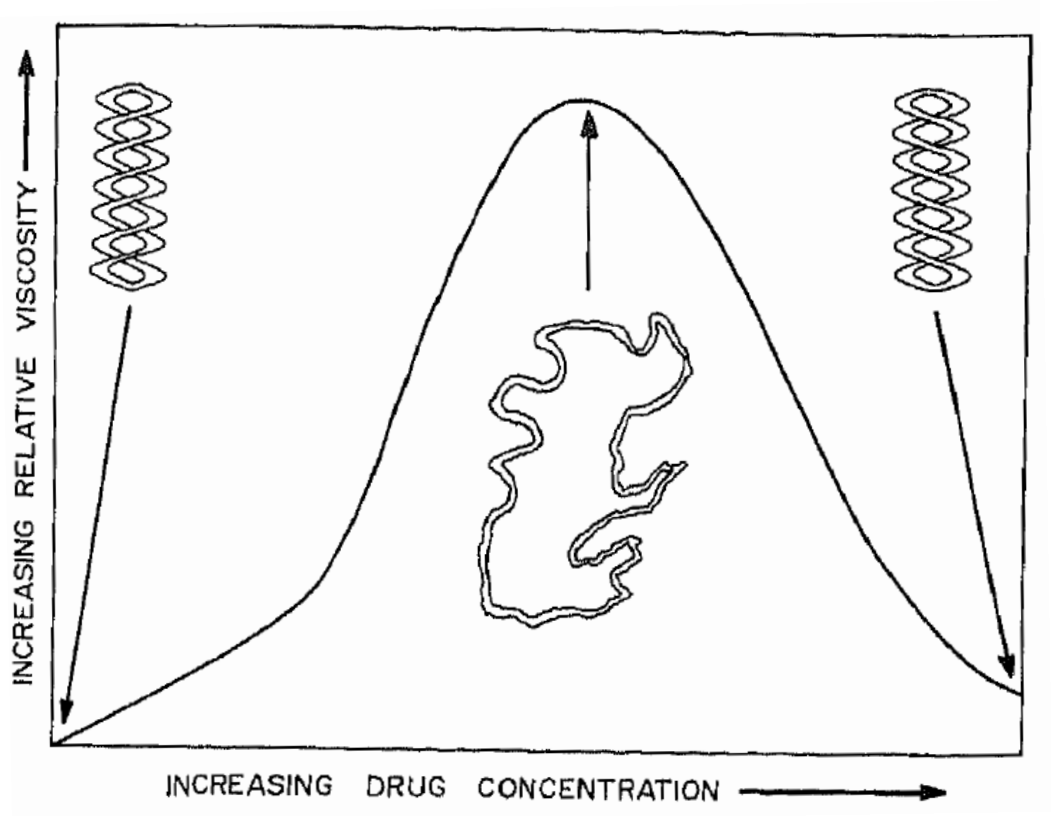

Figure 1-7. *The effects of intercalating drug on solution viscosity of closed superhelical DNA.*[44] As increasing intercalator is added, DNA loses its coiled structure, then regains superhelical coils in the opposite (left-handed) direction. Maximum solution viscosity is reached in the open structure, with minima at minimum and maximum drug concentration. Reproduced from Wilson *et al.*, 1981.

The Binding Affinity of Acridines for DNA

There are a number of factors which must be considered when measuring the affinity of acridine compounds for DNA. Perhaps the most significant of these are the ionic strength of the experimental solution and the structure of the acridine molecule bound. B-form DNA is inherently unstable due to its high charge density. This instability is overcome by "condensation" with mobile counterions in solution.[44,50-52] An intercalating compound will replace some of these counterions when it binds to DNA.

This aspect of the ion-condensation theory relates the observed equilibrium constant for intercalation K_{obs}, to counterion concentration $[M^+]$ (Equation 1-1):

$$\frac{\partial \log K_{obs}}{\partial \log [M^+]} = - m' \Psi$$

Equation 1-1. *Ion Condensation Theory: Quantitative Prediction*.[44] K_{obs} = observed equilibrium constant for intercalation, $[M^+]$ = counterion concentration, *m'* = the number of cationic charges on the drug, $\Psi = 0.88$, the number of cations associated per phosphate.

In this quantitative treatment, $\Psi = 0.88$, and is the number of cations associated per phosphate in the thermodynamic sense. *m'* is related to the number of ion pairs formed between the acridinylated compound and DNA, and in general is equal to the number of cationic charges on the compound. [44] In summary, it is of utmost importance to consider the ionic strength of the solutions in question when comparing the binding affinity of acridinylated compounds for DNA. Wilson and Jones [44] recommend constructing a graph where the logarithm of the observed equilibrium constant (K) for the acridine-DNA complex at different ion concentrations is plotted against the negative logarithm of the concentration of the ion. In the following figure, the equilibrium constants of Ethidium, a monocation, and quinacrine, a dication, are plotted versus the concentration of sodium. The slope of the plots allow a determination of *m'*, the number of ion pairs formed in the DNA-acridine complex, as in Equation 8.

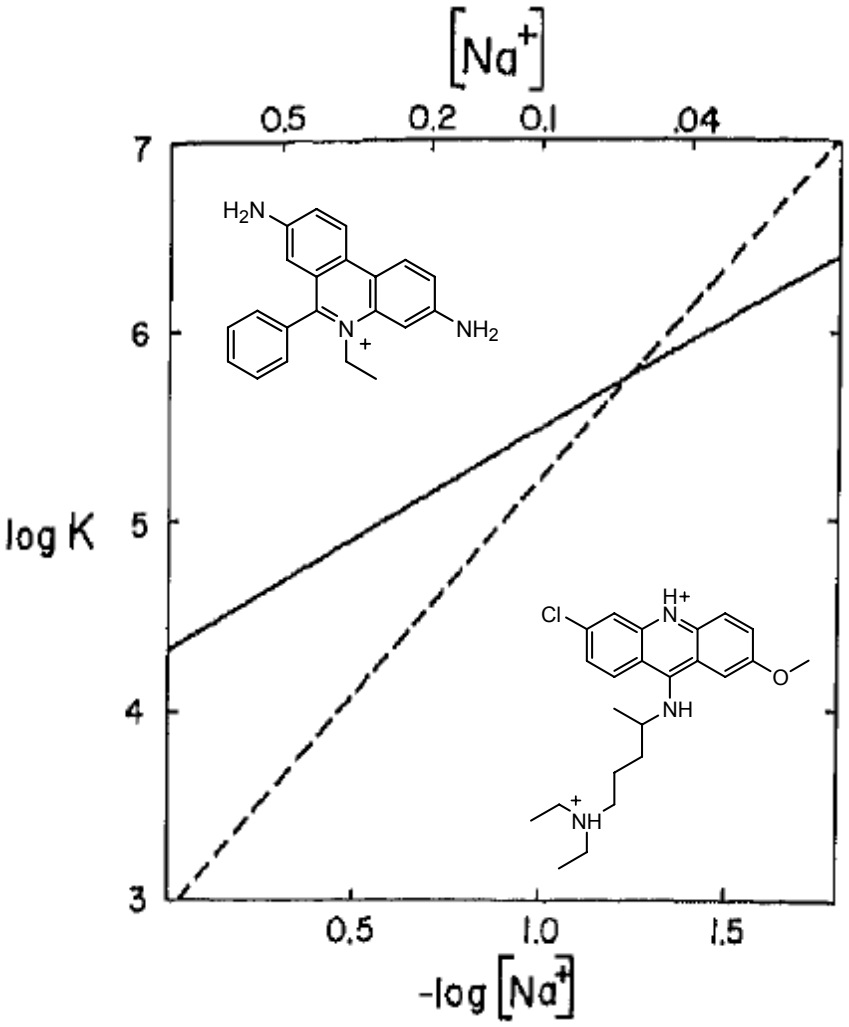

Figure 1-8. *Plot of the Logarithm of the Observed Equilibrium Constants (K) of Ethidium and Quinacrine vs the the Logarithm of the Sodium Ion Concentration*[44] Ethidium : solid line, Quinacrine : broken line. Reproduced with addition of Ethidium and Quinacrine from Wilson *et al.*, 1981.

Ueyama *et. al* conducted a series of binding experiments which are particularly illustrative of the binding capacity of polyintercalators for DNA (Figure 1-8). The first compounds they synthesized were an acridinylated lysine derivative and a peptide containing four acridinylated lysines and three natural lysine residues. [53]

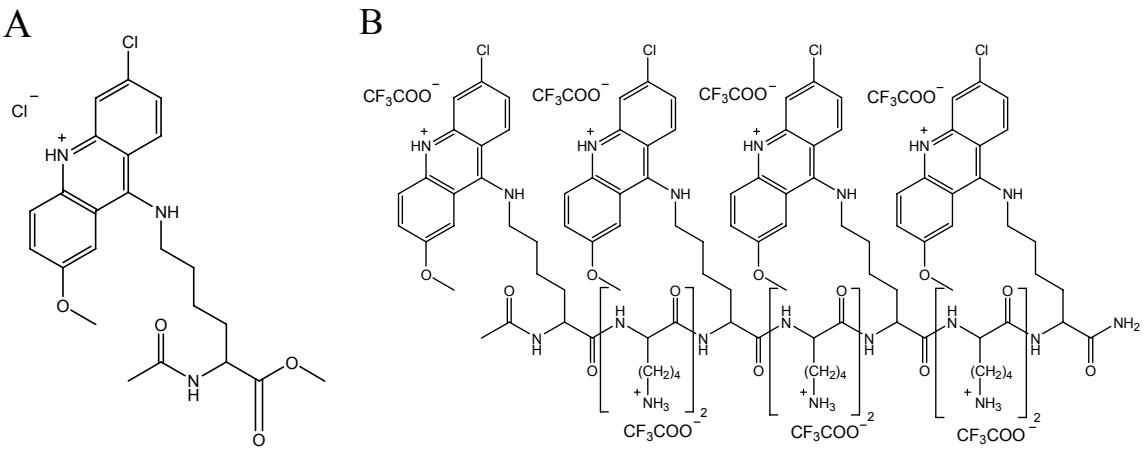

Figure 1-9. *Acridinylated lysine monomer (A) and polyacridinylated peptide (B)* Ueyama *et al*.[53] synthesized a polyacridinylated intercalating peptide on an automated peptide synthesizer.

The absorption spectra of the polyacridinylated peptide (Figure 1-9B) was taken in 10 mM MES and 1 mM EDTA (pH 6.25) in 0.4 M NaCl. Absorption maxima were observed at 423 and 450 nm, with a molar absorptivity of 2.4 x 10^4 cm^{-1} M^{-1}, which is smaller than the sum of four acridinylated lysine monomers, 3.8 x 10^4 cm^{-1} M^{-1} (Figure 1-9A). Sonicated calf thymus DNA was titrated into solution with the polyacridinylated peptide, and a linear increase in viscosity was noted; indicative of intercalation. The researchers also noted a shift in the maxima to longer wavelengths. The peak at 423 nm decreased in intensity, which is consistent with the typical intercalation event (Figure 1-10). The maxima at 450 nm increased, which Ueyama *et. al* did not expect. This may be related to weak acridine-DNA binding, by process (II).

Circular dichroism spectra (not shown) of the polyacridinylated peptide (Figure 1-9B) were measured in the absence and presence of calf thymus DNA. Upon the addition of DNA, the positive Cotton effect at 380-470 nm was enhanced, while the negative effect at 380-470 nm was attenuated, suggesting that the peptide is located on the DNA in a more restricted manner when bound to double stranded DNA.[53]

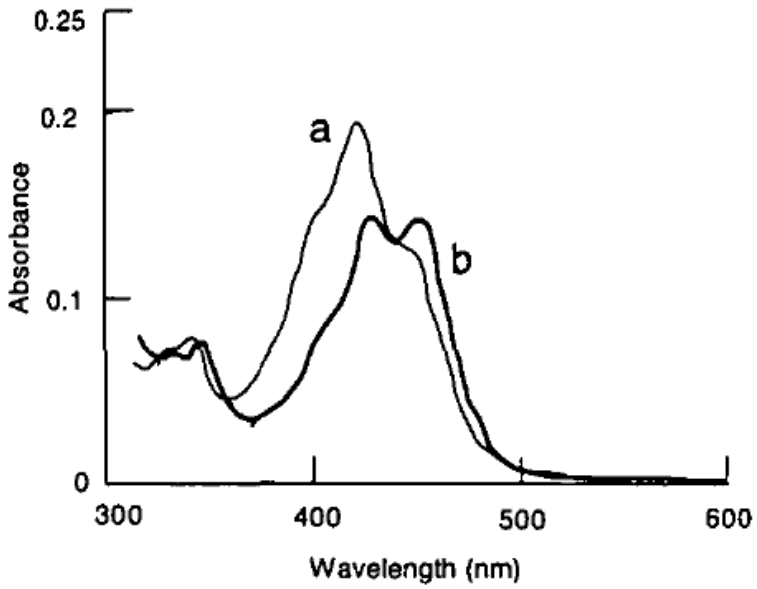

Figure 1-10. *Absorption spectra of Ueyama's polyacridinylated peptide* Spectra taken without (a) and with (b) 68.8 μM-bp calf thymus DNA [in 10 mM MES and 1 mM EDTA, pH 6.25 containing 0.4 M NaCl at 25°C] [53] Reproduced from Ueyama *et al.*, 2000.

A Scatchard analysis of binding was used with the probability method of McGhee and von Hippel [54] to determine the binding constant, $K = (3.0 \pm 0.4) \times 10^6\ M^{-1}$, which they noted as being 1000 times higher than that of quinacrine, $K = 1.6 \times 10^3\ M^{-1}$ (Equation 1-2).

$$\frac{v}{c} = K(1-nv)\left\{\frac{(1-nv)}{[1-(n-1)v]}\right\}^{n-1}$$

Equation 1-2. *Binding constant (K) determination* Ueyama *et al.*[55] adapted McGhee and Von Hippel's [54] conditional probability derivation of Scatchard's equation to determine the binding constant of their polyacridinylated peptide. n = total number of binding sites, c = free peptide concentration, v = moles of peptide bound per base pair, K = observed binding constant.

Ueyama and co-workers [55] continued their acridinylation research with the publication of a series of acridinylated compounds of varying length (Figure 1-11).

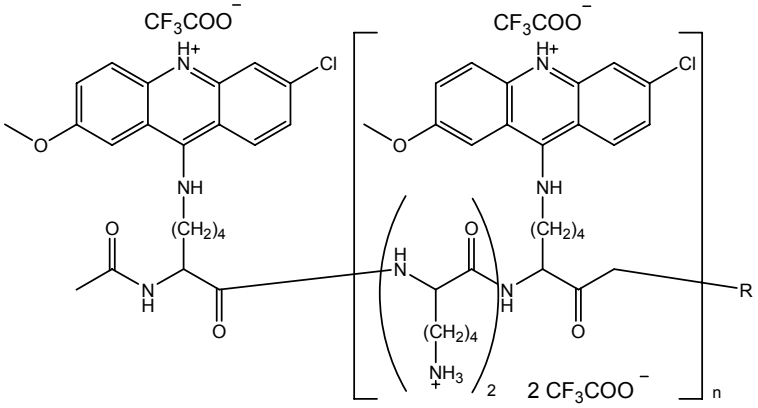

Figure 1-11. *Series of Polyacridinylated Peptides.* [55] For 5 compounds, 1: n = 0, 2: n = 1, 3 : n = 2, 4: n = 3, 5: n = 4 (1: R = OCH_3, 2 – 5: R = NH_2

The authors also plotted the relationship between the peptides and their molar absorptivity, and their respective logarithmic binding constants (Figure 1-12).

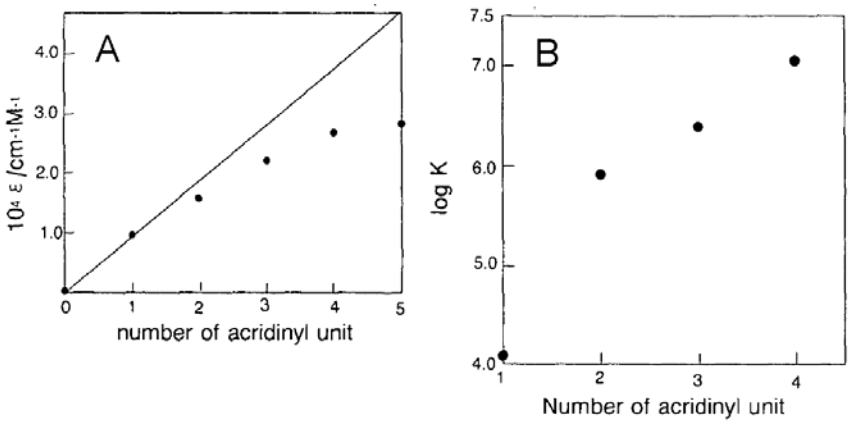

Figure 1-12. *Properties of the series of polyacridinylated peptides.* [55] The molar absorptivity (A) and logarithm of the binding constant (B) of each peptide was determined and plotted. Experiments were performed in 10 mM MES and 1 mM EDTA pH 6.25 at 25°C. Reproduced from Ueyama *et al.*, 2001.

It is interesting to note the behavior of the longer peptides, with four to five acridinyl units. The molar absorptivity of the compounds begins to level off, which suggests aggregation or polymeric behavior. Also, although compound 5 seemed to have high affinity for DNA, it precipitated during Scatchard analysis, and a binding constant could not be obtained. [55]

The DC-SIGN Receptor

The DC-SIGN (Dendritic Cell-Specific Intracellular adhesion molecule-3 Grabbing Non-integrin) receptor was discovered by Curtis and co-workers in 1992. [56] They screened a placental cDNA library via expression cloning and identified a 1.3 kilobase cDNA sequence predictive of a 404 amino acid protein of 45 775 Da organized into three domains: an N-terminal cytoplasmic and hydrophobic region, seven complete and one incomplete tandem repeats, and a C-terminal domain with homology to C-type (calcium-dependent) lectins (Figure 1-13). Curtis *et al*. transfected COS cells with the cDNA and CD4-independent gp120 binding was observed. This was noteworthy because it meant that HIV could bind a receptor protein in the placenta which had previously been unidentified. K_d values of 1.7 ± 0.4 nM and 1.8 ± 0.2 nM were derived for protein - vgp120 (vaccinia virus derived gp120) binding, and protein - ngp120 (native gp120 purified from HIV_{BRU}) binding. A similar K_d (1.3 nM) was obtained for binding between the protein and placental membranes in the presence of CD4a antibodies. The protein was confirmed to be a lectin by analysis of binding and gp120 internalization. Mannan, L-Fucose, α-methyl D-mannoside, D-mannose and N-acetylglucosamine inhibited gp120 binding with an IC_{50} value of 6 μg/ml, and K_i values of 6 mM, 15 mM, 23 mM and 70 mM respectively. Binding between the protein and gp120 required calcium and was blocked by EGTA (K_i 0.3 mM), characteristic of C-type lectins. ^{125}I-gp120 bound to the surface of transfected COS cells was shown to be internalized by an acid stripping procedure used to remove cell surface ligand. [57]

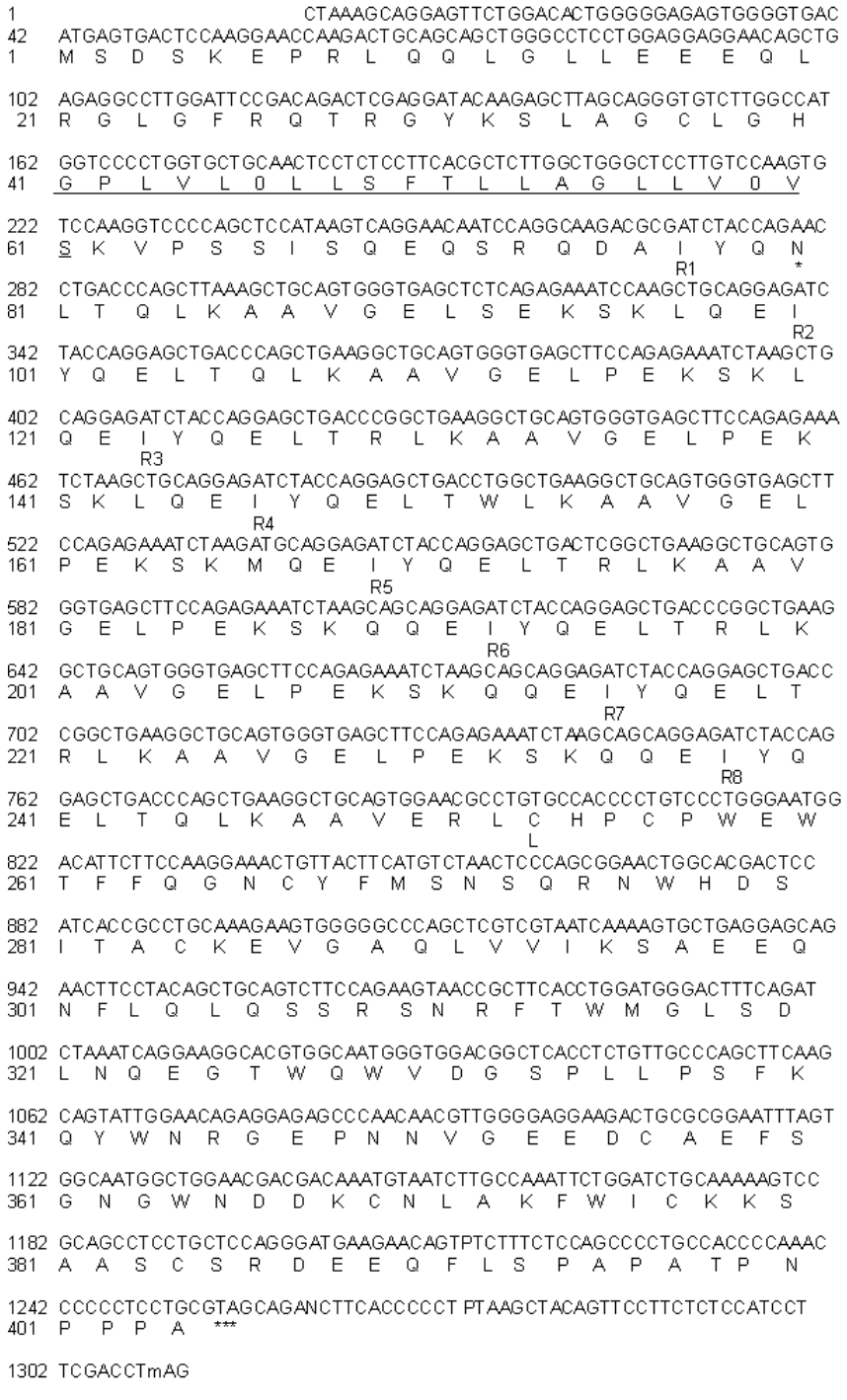

Figure 1-13. *Nucleotide and deduced amino acid sequence of DC-SIGN cDNA* [56] The membrane spanning sequence is underlined and potential N-linked glycosylation site is marked by a star. The beginning of the seven complete and eighth partial repeat (R1-R8) and the beginning of the lectin domain (L) are indicated. Adapted from Curtis *et al.*, 1992.

In 2001, Hadar Feinberg *et al*.[58] published a crystal structure of the carbohydrate recognition domain of DC-SIGN complexed with a $Mannose_3$ N-acetyl $Glucosamine_2$ pentasaccharide (Figure 1-14).

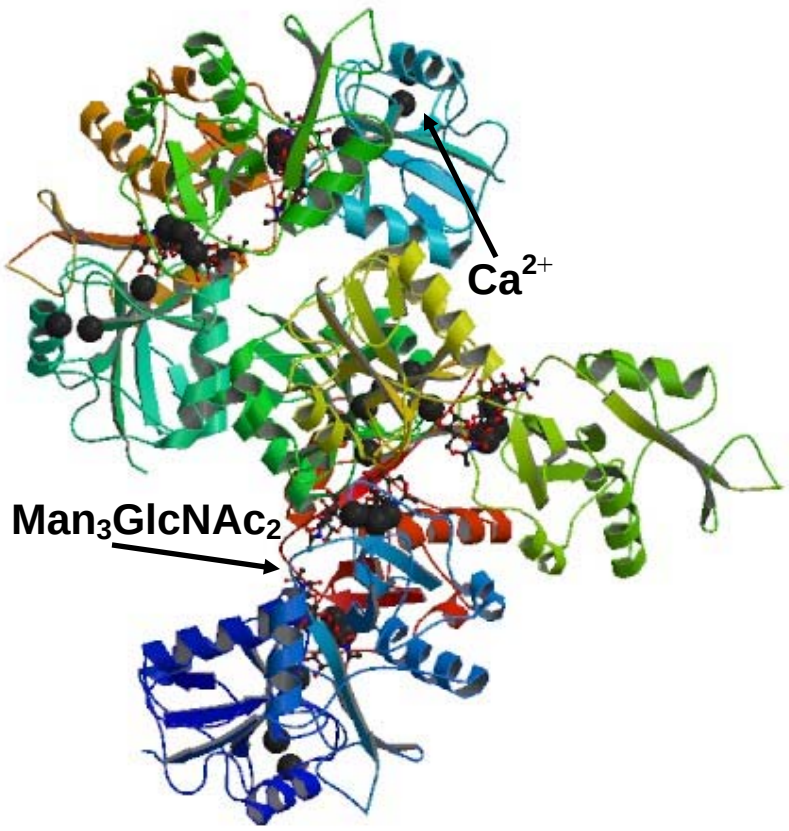

Figure 1-14. *CRD of DC-SIGN with $Man_3GlcNAc_2$ pentasaccharide and calcium.* Structure 1k9i (Protein Data Bank) is the decameric representation of the carbohydrate recognition domain (CRD) of DC-SIGN with the $Man_3GlcNAc_2$ pentasaccharide bound. Ca^{2+} ions are depicted as black spheres, the pentasaccharides are the ball and stick structures.

The publication also contained the more highly resolved structure of the pentasaccharide complexed with DC-SIGNR, a receptor 77% identical in sequence. DC-SIGNR is found

on lymph node and liver sinusoidal endothelia, and in the placental villi, [59-61] while DC-SIGN is expressed on dendritic cells present in the lamina propria of mucosal tissues such as those in the rectum, uterus, and cervix. The bound pentasaccharide (Figure 1-15A) cross-linked two monomeric carbohydrate recognition domains in DC-SIGN exclusively, but in all other respects the conformation of the pentasaccharide was identical for both receptors.

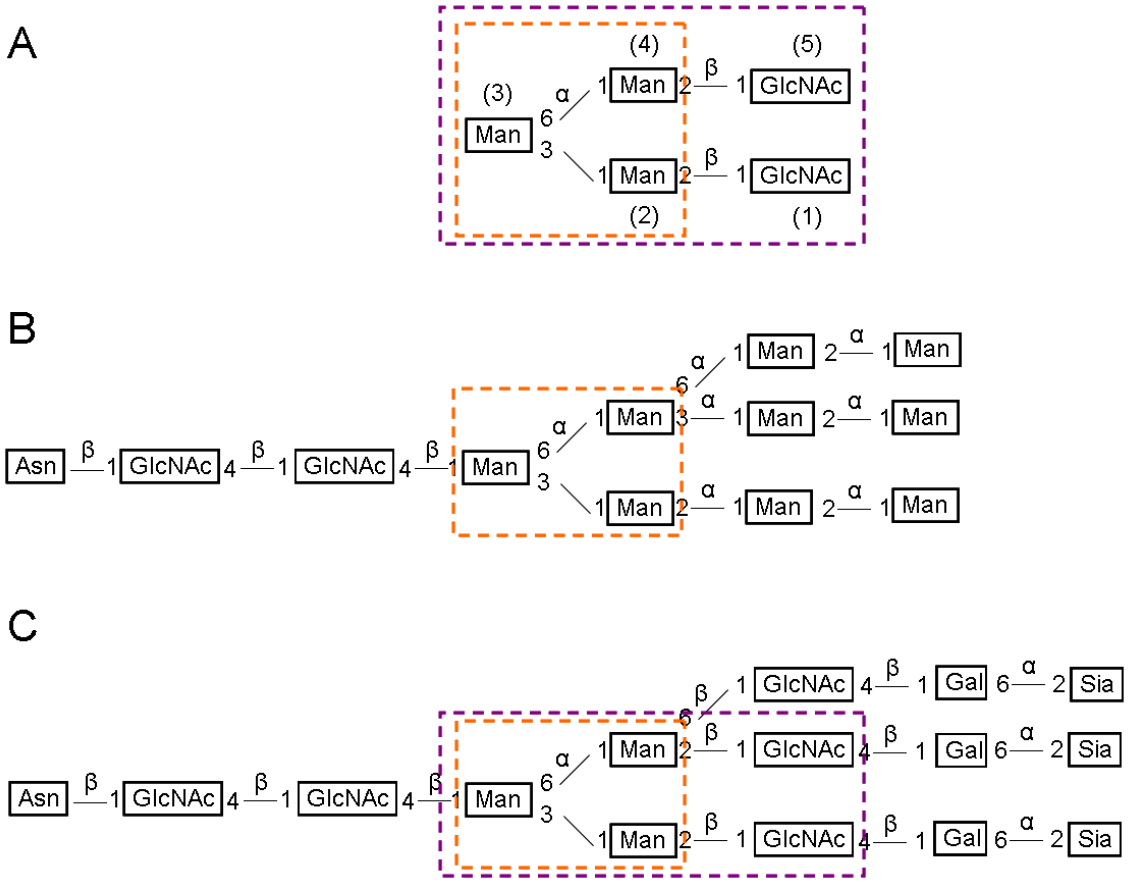

Figure 1-15. *Polysaccharide Structures* [58] (A) Pentasaccharide co-crystallized with the DC-SIGN receptor (B) Man_9 N-glycan – abundant on gp120 (C) A common, complex-type N-glycan. The structure in the purple box is analogous to the structure in (A). Adapted from Feinberg *et al.*, 2001.

The most unusual interaction between the pentasaccharide and DC-SIGN was the interaction between mannose (2), Ca^{2+}, and a set of proximal amino acids. Lectin-carbohydrate reactions typically involve terminal, not internal sugars. In this complex, the equatorial 3- and 4-OHs of mannose (2) form coordination bonds with Ca^{2+}, which in turn bonds to Glu^{354}, Asn^{365}, Asp^{347}, and Asn^{349}. The exocyclic C6 of the sugar forms a water mediated bond with Asp^{367}. The acetamido carbonyl oxygen of GlcNAc (1) forms van der Waals bonds with Val^{351}. GlcNAc (1) also coordinates with a Ca^{2+} ion which cross-links to a partner monomer, forming a dimer (Figure 1-16).

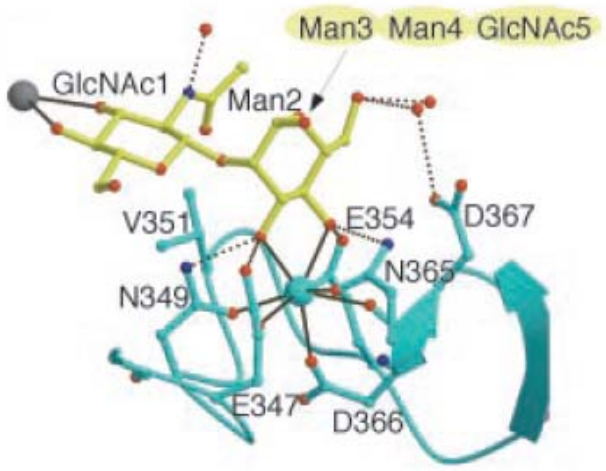

Figure 1-16. *Ball and stick representation of DC-SIGN bound to Man_3 $GlcNAc_2$.* [58] The large gray and cyan spheres are Ca^{2+}, the red spheres are oxygen and the blue spheres represent nitrogen. Reproduced from Feinberg *et al.*, 2001

The crystal structures reported in 2001 by Feinberg *et al*. [58] were the first published containing DC-SIGN and a bound polysaccharide. The study was a landmark and it serves as a valuable model. However, the $Man_3GlcNAc_2$ pentasaccharide used had weak affinity for DC-SIGN relative to a number of high mannose and fucosylated carbohydrates (Table 1-3 and Figure 1-17, structures on Figure 1-18).

Binding Competition Assays	
Ligand	($K_{D,\ Man}/K_D$)
Man α1-2 Man	4.1 ± 0.1
Man α1-3 Man	1.8 ± 0.3
Man α1-4 Man	1.8 ± 0.4
Man α1-6 Man	1.6 ± 0.1
Man α1-3 [Man α1-6] Man	3.9 ± 0.5
Man α1-3 [Man α1-3 [Man α1-6] Man α1-6] Man	7.3 ± 0.4
GlcNAc β1-2 Manα 1-3 [GlcNAc β1-2 Man α1-6]Man [A]	17 ± 6.4
$Man_9GlcNAc_2$	131 + 26

[A] GlcNAc β1-2 Man α1-3[GlcNAc β1-2 Man α1-6]Man is the $Man_3GlcNAc_2$ pentasaccharide reported in the crystal structure, Figure 16.

Table 1-3. *Binding of Oligosaccharides to DC-SIGN.* [58] Competition binding assays with the immobilized CRD of DC-SIGN were performed. The K_Ds relative to the K_D for mannose were reported. Adapted from Feinberg *et al.*, 2001.

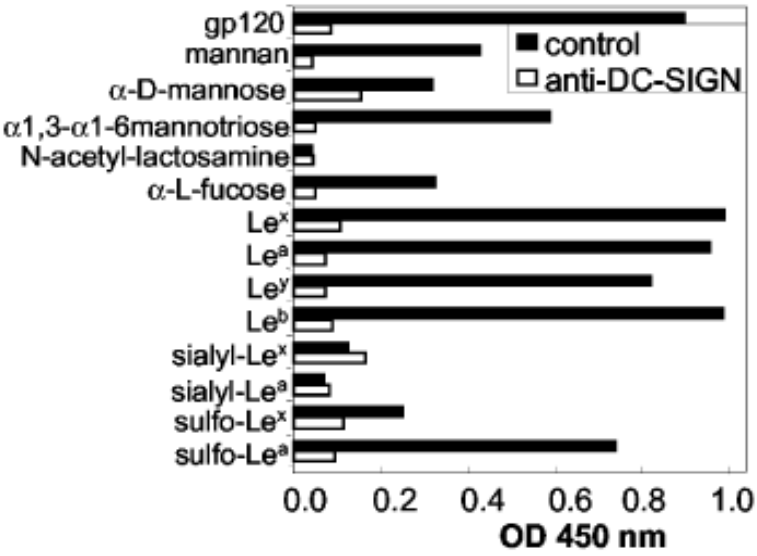

Figure 1-17. *Comparative affinity of carbohydrate ligands for DC-SIGN.* [62] Synthetic glycoconjugates were screened for affinity to a chimeric DC-SIGN with a human IgG1-Fc tag in an ELISA-type assay. Anti-DC-SIGN mAb AZN-D1 was used to block binding. Reproduced from Appelmelk *et al.*, 2003.

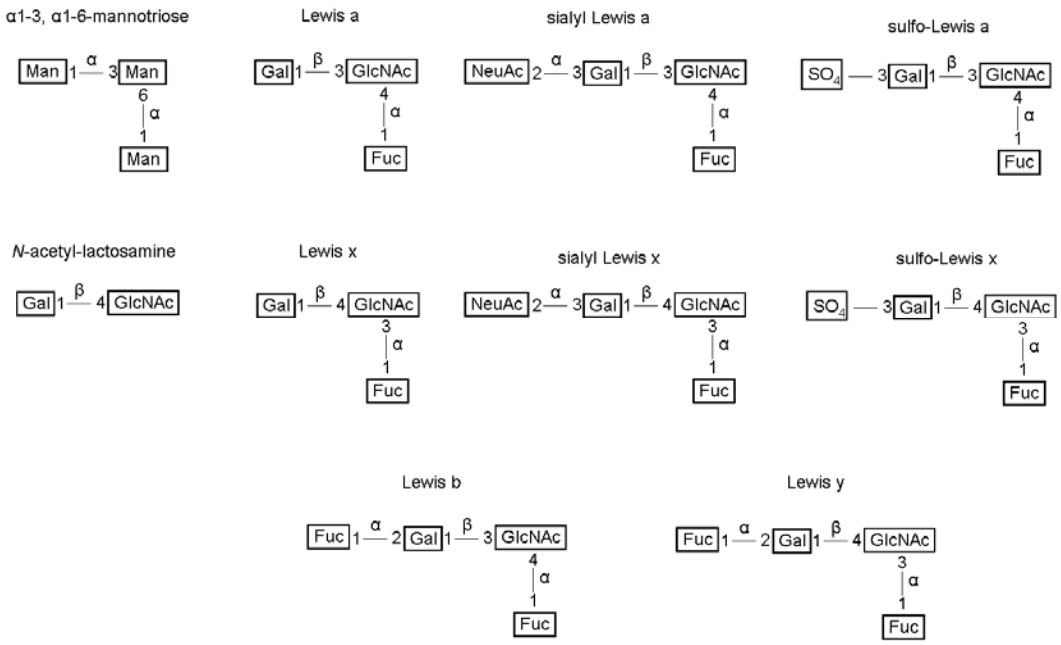

Figure 1-18. *Schematic diagram of the synthetic glycoconjugate ligands used in the DC-SIGN binding assay*. [62]

In 2007, Feinberg *et al*. published a second paper on DC-SIGN with crystallographic analysis of bound polysaccharides. [63] The Man_6 structure reported is of special interest because it is part of the structure of the $Man_9GlcNAc_2Asn$ N-glycan, present on the coating of the HIV virus, Ebola virus, and the Leishmania pifanoi parasite. [64] The binding competition assay was performed with Man_6, Man_9, and $Man_9GlcNAc_2$. Man_6 bound 14 times more tightly than mannose, but Man_9 bound 32 times more tightly, and $Man_9GlcNAc_2$ bound with 88 times the affinity (Table 1-4 and Figure 1-19). The researchers did not report the binding affinity of the full-length N-glycan, $Man_9GlcNAc_2Asn$. The addition of a single amino acid into the spacer arm may have created a significant increase in binding affinity.

Binding Competition Assays		
Ligand	DC-SIGN	
	K_I	K_I vs. mannose
	μM	*fold increase*
Man	2300 ± 100	1
Manα 1-2Man[a]	--[a]	4.1 ± 1
Man_{6a}	183 ± 18	12 ± 3
Man_{6b}	157 ± 17	14 ± 1
Man_9	73 ± 6	32 ± 4
$Man_9GlcNAc_2$	26	88

[a] – absolute and relative K_I vs. mannose values taken from Feinberg *et al*, 2001. [58]

Table 1-4. *Binding of High Mannose Oligosaccharides to DC-SIGN.* [63] Competition binding assays with the immobilized CRD of DC-SIGN were performed. Absolute K_I value omitted due to experiment with a different batch of ^{125}I Man-bovine serum albumin. Adapted from Feinberg *et al.*, 2007.

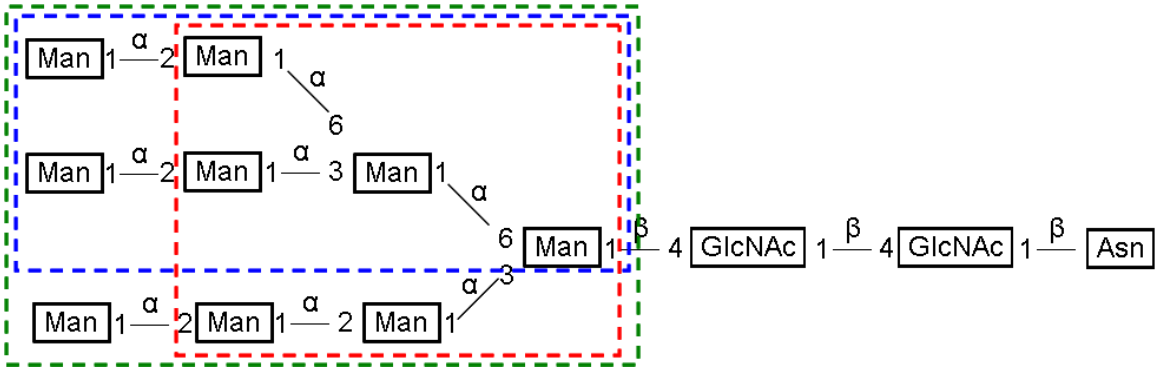

Figure 1-19. *Asparagine linked high mannose structures.* [63] Man_{6a} is shown in the red box, Man_{6b} is in the blue box, and Man_9 is in the green box. Adapted from Feinberg *et al.*, 2007.

The researchers found that the crystal structure of Man_{6b} bound to the receptor was the same as that of $Man_3GlcNAc_2$, from their 2001 paper. However, they observed Man_{6b} bound in two overlapping orientations in a 3:1 ratio, designated major and minor. Only three mannose residues were visible in the major orientation; two were visible in the

minor orientation. The penultimate α1-3 linked mannose binds to the primary Ca^{2+} site and is seen in both orientations (Figure 1-20). In the minor orientation, the same mannose is seen, but it is rotated 180° around an axis bisecting the pyranose ring through the C-3 – C-4 bond.

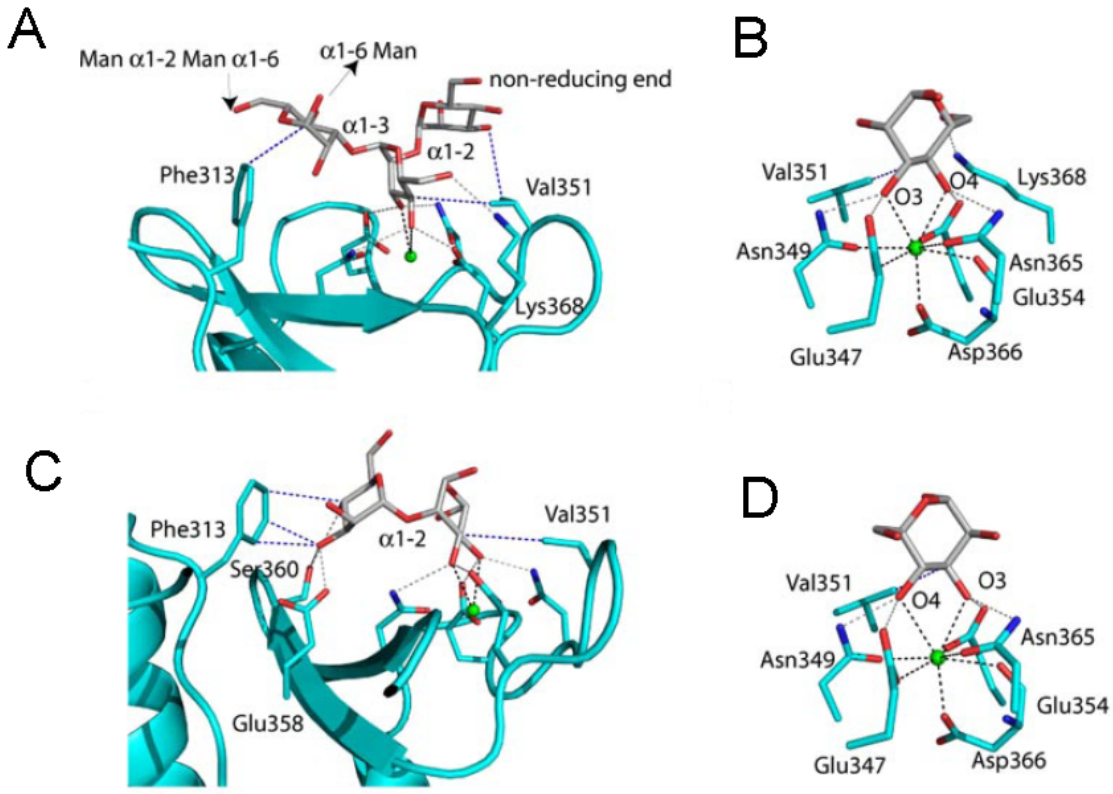

Figure 1-20. *Ball and stick representation of DC-SIGN bound to Man_{6b}.* [63] The green spheres represent Ca^{2+}, The red sticks are oxygen, nitrogen is blue. Ca^{2+} coordination bonds are dashed black lines, van der Waals interactions are dashed blue lines, hydrogen bonds are dashed gray lines. **A** is the major orientation of the bound ligand, **B** is a magnified view of **A**, **C** is the minor orientation of the ligand, **D** is a magnified view of **C**. Reproduced from Feinberg *et al.*, 2007

One of the primary challenges in quantifying the affinity of DC-SIGN for high mannose N-glycans is the difficulty involved in obtaining material. For instance, in the

competition, binding assays performed by Feinberg and co-workers, [63] the $Man_9GlcNAc_2$ glycan was assayed only once in duplicate because only limited quantities were available. This is also part the reason the group did not produce a crystal structure of the ligand-receptor complex. The Man_9 nonasaccharide was synthesized by the lengthy procedure shown below (Scheme 1-8,9 and 10):

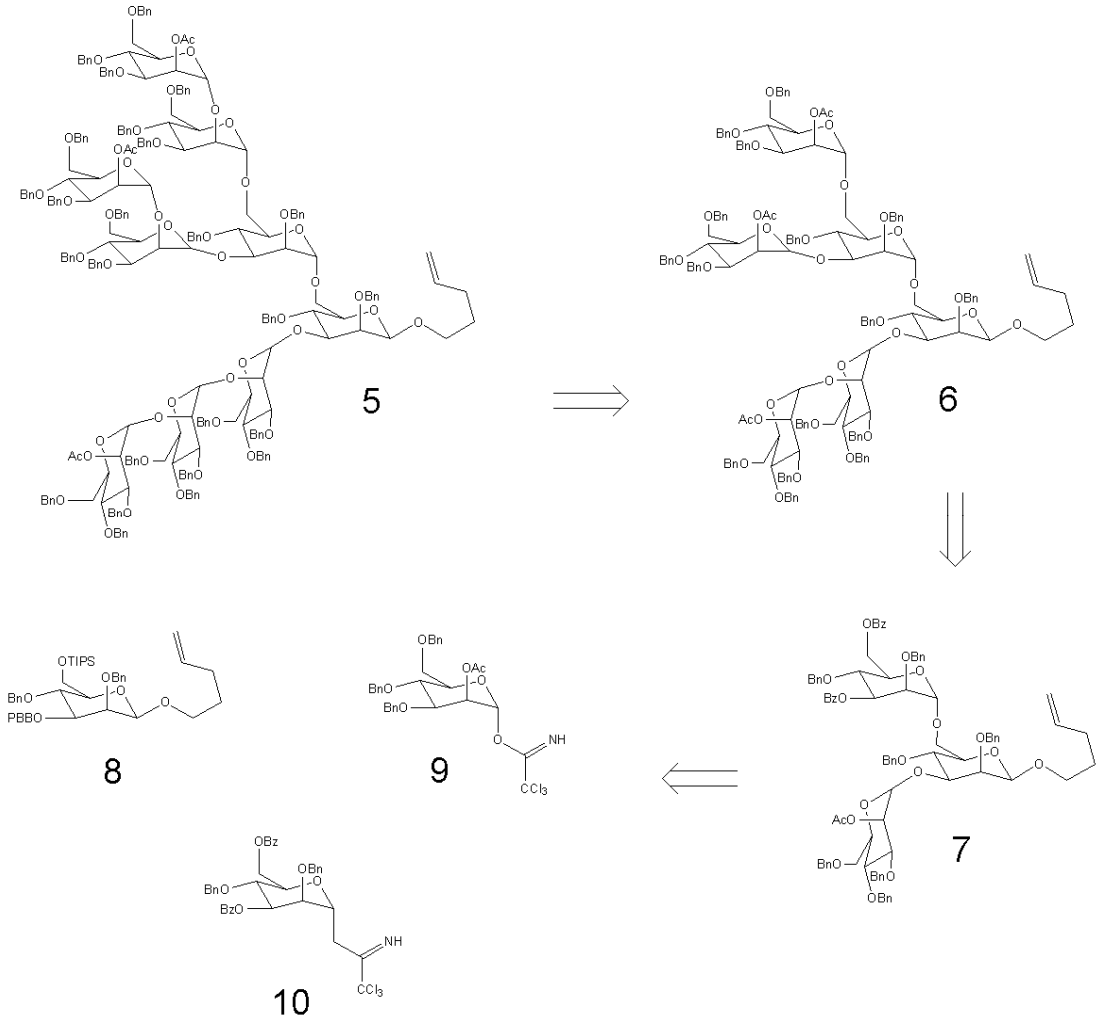

Scheme 1-8. *Retrosynthesis of the Man_9 nonasaccharide*. [65] Seeberger's retrosynthetic method for producing Man_9 was adopted. Man_{6b} was produced by the same approach, using methyl 2,3,4-tri-O-benzyl-α-D-manopyranoside as the core sugar unit. [63,66,67]

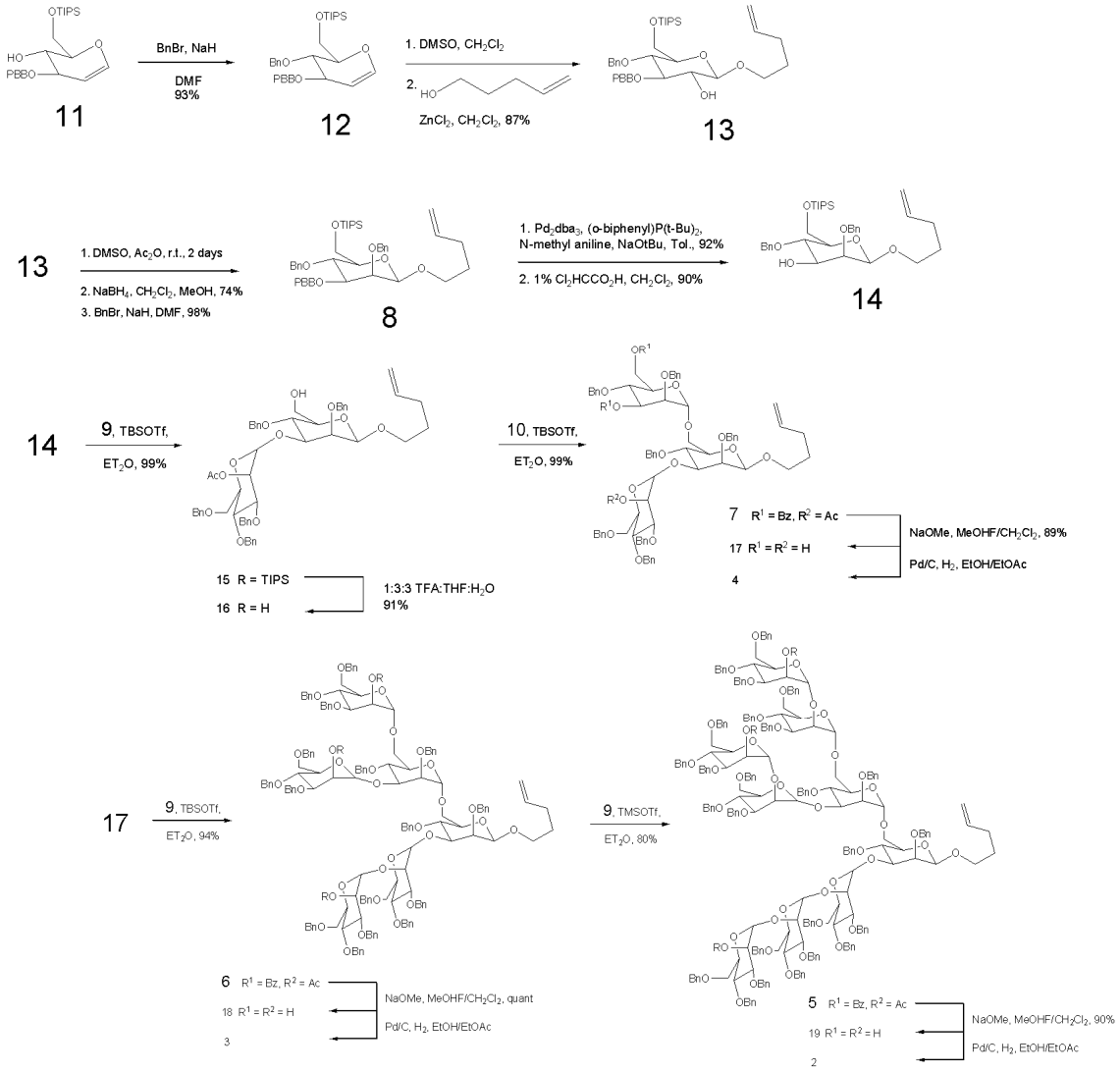

Scheme 1-9. *Reaction conditions for the Man_9 nonasaccharide.* [65] Seeberger's 15 step synthesis produces Man_9 at a 25% overall yield. It is linear, and was designed to be automated.

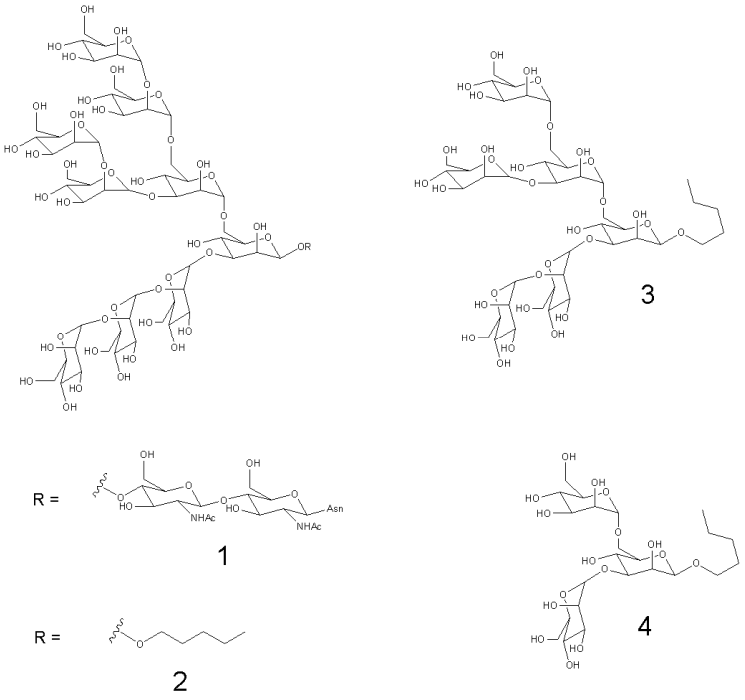

Scheme 1-10. *High mannose oligosaccharide target compounds.* [65] Compounds 2-4 were synthesized, compound 1, the native N-glycan, has never been synthesized to date.

The carbohydrate chemistry used in the synthesis of compounds 2-4 is unique in many ways and the methodology could potentially be used in an automated setting. However at this time, the chemical synthesis of natural glycans is still much less practical than natural product isolation. Seeberger's synthesis provides specific evidence of this, particularly because the research group could not synthesize the full N-glycan.

The Functions of DC-SIGN

The membrane associated mannose binding lectin discovered by Curtis and co-workers in 1992 [56] was renamed DC-SIGN (dendritic cell-specific intracellular adhesion molecule-3 grabbing non-integrin) by Geijtenbeek *et al*. in 2000.[68] Steinman and Cohn discovered dendritic cells (DCs) in 1973 [69] and over the next three decades it became well established that dendritic cells were essential to the initiation of a primary immune

response. DCs do this by capturing antigens in peripheral tissue and processing them to form a major-histocompatibility (MHC) – peptide complex. The DCs then migrate from the periphery to the T-cell areas of secondary lymphoid organs (Figure 1-21). The cells mature during the migration and their surface profile is altered. At that point resting T-cells are attracted to DCs, and when the cells bind, the antigen payload in the DC is transferred to the T cells. [2,70,71]

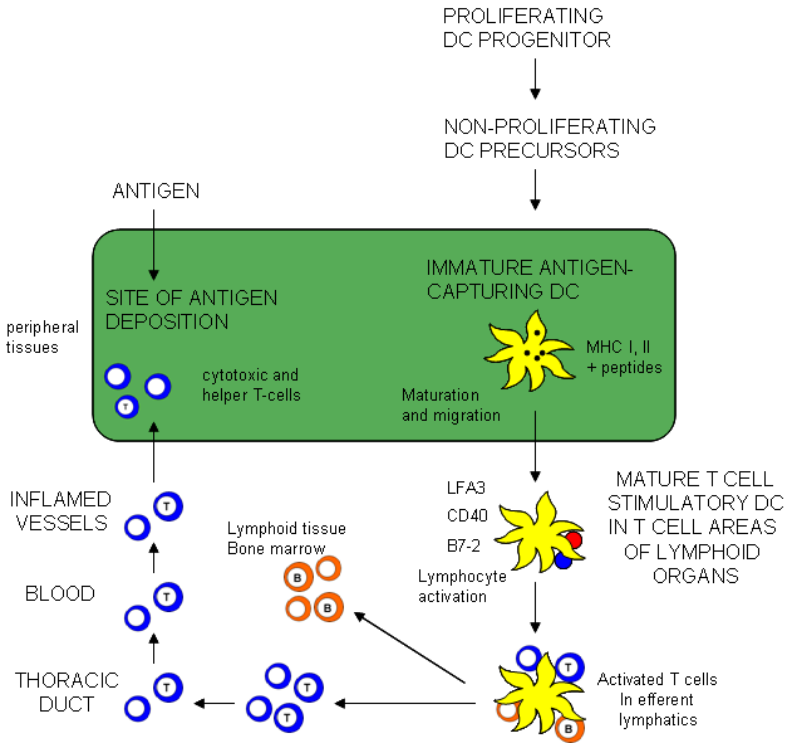

Figure 1-21. *DC Activation In Vivo*. [66] Antigens are captured by DCs in peripheral tissues and processed to form MHC-peptide complexes. The immature DCs derive from proliferating and non-proliferating precursor cells. Antigen deposition and inflammation matures the DCs and they express molecules which will lead to binding and stimulation of T cells in the T-cell areas of lymphoid tissues. If the antigen has also been bound by B cells, then B and T cells can cluster with DCs. After activation, T and B blasts leave the T cell area. B blasts move to the lining of the intestine, bone marrow and other parts of the lymphoid tissue. Some become antibody-secreting plasma cells. T blasts leave the blood at the original site of antigen deposition, recognize changes in the inflamed blood vessels and respond vigorously to cells presenting antigen. Adapted from Geijtenbeek *et al.*, 2000.

The discovery of DC-SIGN by Geijtenbeek and his co-workers began with their observation of high levels of ICAM-3 (intracellular adhesion molecule 3) expression on the surface of resting T cells. The β2 integrins LFA-1 (lymphocyte function associated integrin-1, also known as αLβ2) and αDβ2, both present on DCs, had been described as the primary receptors for ICAM-3, although their affinity for ICAM-3 is low. [72-75] In addition to these observations, the investigators knew that ICAM-3 is a heavily glycosylated transmembrane protein. [76,77] The researchers then used these facts to design a set of experiments which would show that DC-SIGN, (and neither LFA-1 nor αDβ2) a novel ICAM-3 binding C-type lectin exclusively expressed by DCs, mediated strong adhesion between DCs and ICAM-3 on resting T-cells and was essential for DC-induced T cell proliferation. [68]

Geijtenbeek *et al*. published an additional article in 2000 revealing a second function of DC-SIGN. [78] It was well known that immature DCs migrate from the blood to peripheral tissue, and then ultimately to secondary lymphoid organs.[66] This migration is part of the immune response to inflammation, and necessary for interaction with T-cells. Immature DCs express high levels of DC-SIGN,[68] and lectins often function as rolling receptors for leukocyte transendothelial migration.[79] Thus, they hypothesized that DC-SIGN might play a role in the migratory ability of DCs. They focused their investigation on ICAM-2, a transmembrane glycoprotein with high sequence similarity to ICAM-3. They found that DC-SIGN has high affinity for ICAM-2; higher in fact than ICAM-3 (IC_{50} = 1 μg/mL vs 6 μg/mL). However, unlike ICAM-3, ICAM-2 is abundantly expressed by vascular and lymphoid epithelia.[80] The data showed that 1) adhesion of DCs to ICAM-2 was almost entirely mediated by DC-SIGN and not LFA-1, and could be inhibited by EGTA or mannan, 2) DC-SIGN positive-precursors are present in the blood, 3) DC-SIGN mediated tethering and rolling was observed over the entire range of physiological shear stress (flow conditions) reported to occur in postcapillary venules known to support leukocyte emigration.[81] These results illustrate the role of DC-

SIGN in DC function as a rolling receptor that mediates ICAM-2 dependent migration processes in addition to its function in mediating naïve T cell interaction through ICAM-3.

In 2008, Juan García-Vallejo *et al*.[82] determined that the Lewis^{Y} antigen expressed on ICAM-2 was responsible for DC-SIGN mediated adhesion and rolling. They discovered this with human umbilical vein endothelial cells. They determined experimentally that ICAM-2 expressing CHO cells only served as a ligand for DC-SIGN when correctly glycosylated. Additionally, when the FUT1 gene (the gene necessary for the expression of Le^{Y} in endothelial cells) was silenced, the rolling and adhesion of immature DCs over endothelial cells was reduced.

Unfortunately, DC-SIGN can be exploited by a variety of pathogens to subvert immune response (Table 1-5). HIV-1 was the first pathogen discovered to have this ability, [56,83] and since then several others have been found capable.

DC-SIGN-Binding Pathogens		
Pathogen	Antigen	Carbohydrate Structure
Viruses		
HIV-1	gp120	High mannose
Ebola Virus	GP	High mannose
Bacteria		
Helicobacter pylori	LPS	Lewis-x
Parasites		
Leishmania pifanoi	LPG	High mannose
Schistosoma mansoni	SEA	Lewis-x

Table 1-5. *DC-SIGN Binding Pathogens*.[64] gp120, glycoprotein 120; GP, glycoprotein; LPS, lipopolysaccharide, LPG, lipophosphoglycan; SEA, soluble egg antigen. Adapted from van Kooyk *et al.*, 2003.

It is now commonly accepted that immature DCs capture HIV-1 in the mucosa by binding HIV-I's envelope glycoprotein120 via DC-SIGN, and internalize and transmit the virus to lymphoid tissue, where the HIV-I is transferred to $CD4^+$ T cells.[84,85] Viral particles endocytosed by DC-SIGN are sequestered into acidic, non-lysosomal vesicles near to the cell membrane, and are somehow protected from degradation and processing. This is unusual because studies have shown that DC-SIGN bound antibodies internalized into lysosomal compartments for processing and presentation to T cells while DC-SIGN bound HIV-1 particles are stable and retain infectivity for days.[85,86] *In vitro* studies also showed that at low HIV-1 titres, T cells are not infected without the assistance of DC-SIGN *in trans*.[84,85] *In vivo* studies in a primate model showed that the addition of a glycan to a protein domain of a chimaeric HIV virus resulted in enhanced binding to DC-SIGN.[87]

A second class of pathogen capable of manipulating the immune response comprise certain members of the genus mycobacterium. Two examples are *M. tuberculosis*, and *M. bovis* bacillus Calmette-Guérin. They contain ManLAM (mannose-capped lipoarabinomannan), a component of their cell wall, which binds strongly to DC-SIGN.[88-90] When *M. tuberculosis* is endocytosed, it is targeted to late endosome/lysosomal compartments where the particles are destined to be degraded;[88,91] however the immune system typically cannot totally eradicate the pathogen. DCs (and some macrophages bearing the mannose receptor) infected with *M. tuberculosis* secrete the virulence factor ManLAM which binds DC-SIGN on DCs attracted to the inflammatory site, thus interefering with immune response.[92,93] Toll-like receptors (TLRs) present on the DCs also recognize *M. tuberculosis*, resulting in the activation of nuclear factor κB (NF-κB), leading to maturation of DCs, and the production of inflammatory cytokines to enhance T-cell responses to eliminate the pathogen.[64] However, high levels of ManLAM secretion by infected DCs inhibits the activation of NF-κB and the maturation of DCs, and results in production of the immunosuppressive

cytokine interleukin-10 (IL-10).[88,94] The central problematic characteristic of the pathogens which interact with DC-SIGN is that they cause chronic infections which can last a lifetime, and they do this by manipulation of the T_H1 (T helper 1) versus T_H2 (T helper 2) immune response. [64] T_H1 cells induce cellular immunity, while T_H2 cells induce humoral immunity, and it may be possible that some microorganisms target DC-SIGN specifically to induce a T_H2 dominant response.[88] This phenomena is seen with *Leishmania mexicana*, where a T_H1 to T_H2 shift is necessary for virulence and persistence. This is also the case with the parasite Schistosoma mansoni, where the T_H2-type immune response to infection is associated with persistence, driven by its major glycan antigen Le^x.[95]

Research Objective

For several years the objective of research in our laboratory has been to design and synthesize non-viral gene delivery vectors. Designing an effective vector of this type generally requires 1) a method of binding or enveloping DNA,[96] 2) preventing the vector-DNA complex from binding non-specifically with blood plasma proteins, undesired cells, and the extracellular matrix, [97] 3) inducing cell or tissue specific binding and endocytosis, 4) a method for the release of the DNA from liposomal or endosomal enclosure, 5) resistance to cytoplasmic degradation, and 6) localization to and passage through the double-membrane of the nuclear envelope surrounding the nucleus.[98,99]

The focus of the research in the following chapters is on advances made in vector design and application in two areas: the synthesis of acridine derivatives which reversibly bind to DNA, and the development of new targeting ligands for gene transfer to dendritic cells.

Cationic lipids, polymers, and peptides are commonly used to encapsulate and complex DNA. The binding interaction results from electrostatic attraction between the anionic phosphate backbone of the nucleic acid and positively charged moieties on the

carriers.[100] DOTMA, PEI, and poly-arginine peptide belong to this group of compounds. I adopted an approach which combines a cationic amino acid and a derivatized, intercalating amino acid into a single DNA-binding peptide.

Antibodies, proteins, and oligosaccharides are often utilized as targeting agents for non-viral vectors. The single-chain antibody to the tumor associated cell surface ERBB2 antigen,[101] the glycoprotein transferrin,[97] and sialyl Lewis X [102] are examples of targeting ligands used with synthetic vectors. We used the high-mannose N-glycan $Man_9GlcNAc_2Asn$ as the targeting ligand for our vector.

Haensler and Szoka [103] synthesized a targeted vector similar in design to the vector designed in this publication. It contained a bisacridine moiety for intercalating into plasmid DNA and galactose monosaccharides for binding the asialoglycoprotein receptor on primary hepatocytes. While the compound bound the pCLUC4 plasmid encoding firefly luciferase with micromolar affinity, it did not induce transfection of the hepatocytes. Our hypothesis was that we could achieve targeted gene delivery with a vector containing carbohydrate and intercalative functionality. The objective of this research project was to synthesize a vector containing acridine for non-covalent complexation of DNA, and a glycan ligand for targeting the DC-SIGN receptor on dendritic cells. Gene expression in the target cells would be quantified by luciferase analysis of the translated pGL3 reporter gene.

CHAPTER 2

AN IMPROVED METHOD FOR PREPARING SEPHAROSE N-CAPROYL GALACTOSAMINE AFFINITY RESIN FOR THE PURIFICATION OF SOYBEAN AGGLUTININ FROM SOY FLOUR

Introduction

Soybean Agglutinin (SBA) is a glycoprotein and a lectin. SBA was initially identified as a toxin with hemagglutinating activity found in defatted soybean flour by Irvin Liener in the 1950s.[104] This discovery soon led to collaboration with Nathan Sharon, who published articles on the structure, purification and application of SBA and other lectins over the next four decades.[105,106,107] Lectins bind carbohydrates through non-covalent interaction, and as such are used experimentally to investigate intracellular, extracellular, and membrane bound glycoproteins. SBA has been used clinically to purge mononuclear bone marrow cells, enriching CD34+ hematopoietic progenitor cells, thereby preventing graft-vs-host disease in bone marrow transplants.[108] SBA is also of interest because it contains Mannose-9 N-Glycan, an N-Glycan on the HIV glycoprotein 120 which binds the mannose binding lectin (MBL), DC-SIGN, and other lectins in the innate immune system, facilitating HIV infection of T cells.[109] Previously, we incorporated Man_9 into a non-viral gene delivery vector to target the mannose receptor on Kupffer cells in the liver.[110]

My initial research into improving our ammonium sulfate precipitation procedure for isolating SBA led to the discovery of Sharon's affinity purification method.[106] Low-pressure chromatography was an ideal means for purification of the quantity of N-glycan necessary to synthesize our bioconjugate vectors. We found the affinity absorbent preparation procedure of Allen and Neuberger[111] easy to follow and an improvement over the method published by Gordon et. al.[106] The former procedure can be completed in much less time than the latter with fewer steps and under milder conditions. We produce

the same Sepharose-N-caproylgalactosamine conjugate as Allen and Neuberger[111] at significantly lower cost as unfunctionalized sepharose is used instead of sepharose containing N-hydroxysuccinimide protected 6-aminohexanoic acid. This was done by adopting the 1,1'Carbonyldiimidazole (CDI) sepharose activation procedure published by Bethel and Ayers.[112] Mild, benchtop chemistry is employed to synthesize affinity resin which consistently produces approximately 3 mg of pure SBA per gram of soy flour.

Materials and Methods

Sepharose-N-caproylgalactosamine affinity resin

Sepharose CL-4B, D-Galactosamine HCl, and 6-aminocaproic acid were from Sigma-Aldrich. 1,1'Carbonyldiimidazole, and N-(3-Dimethylaminopropyl)-N'-ethyl-carbodiimide HCl were Fluka Biochemica products. Trypsin used for LC-MS identification of SBA was SIGMA proteomics grade. All of the other solvents and buffer solutions were reagent grade material from Fisher or Sigma. The soy flour was a sample from Archer Daniels Midland. Centrifugation was done on a Sorvall RC 5B Plus centrifuge, and low pressure chromatography was monitored with an ISCO UA-6 UV/VIS detector and Type 12 optical unit.

SBA Analysis

NuPAGE® Novex Bis-Tris Gels from Invitrogen were used with the NuPAGE® Gel System for protein analysis. Staining was done with the PIERCE GelCode® Blue Stain Reagent. Protein concentration was determined with a Beckman DU-640 spectrophotometer and LC-MS/MS identification of SBA was performed with an Agilent 1100 series HPLC system on a Vydac C_{18} column with an inline 1100 series LC/MSD trap.

Results

Preparation of the Sepharose-N-caproylgalactosamine conjugate

6-Aminocaproic acid was bound to activated Sepharose CL-4B as described.[112] A moist cake (50 g) of Sepharose CL-4B was washed with sequential 200 mL washes of water, 3:7 acetone water, 7:3 acetone water, and acetone. The sepharose was suspended in 50 mL acetone. 1,1'Carbonyldiimidazole (1.2 g) was added with stirring for 15 min at RT. A solution of 14 g of 6-aminocaproic acid in 90 mL of water was prepared. After a 15 min reaction with CDI, the mixture was washed with 1 L of acetone, and the 6-aminocaproic acid solution was immediately used to transfer the activated sepharose into a round-bottomed flask, where the pH was raised to 10 with 1 M NaOH. The mixture was stirred overnight at 4°C.

Galactosamine was coupled to the carbonyl of 6-aminocaproic acid with a water soluble carbodiimide (Scheme 2-1).[111] The linker-bound sepharose was washed with 2 L of water, 1 L of 1 M NaCL and again with 2 L of water. A slurry was (125 mL) was prepared with water, and 600 mg of Galactosamine HCl was added followed by adjustment of the pH of the mixture to 5.0 with 0.1 M NaOH. A solution 300 mg of fresh N-(3-Dimethylaminopropyl)-N'-ethyl-carbodiimide HCl in 8 mL of water was prepared, and added to the slurry over 5 min, and after 10 min a pH of 5.2 was determined. The slurry was stirred for 1 hr, and then left at RT for 20 hr without stirring. The gel (30 mL, 31.2 g) was loaded into a glass column (2.5 x 10 cm) and washed successively with 3 column volumes each of 1 M NaCl, 1 M NaCl containing 100 mM Tris-HCl pH 8.6, 1 M NaCl containing 50 mM sodium formate pH 3.0, 1 M NaCl containing 100mM Tris-HCl pH 8.6, water, and PBS. The gel was then ready for use, or could be stored at 4°C in 2 M NaCl.

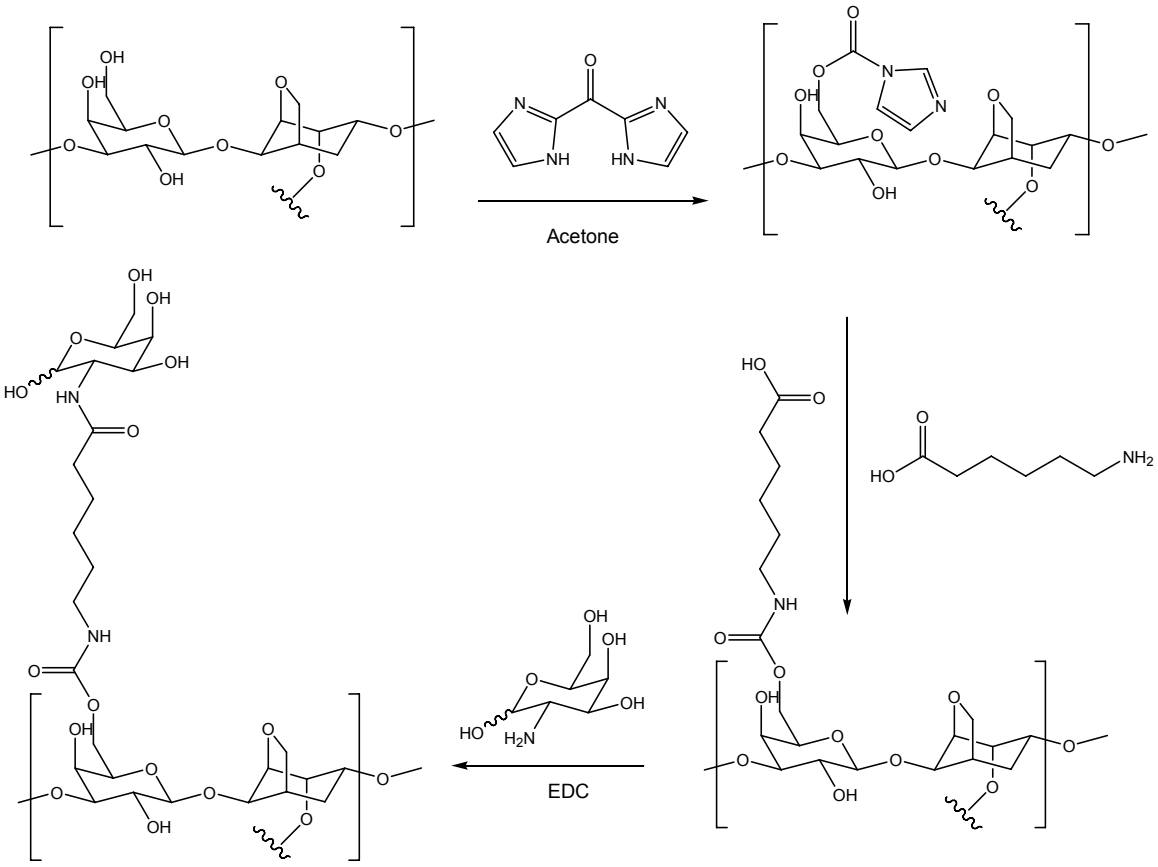

Scheme 2-1. *Synthesis of Sepharose-N-caproylgalactosamine Affinity Resin*. Sepharose CL-4B is brought up in acetone and activated with 1,1'carbonyldiimidzole. The 6-aminohexanoic acid linker is then bound, followed by galactosamine coupling with a water soluble carbodiimide.

Purification of SBA

Soy flour (10 g) was added to 200 mL of PBS and stirred overnight at 4°C. The solution was then centrifuged at 9 000 g for 15 min, and the supernatant was applied to the galactosamine affinity column at RT. The column was washed with PBS until the absorbance of the effluent was below 0.02 at 280 nm. SBA was eluted in 8 mL fractions by the addition of 30 mL of 0.2 M D-Galactose in PBS. SBA was then pooled and dialyzed in 12-14 kDa MWCO tubing for 48 hrs against running water and freeze dried. The yield was then determined by measuring absorbance at 280 nm with ε_{280} = 40, 250 M^{-1} cm^{-1} as the molar absorptivity (Figure 2-1).

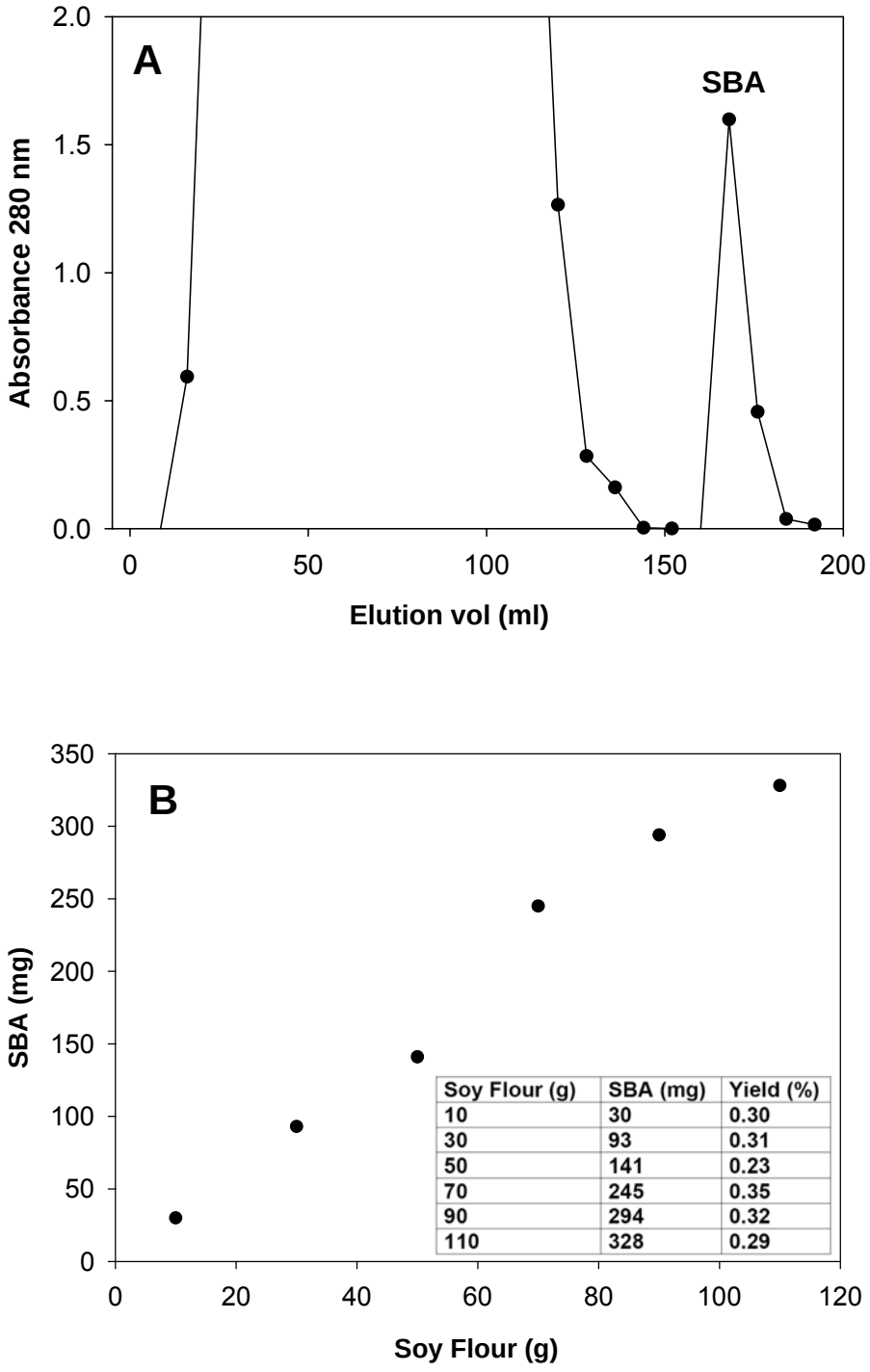

Figure 2-1. *Sepharose N-caproyl Galactosamine Affinity Column*. Soy flour is dispersed in PBS, centrifuged, and the supernatant is loaded onto a 30 mL affinity column A 200 mM galactose solution is loaded for elution. Panel A: Chromatogram of the affinity purification of 10 g of soy flour. Panel B: Galactosamine affinity column yields. The column bound 11 mg SBA per mL of resin, and the soy flour contained 3 mg SBA per gram of soy flour.

Protein Electrophoretic Analysis and LC-MS/MS Identification

The soy flour-PBS suspension, soy flour supernatant, affinity purified pool of SBA, and dialyzed SBA were analyzed by PAGE according to the NuPAGE® protocol. The PAGE gel was loaded with 6.5 µL samples and compared to a 1 µg sample of purified SBA (Figure 2-2).

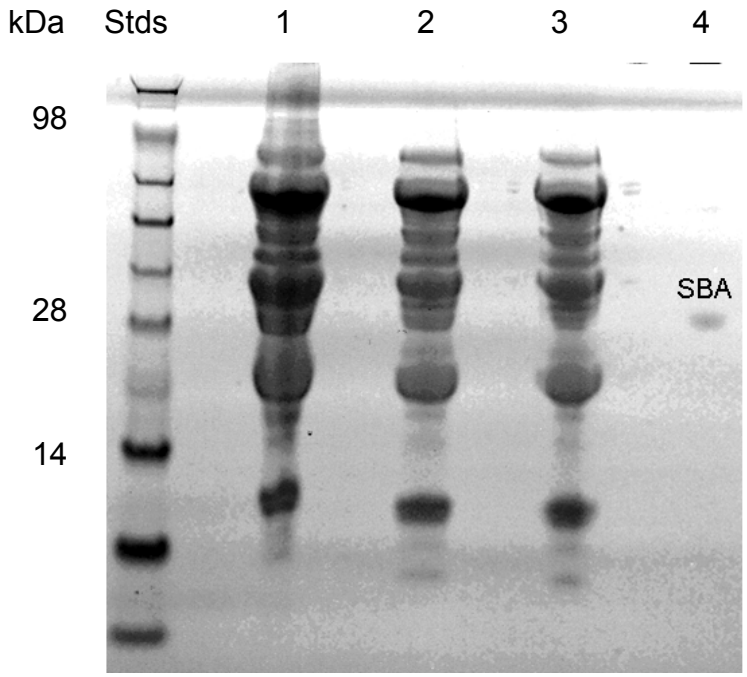

Figure 2-2. *SDS-PAGE Gel Analysis of SBA Affinity Purification* Lane 1: soy flour/PBS suspension, Lane 2: supernatant from soy flour/PBS suspension, Lane 3: unbound protein, Lane 4: purified soybean agglutinin. SBA is seen in reduced monomeric form, at 30 kDA.

To prepare a sample for LC-MS/MS identification, 1 mg of purified SBA in 40 µl H_2O was mixed with 40 µl 0.05% SDS. The sample was then heated at 95°C for 7 min Then two weight percent trypsin (SIGMA Proteomics Grade) 50 mM Tris HCl, pH 8 was

added and incubated at 37°C overnight. The digest was then freeze dried and redissolved in 0.5 mL water. A portion of the digest (75 µl, 5 nmol) was injected onto the RP-HPLC and eluted with a 10-60% acetonitrile in 0.1% acetic acid 60 min gradient, eluting at 0.7 ml/min The peaks were detected by an ESI-MS ion trap in the positive mode with 50 psi nebulizer pressure, 10 L/min dry gas flow with a source temp of 350°C (Figure 2-3). The data files were exported to the MASCOT (Matrix Science) search engine where an MS/MS Ion Search was conducted with the SwissProt database to identify SBA from peptides deconvoluted with the Agilent software (Table 2-1).

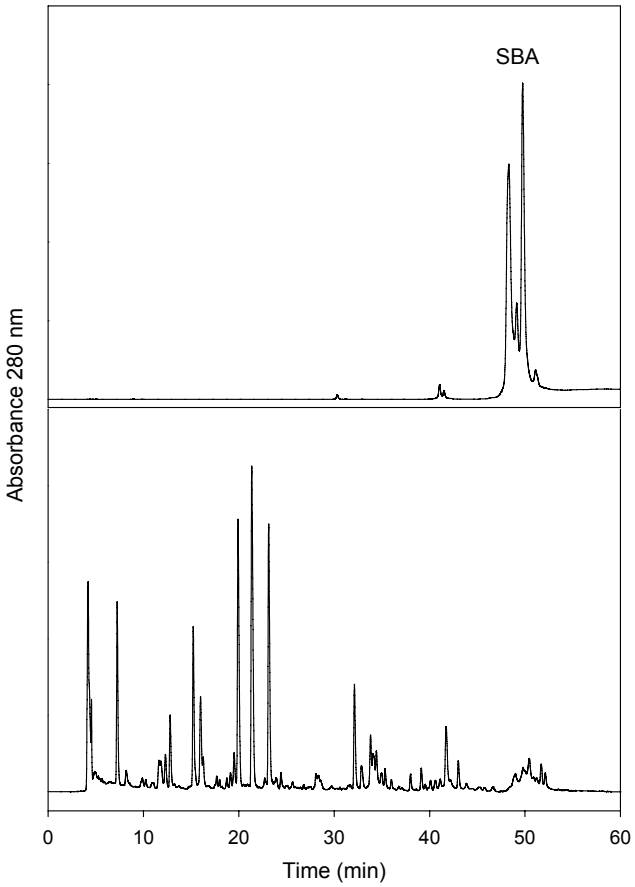

Figure 2-3. *Tryptic Digestion of SBA*. Soybean agglutinin (top panel) was digested with a 2 wt/% trypsin solution and injected on an ESI LC-MS (bottom panel).

Soybean Agglutinin Mass: 30,909		
Observed Mass (m/z)	Calculated Mass (g/mol)	Peptide
988.10	986.52	K.TSLPEWVR.I
1150.43	1148.55	K.TTSWDLANNK.V
1304.28	1302.70	R.TSNILSDVVDLK.T

Table 2-1. *Mascot MS/MS Ion Identification.* Three peptides were identified in the MS/MS ion search of the tryptic digest. SBA had the highest probability-based Mowse score of all the proteins identified by the deconvolution algorithm.

Discussion

The N-caproylgalactosamine affinity column described here purified 328 mg of SBA from 110 g of soy flour. The experimentally determined resin capacity of 11 mg/ml is close to the previously reported 12 mg/mL capacity. [111] While loading 120 g soy flour would likely have yielded 360 mg SBA at a capacity of 12 mg/mL, loading 130 g soy flour clogged the column on two occasions.

The affinity resin used here is essentially the same as that described by Allen and Neuberger[111], however, we activate our resin to covalently link 6-aminohexanoic acid using 1, 1'carbonyldiimidazole, thereby lowering the cost of synthesis several fold. CDI activation results in a greater number of linker functional groups to the resin compared to cyanogen bromide activation. This is because the imidazole carbamate is the sole reaction product, while CNBr activation produces isourea, carbamate and carbonate products of varying reactivity.[113] Also, when using CDI, N-hydroxysuccinimide activation of 6-aminohexanoic acid is unnecessary, since the amide bond between the acid and Galactosamine is formed directly with the water soluble carbodiimide. Acetone is the only organic solvent needed, and the series of reactions are completed in two days under mild conditions and with basic laboratory equipment. We have made 500 milliliters of the affinity resin by this method for gram scale purification of SBA.

CHAPTER 3

ENZYMATIC RELEASE OF $MAN_9GLCNAC_2ASN$ FROM SOYBEAN AGGLUTININ AND DERIVITIZATION OF $MAN_9GLCNAC_2ASN$ ANALOGS

Introduction

Glycans are often integrated into drug delivery vehicles as bioactive ligands to confer target recognition and specificity, or to impart structural stability and integrity in *in vivo*. They are also applied to take advantage of intrinsic pharmacological properties. They have been shown to posses immuno modulatory, anti-tumor, anti-inflammatory, anti-coagulant, hypoglycemic, and antiviral activity.[114]

In our laboratory we have constructed non-viral gene delivery vectors containing either Man_9 N-glycan, or Triantennary N-glycan, for selective *in vivo* targeting to the liver; to the mannose receptor on Kuppfer cells or the asialoglycoprotein receptor on hepatocytes.[110,115]

In the present study we sought to improve the design of the high mannose targeted gene delivery vector. This chapter describes a greatly improved method of proteolytic release of Man_9 from affinity purified SBA. To endow this N-glycan with affinity for DNA we attached Acridine to the Asn residue on the reducing end of the oligosaccharide. This was achieved by preparing 6-(9-Acridinylamino) hexanoic acid. [116] The acridine acid was converted to an NHS ester via DCC coupling and used to make two novel $Man_9GlcNAc_2Asn$ analogs; $Man_9GlcNAc_2Asn$-Acridine, and $Man_9GlcNAc_2Asn$-Tyrosine Acridine. $Man_9GlcNAc_2Asn$-Acr was the more efficient acridinylated compound from a synthetic and purification standpoint, however as demonstrated, it displayed weak binding affinity for plasmid DNA.

Materials and Methods

Liquefied phenol was from J.T. Baker, and the concentrated sulfuric acid was a Fisher Scientific reagent. D_2O was from Cambridge Isotope Laboratories. NuPAGE® Novex Bis-Tris Gels from Invitrogen were used with the NuPAGE® Gel System for protein analysis. SDS PAGE gel staining was done with PIERCE GelCode® Blue Stain Reagent. The Sephadex G-50 resin was from Amersham Biosciences. The AG 50W-X2 cation exchange resin was from Bio-Rad. The centrifuge was an IEC HN-SII, and the freeze dry system was a Labconco Freezone 4.5 with a centrivap concentration accessory. An ISCO UA-6 UV/VIS detector and Type 12 optical unit were used to monitor the eluate during gel filtration and ion exchange chromatography. A Milton Roy Spectronic 20D was used for colorimetric detection in the phenol sulfuric assay. The MALDI-TOF was a Bruker Biflex III, and the NMR spectrometer was a 600 MHz Bruker Oxford AS600.

Pronase was a *BioChemika* product from Sigma-Aldrich. Tris, pyridine, acetic acid, and trifluoroacetic acid were certified ACS grade Fisher reagents or an equivalent.

Boc-Tyrosine N-hydroxysuccinimide was a *Chemika* reagent from Sigma-Aldrich. Sodium bicarbonate and N,N-dimethylformamide (DMF) were Fisher reagents.

The 9-Chloroacridine (97%) was a Sigma-Aldrich product, the solid phenol was a Riedel-de-Haën product (ACS grade) through Sigma-Aldrich. The sodium hydroxide pellets were a Mallinckrodt product through Fisher Scientific. The N,N-Dimethylformamide and anhydrous ethyl ether were Fisher reagents, and the 95% ethanol was a USP reagent from the university Biochemistry store. The N-hydroxysuccinimide (NHS) was a Sigma-Aldrich product, and the N,N'-Dicyclohexylcarbodiimide (DCC) was a Fluka product through Sigma-Aldrich. NMR spectra were taken with a 300 MHz Bruker NMR.

The 0.1% Agarose gel was made with agarose from GIBCO, Tris and Boric acid from Fisher Scientific, and EDTA from Sigma-Aldrich. SEAP plasmid was obtained from the Promega corporation. The Ethidium bromide stock solution was from Bio-Rad.

Enzymatic Digestion of SBA

Affinity purified SBA (600 mg) was freeze dried and brought up in 8 mL of 100 mM HCl. The protein was then denatured at 50°C for 15 min The pH was raised to 8.5 with 600 μL 1M NaOH resulting in the formation of a gel. The SBA gel was dissolved by adding 2 ml of water and 100 μL 2M NaOH followed by the addition of 7 mg of pronase in 2 ml of 30 mM $CaCl_2$ in 50 mM Tris pH 8.5. The digestion was carried out for 24 hours at 37°C, after which an additional 5 mg of pronase in 1 mL of Tris was added, and the digestion continued for an additional 24 hr period.

Low Pressure Chromatographic Purification of $Man_9GlcNAc_2Asn$

The digested SBA (3 μg) was loaded on a PAGE gel to verify digestion. The digest was centrifuged at 4000 g for 8 min, and the supernatant was freeze dried. The centrifugation and lyophilization were repeated, and the sample was brought up in 1.5 ml water. An aliquot was analyzed by phenol sulfuric assay,[117] a colorimetric assay for carbohydrates. The 490 nm absorbance was converted to estimate mannose content using the conversion of 1 AU = 18.5 nmol Man_9. Man_9 was quanified throughout the purification. Approximately 15 μmol of Man_9 (from 20 μmol digested) was recovered. The pronase digest was applied to Sephadex G-50 resin in a column (1.5 x 170 cm) and eluted with 10 mM acetic acid. The eluant was collected in 8.5 mL fractions, with detection by absorbance at 280 nm and by assaying fractions with PSA. The carbohydrate containing fractions (200 mL) were pooled, concentrated by roto-evaporation, freeze-dried, and brought to 1.5 ml. The PSA was used to determine that 14.1 μmol were recovered from the first gel filtration column. The gel filtration was

repeated, and the glycan containing fractions were pooled, dried, and brought up in 1.5 mL for polishing on a cation exchange column. The PSA recovery at this point was 11.7 μmol.

The Man_9 was applied to a cation exchange column (1.5 x 50 cm) and eluted with pyridine/acetic acid, pH 3.2. The glycan (1.1 L) was pooled, dried, and brought up in 1.5 mL. Total recovery was determined to be 6.7 μmol by PSA, a 45% overall yield.

A 2 nmol sample of Man_9Asn was analyzed by MALDI-TOF with a super-DHB matrix in linear mode. Likewise, a 1 mM sample in D_2O with an acetone internal standard was analyzed by NMR.

$Man_9GlcNAc_2Asn$ Tyrosine Analogs

$Man_9GlcNAc_2Asn$ (500 nmol) was freeze dried and reconstituted in 300 μl DMF. Boc Tyrosine NHS (5 μmol) was brought up in 200 μl of DMF, added to Man_9Asn and reacted for 3 hr. The reaction was loaded onto Sephadex G-25 resin in a 1.5 x 50 cm glass column, eluting with a 10 mM acetic acid mobile phase, detecting by absorbance at 280 nm. The derivatized Boc-$Man_9GlcNAc_2Asn$-Tyr (50 ml) was pooled, dried, reconstituted in water, and analyzed by UV/VIS and HPLC ESI-MS. The yield was determined by measuring tyrosine absorbance at 274 nm with a molar absorptivity of 1400 $M^{-1}cm^{-1}$. The purity and identity of Boc-$Man_9GlcNAc_2Asn$-Tyr was determined by RP-HPLC. The sample was analyzed on an 1100 series Agilent HPLC with a GraceVydac C_{18} column (0.46 x 25 cm) and an inline 1100 series LC/MSD trap, eluting with 1-30% ACN in 0.1% TFA over 30 min, while detecting in negative mode. The yield was quantitative and no contaminating peaks were visible in the chromatogram.

Boc-$Man_9GlcNAc_2Asn$-Tyr (253 nmol) was freeze dried and reconstituted with 150 μl of 95% TFA for 5 min The de-protection reaction was then quenched on dry ice, and dried by speedvac for 1 hr. The compound was reconstituted with 1 mL of water, and a quantitative yield was determined by UV/VIS. The derivatized glycan was then

analyzed for purity on an ISCO HPLC system with a Vydac C_{18} column and a model 2360 gradient programmer, model 2350 pump, and a V^4 absorbance detector. The gradient was the same as used in the previous analysis. The $Man_9GlcNAc_2Asn$-Tyr chromatograms were free of contaminating peaks.

Synthesis of the 6-(Acridin-9-ylamino)-hexanoic acid 2,5-dioxo-pyrrolidin-1-yl-ester

Sodium hydroxide (720 mg) was added to 12 g of phenol, and heated with stirring at 100°C. 9-Chloroacridine (2.8 g) was added, and the reaction continued for 1.5 hrs. The heat was removed, and 100 mL of 2N NaOH was added. The mixture was stirred briefly, and left at RT for 24 hrs, after which the precipitate was collected by filtration, washed with water, and dried. The reaction yielded 3.4 g (95%) 9-Phenoxyacridine, which had a m.p. of 123-124°C. (300 MHz, DMSO-d_6): δ = 8.23 (d, 2H), 8.03 (d, 2H), 7.86 (t, 2H), 7.56 (t, 2H), 7.29 (t, 2H), 7.08 (t, 1H), 6.87 (d, 2H).

9-Phenoxyacridine (1.5 g) was added to 3 g of phenol under an argon atmosphere and stirred at 50°C. After the solid was in solution, 6-aminocaproic acid (725 mg) was added and the temperature was increased to 100°C for 6 hr. The reaction was cooled to 50°C, 25 mL ethyl ether was added with vigorous stirring and the precipitant was collected on filter paper, washed with ethyl ether, ethanol, and water, and dried overnight. The reaction yielded 1.59 g (94%) 6-(9-Acridinylamino) hexanoic acid, which had a m.p. of 192°C. (300 MHz, CF_3CO_2D): δ = 8.39 (d, 2H), 7.99 (dd, 2H), 7.63 (dd, 2H), 7.26 (br, 2H), 4.28 (t, 2H), 2.60 (tri, 2H), 2.13 (qui, 2H), 1.89 (m, 4H)

6-(9-Acridinylamino) hexanoic acid (25 mg), DCC (16 mg), and NHS (13 mg) were combined and brought into DMF (2 mL) with stirring. After 24 hrs, the reaction was centrifuged and the supernatant was collected. The ester was then analyzed by HPLC and used *in situ*.

Synthesis of the $Man_9GlcNAc_2Asn$ Acridine Analogs

$Man_9GlcNAc_2Asn$ (1 μmol) was prepared and brought up in 250 μl of 100 mM $NaHCO_3$. 6-(9-Acridinylamino) hexanoic acid 2,5-dioxo-pyrrolidin-1-yl-ester (10 μmol) in 250 μL DMF was added to the glycan and stirred for 24 hrs. The reaction was loaded onto a Sephadex G-25 column (1.5 x 50 cm), and eluted with 0.1% acetic acid while detecting by absorbance at 280 nm. The $Man_9GlcNAc_2Asn$-Acr was then pooled, concentrated, and quantified by absorbance via acridine ($\varepsilon_{409\ nm} = 9266\ M^{-1}\ cm^{-1}$), resulting in the recovery of 945 nmol (95%) yield. $Man_9GlcNAc_2Asn$-Acr was analyzed for purity by RP-HPLC by injecting 1 nmol while eluting with a gradient of 1-30% acetonitrile in 0.1% TFA over 30 min, with ESI-MS in the negative mode.

$Man_9GlcNAc_2Asn$-Tyr (200 nmol) was prepared and brought up in 50 μl 100 mM $NaHCO_3$. 6-(9-Acridinylamino) hexanoic acid 2,5-dioxo-pyrrolidin-1-yl-ester (2 μmol) in 50 μL DMF was added and reacted for 24 hrs. The reaction product was purified by Sephadex G-25 as described above. The product was analyzed for purity by analytical RP-HPLC and determined to 83%, with an isolated yield of 107 nmol (54%).

$Man_9GlcNAc_2Asn$-Acridine - Plasmid DNA Binding: The Band Shift Assay

Six experimental samples were made adding SEAP plasmid DNA (0.6 μg) to 0.03, 0.32, 3, 8, 16, and 32 nmol Man9GlcNAc2Asn-Acr. Each sample was incubated for 30 min and loaded into an agarose gel. The gel was electrophoresed with an 80V electric field for 90 min and stained overnight at 4°C with 200 ml 0.1 μg/μl ethidium bromide. The gel was analyzed with a UVP Dual Intensity Ultraviolet Transilluminator and a Fisher Electrophoresis photodocumentation system.

Results

Enzymatic Digestion of SBA and Chromatographic Purification of $Man_9GlcNAc_2Asn$

Affinity purified SBA was digested with 2 wt % pronase solution for 48 hours, followed by purification by low pressure gel filtration and ion exchange chromatography, as in Lis and Sharon (Figure 3-1).[118]

The digestion was monitored by determining the loss of protein bands on SDS-PAGE to establish reaction completion. The SBA digest was fractionated as a glycopeptide. The glycopeptide lacked 280 nm absorbance but could be detected by performing a phenol sulphuric assay specific for detecting monosaccharides and oligosaccharides (Figure 3-2). While gel filtration enriched the glycopeptide, there was still significant protein and peptide contamination. The $Man_9GlcNAc_2Asn$ was further enriched by a second gel filtration purification followed by a cation exchange column (Figure 3-3). The final column step led to $Man_9GlcNAc_2Asn$ that was substantially free of peptide. MALDI-TOF analysis indicated the purified Man_9 possessed two major ions, corresponding to the mono and di-sodium adducts (Figure 3-4). Further confirmation of the proposed structure was obtained by high field NMR. By comparison with the chemical shifts and coupling constants from previously indentified $Man_9GlcNAc_2Asn$, [119,105] it was possible to make assignments for most of the anomeric protons (Figure 3-5). Most importantly, the chemical shifts of the D1-D3 residues were identified with chemical shifts of 5.04, 5.05, and 5.03 ppm.

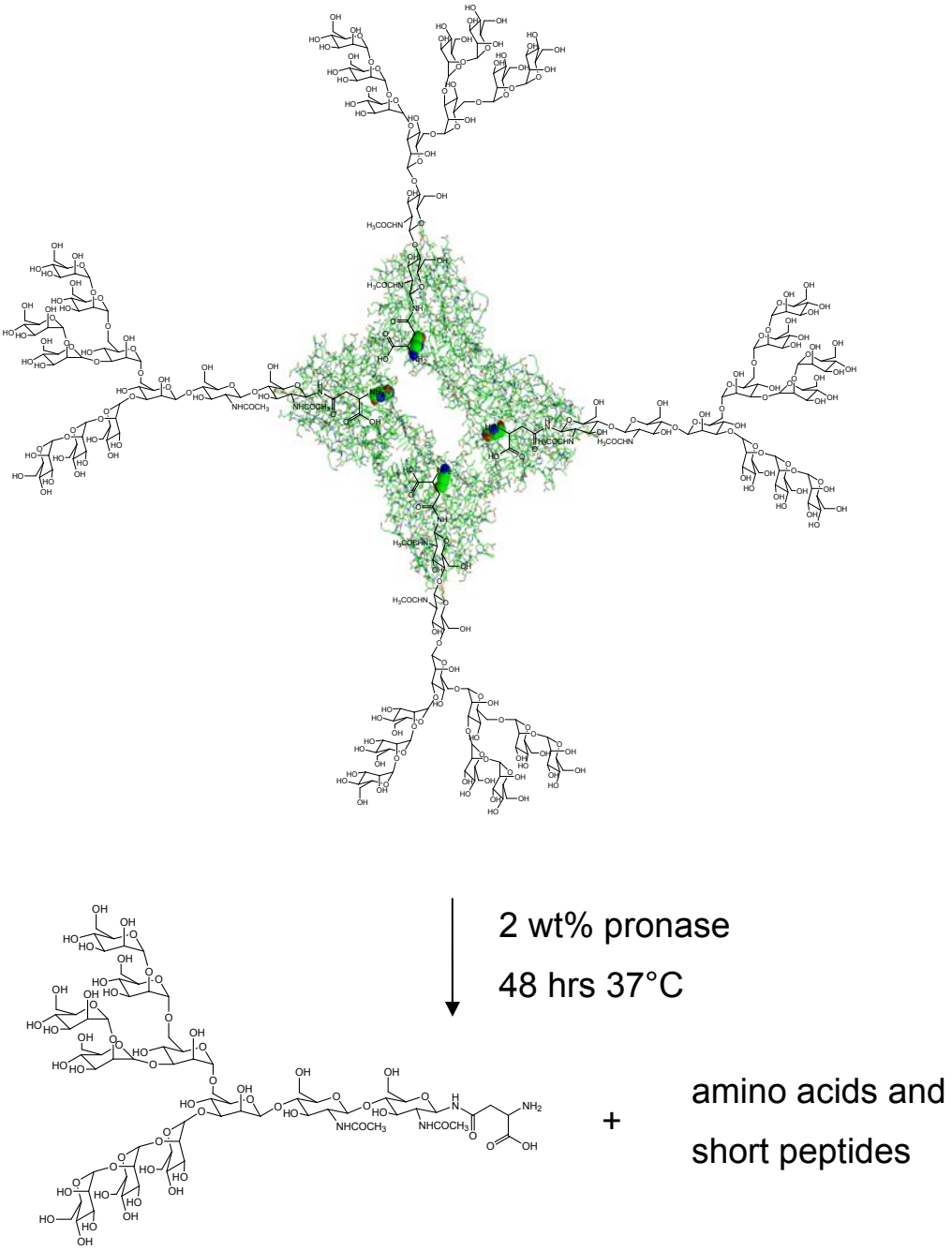

Figure 3-1. *SBA Digestion by Pronase*. Pronase, an enzyme preparation from *Streptomyces griseus*, with three proteolytic activities and a wide range of substrate specificity digests the SBA glycoprotein allowing isolation of the glycan.

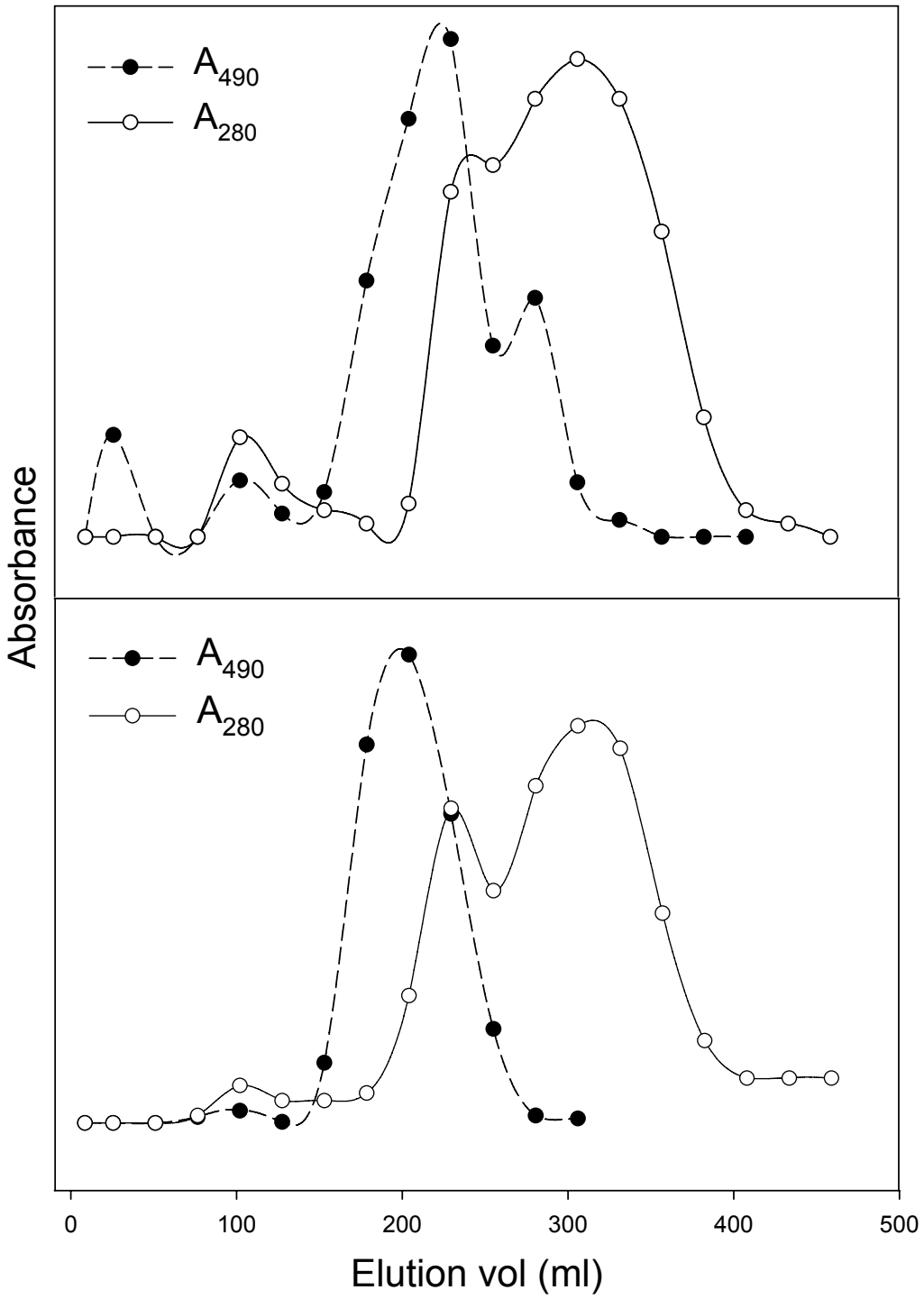

Figure 3-2. *Gel Filtration of the SBA Pronase Digest*. Mobile phase was 10 mM acetic acid, with UV peptide and amino acid detection at 280 nm and carbohydrate detection at 490 nm by the phenol sulfuric acid assay.

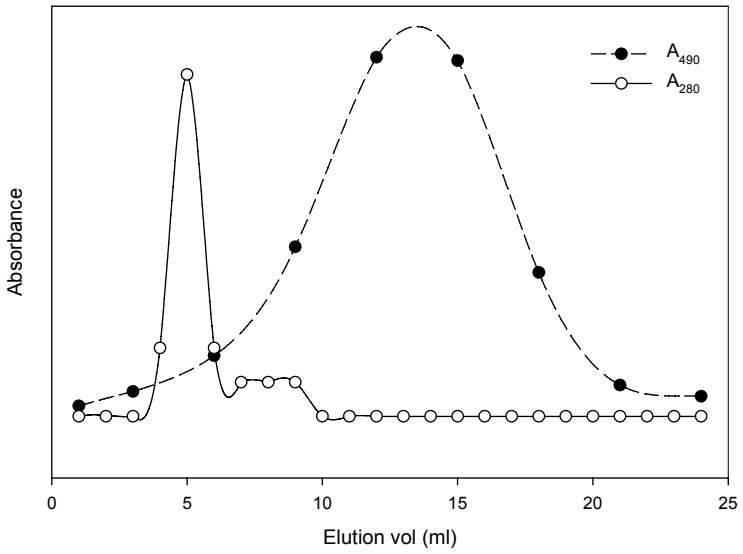

Figure 3-3. *Cation Exchange Purification of $Man_9GlcNAc_2$.* $Man_9GlcNAc_2Asn$ binds weakly to the cation resin through its Asn residue. The contamination peak with 280 nm absorbance contains peptides with a pI below 3.2.

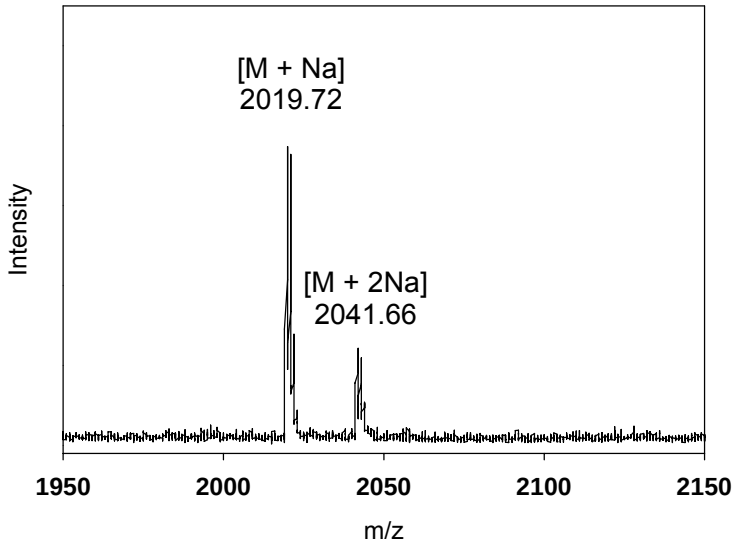

Figure 3-4. *MALDI-TOF Analysis of Purified $Man_9GlcNAc_2Asn$*. The glycan was ionized with a super 2,5 DHB matrix and analyzed in reflectron mode with. It was identified with sodium atoms adducted.

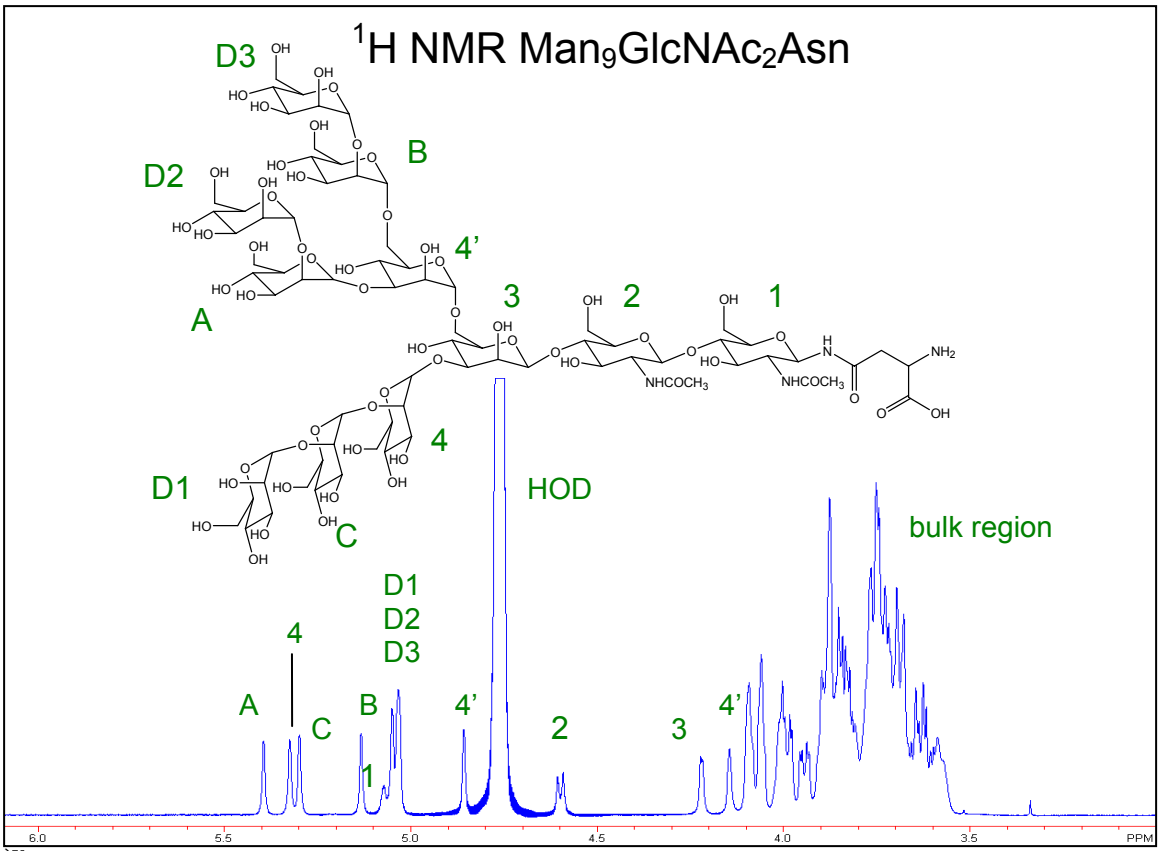

Figure 3-5. *600 MHz ^{1}H NMR of Man$_9$GlcNAc$_2$Asn.* Spectra taken with a 1 mM sample in D_2O. The numbers and letters in the spectrum correspond to the monosaccharide residues in the structure. A large signal corresponding to the unexchanged proton of HOD can be seen at 4.7 ppm.

Man$_9$GlcNAc$_2$Asn Tyrosine Analogs

We have previously developed N-glycans for receptor targeting in non-viral gene delivery by incorporation of tyrosine.[120] The phenyl group confers absorption at 280 nm and provides a site for ^{125}I iodination; which facilitates *in vivo* biodistribution studies. When a Boc-protected tyrosine is used and Boc is removed, the 1° amine can be further derivatized, typically with a peptide which will condense DNA. In past years the laboratory has produced tyrosinamide Man$_9$ from Man$_9$GlcNAc$_2$ obtained through preparative hydrazinolysis of semi purified SBA.[119] The tyrosinamide Man$_9$ analogs in the following pages were produced through a more efficient process, from affinity

purified SBA and enzymatically released $Man_9GlcNAc_2Asn$. Additionally, no HPLC purification was employed, and the products were isolated via low pressure gel filtration chromatography.

Boc-protected $Man_9GlcNAc_2Asn$ Tyrosine was prepared by reaction of $Man_9GlcNAc_2Asn$ and a 10-fold excess of Boc-Tyrosine N-hydroxysuccinimide. After the reaction was complete, the product was isolated with a Sephadex G-25 column, which sufficiently separated the derivatized product from excess reagent (Figure 3-6). The eluting Boc-$Man_9GlcNAc_2Asn$-Tyr fractions were pooled, concentrated, and freeze dried prior to analysis by NMR and HPLC-MS. The upfield signals coming from the Boc group can be clearly seen. Two doublets in the aromatic region resulting from tyrosine are visible as well (Figure 3-7). The de-protected Man_9 was prepared in water and analyzed as described above. The loss of Boc resulted in a loss of 100 mass units and a distinct 13 min shift in retention time on the LC-MS chromatogram, as the compound became distinctly more hydrophilic (Figure 3-8).

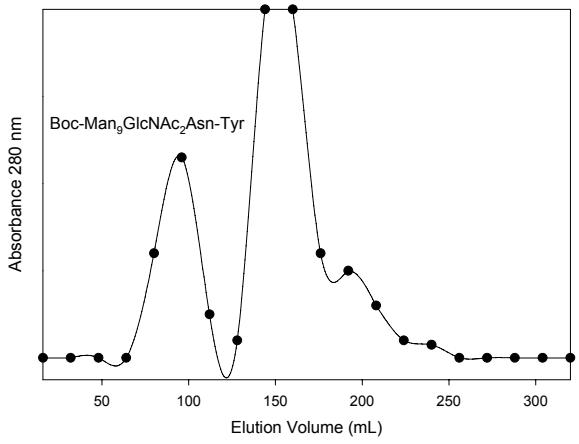

Figure 3-6. *Gel Filtration Purification of Boc-$Man_9GlcNAc_2Asn$-Tyr*. The reaction mixture was loaded onto a gel filtration column containing Sephadex G-25 resin and eluted with 0.1% acetic acid. The Man_9 tyrosinamide was separated from the excess Boc-tyrosine-NHS reagent.

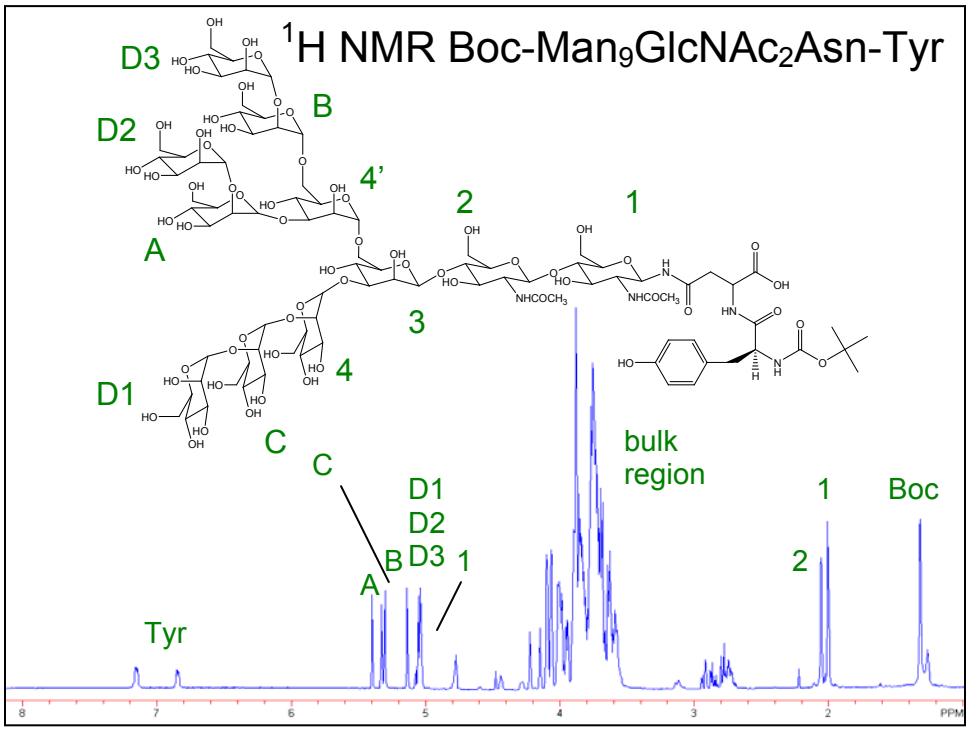

Figure 3-7 *600 MHz ^{1}H NMR of Boc-Man$_9$GlcNAc$_2$Asn*. Spectra taken with a 1 mM sample in D_2O. The numbers and letters in the spectrum correspond to the monosaccharide residues in the structure. HOD was suppressed. The shift equivalent signals corresponding to the methyl protons of the Boc group are seen furthest upfield. The pair of doublets from tyrosine's phenyl ring appear downfield in the aromatic region. The '1' and '2' signals immediately downfield of Boc correspond to the protons on the N-acetyl groups.

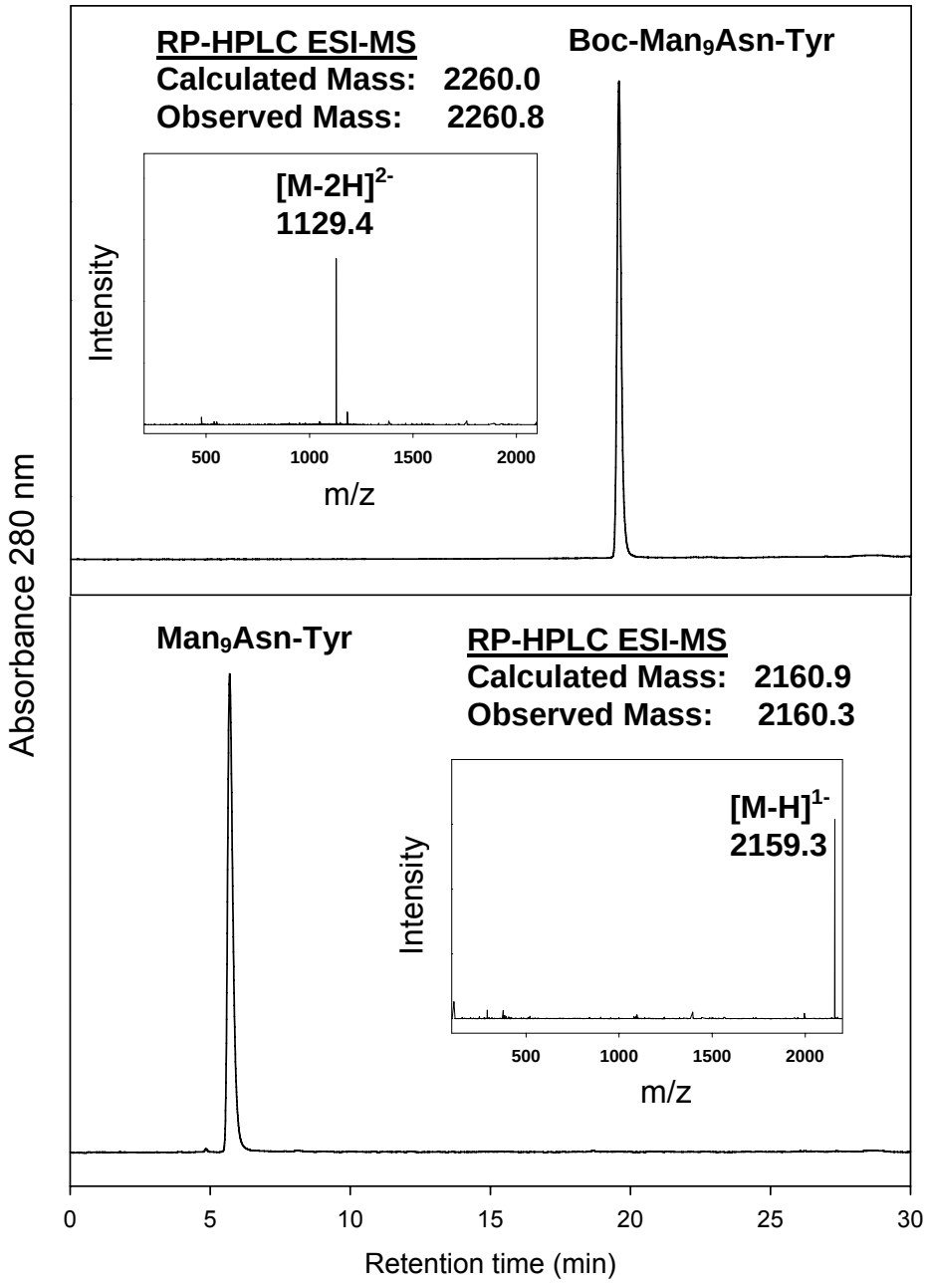

Figure 3-8. *Characterization of $Man_9GlcNAc_2Asn$ Tyrosinamide Analogs*. The Boc protected and de-protected compounds were analyzed by HPLC on a 1-30% ACN in 0.1% TFA gradient over 30 mins, and infused into an in-line ESI-MS detecting in negative mode.

Synthesis of the 6-(Acridin-9-ylamino)-hexanoic acid 2,5-dioxo-pyrrolidin-1-yl-ester

To investigate a novel method of reversibly attaching Man_9 to plasmid DNA, we began by attaching a single acridine to the N-glycan. This was accomplished by first synthesizing the 6-(9-Acridinylamino)-hexanoic acid ester.

The synthetic procedure described by Karup et. al.[116, 121] was followed to produce the acid, as indicated below (Scheme 3-1). Subsequent activation of the acid to the NHS ester was accomplished with DCC. Proton NMR was used to characterize the 9-phenoxyacridine and 6-(9-Acridinylamino)-hexanoic acid intermediates (Figure 3-9). The six aromatic signals seen in the 9-phenoxyacridine spectrum were essentially the same as those recorded in the literature. Likewise, the chemical shifts seen in 6-(9-Acridinylamino)-hexanoic acid spectra matched the literature, although minor impurities were present (Table 3-1).

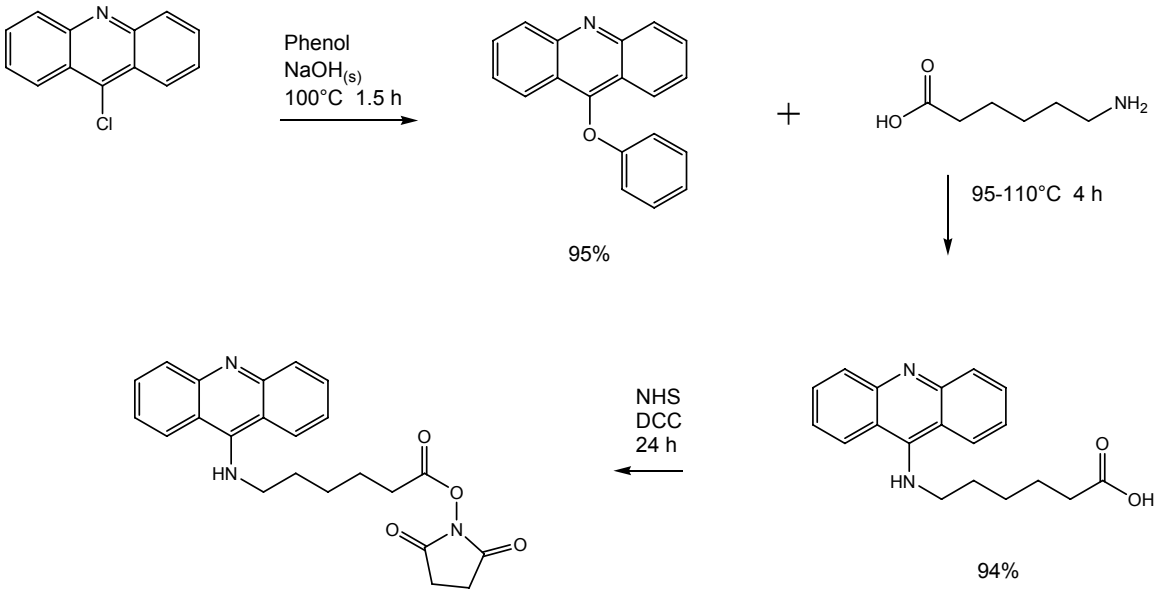

Scheme 3-1 *Synthesis of the Acridine Ester*. The literature procedure of Karup et. al. was adopted to make 6-(9-Acridinylamino)-hexanoic acid. The acid was converted into the ester with DCC.

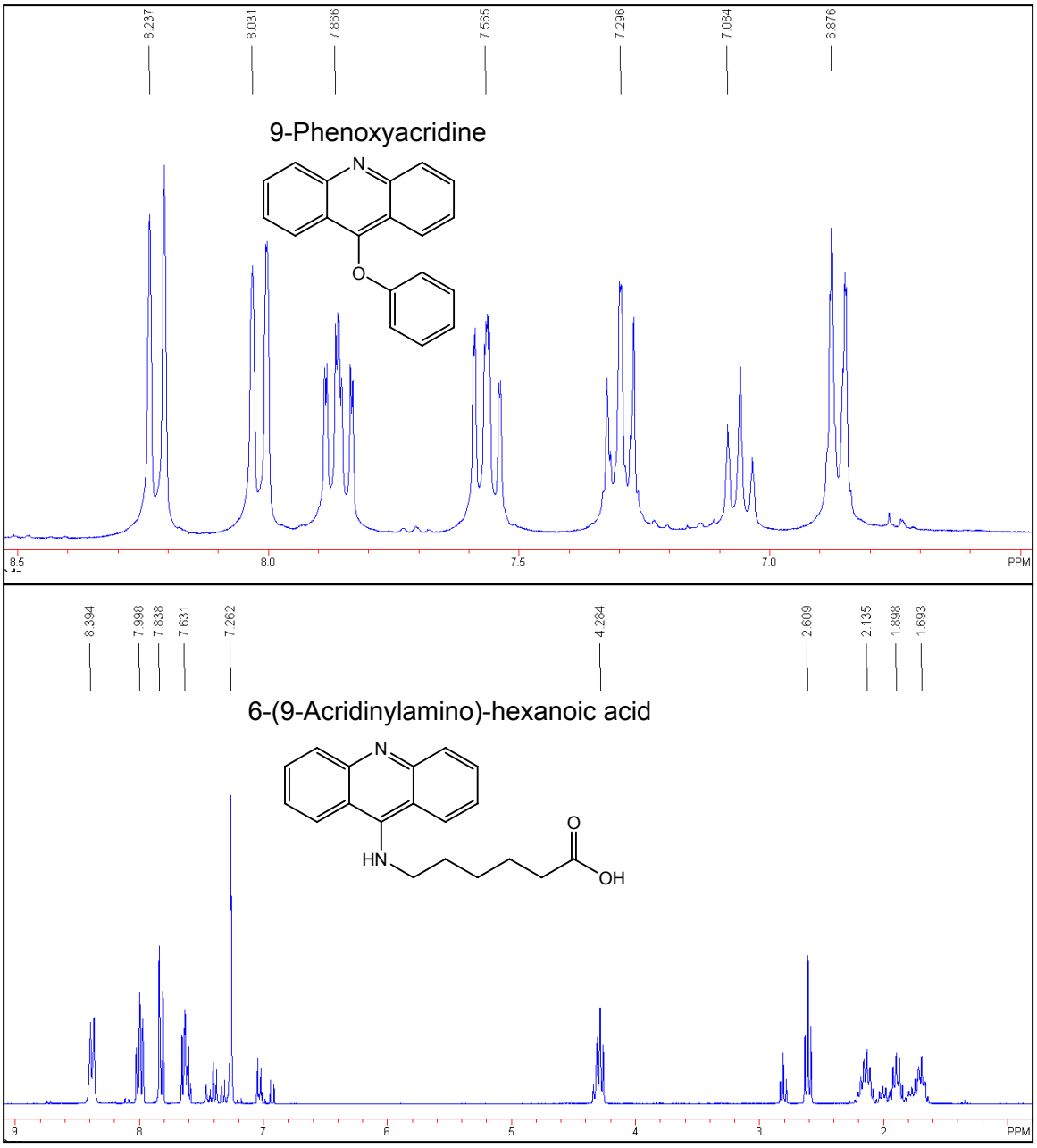

Figure 3-9. *300 MHz ^{1}H NMR Characterization of 9-Phenoxyacridine and 6-(Acridin-9-ylamino)-hexanoic acid*. Phenoxyacridine in DMSO-d_6 , Acridine acid in CF_3CO_2D.

	^{1}H NMR δ
9-Phenoxyacridine	8.23 (d, 2H), 8.03 (d, 2H), 7.86 (t, 2H), 7.56 (t, 2H), 7.29 (t, 2H), 7.08 (t, 1H), 6.87 (d, 2H),
6-(Acridin-9-ylamino)-hexanoic acid	8.39 (d, 2H), 7.99 (dd, 2H), 7.67 (dd, 2H), 7.26 (br, 2H), 4.28 (t, 2H), 2.60 (t, 2H) 2.13 (qui, 2H), 1.79 (m, 4H)

Table 3-1. *300 MHz ^{1}H NMR Chemical Shift Data for 9-Phenoxyacridne and 6-(Acridin-9-ylamino)-hexanoic acid*

9-Phenoxyacridine (3 nmol) was prepared in methanol and analyzed with a 30 min 30-60% acetonitrile in 0.1% TFA gradient (Figure 3-10). The compound was monitored at 280 nm, but was also visible at 409 nm. The four phenyl rings in the structure confer hydrophobicity, and it elutes at approximately 40% acetonitrile under these gradient conditions. The synthesized 9-phenoxyacridine was 86% pure without silica purification, and was used directly to synthesize the 6-(9-Acridinylamino)-hexanoic acid.

6-(9-Acridinylamino)-hexanoic acid (2 nmol) and 6-(9-Acridinylamino)-hexanoic ester (2 nmol) were prepared in DMF and analyzed with a 30 min 15-45% acetonitrile in 0.1% TFA gradient (Figure 3-11). These compounds were also analyzed without purification, and were 99% and 83% pure, respectively. Conversion of the acid functional group to the more hydrophobic ester moiety resulted in a five minute shift in retention time.

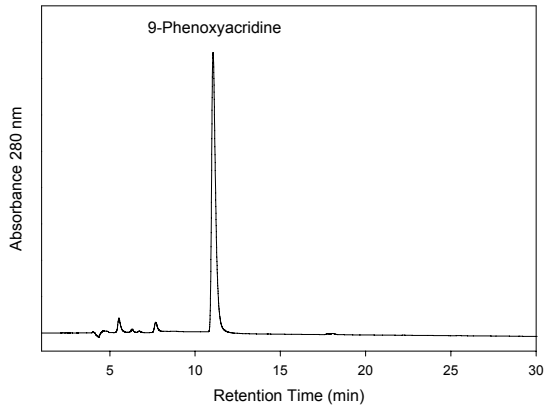

Figure 3-10. *RP-HPLC of 9-Phenoxyacridine*. A 3 nmol sample of 9-phenoxyacridine was analyzed with a 30-60% ACN in 0.1% TFA 30 min gradient.

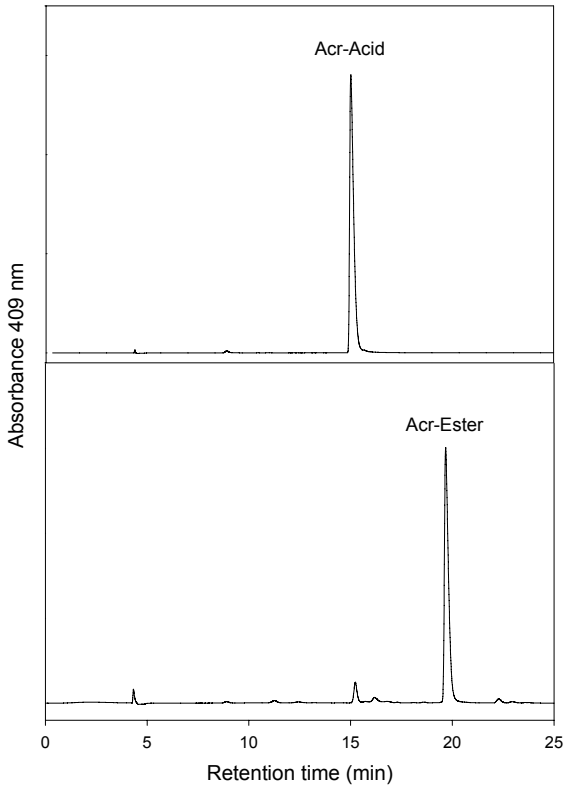

Figure 3-11. *RP-HPLC Characterization of Acridine Acid and Acridine Ester*. Acridine acid (2 nmol) and acridine ester (2 nmol) were analyzed on a 30 min 15-45% ACN in 0.1% TFA 30 min gradient. The conversion of the acid moiety to more hydrophobic ester results in an increase in retention time.

Synthesis of the $Man_9GlcNAc_2Asn$ Acridine Analogs

Two Man_9 Acridine compounds were made with the acridine ester. The first compound was $Man_9GlcNAc_2Asn$ directly derivatized with the acridine ester. The second was $Man_9GlcNAc_2Asn$-Tyr derivatized with the ester. In both reactions, a 10-fold excess of the ester was used, and the product was purified by gravity-fed gel-filtration chromatography (Figure 3-12). However, additional preparative HPLC purification was employed for the $Man_9GlcNAc_2Asn$-TyrAcr.

Both compounds were analyzed by HPLC on 30 min 1-30% acetonitrile in 0.1% TFA gradients and characterized by ESI-MS in the negative mode (Figure 3-13 and 3-14). Each displayed an observed mass which was within 1 mass unit of the calculated mass. The derivatized glycans were also analyzed by high field nmr, and characteristic anomeric proton shifts were noted (figs. 3-13 and 3-14).

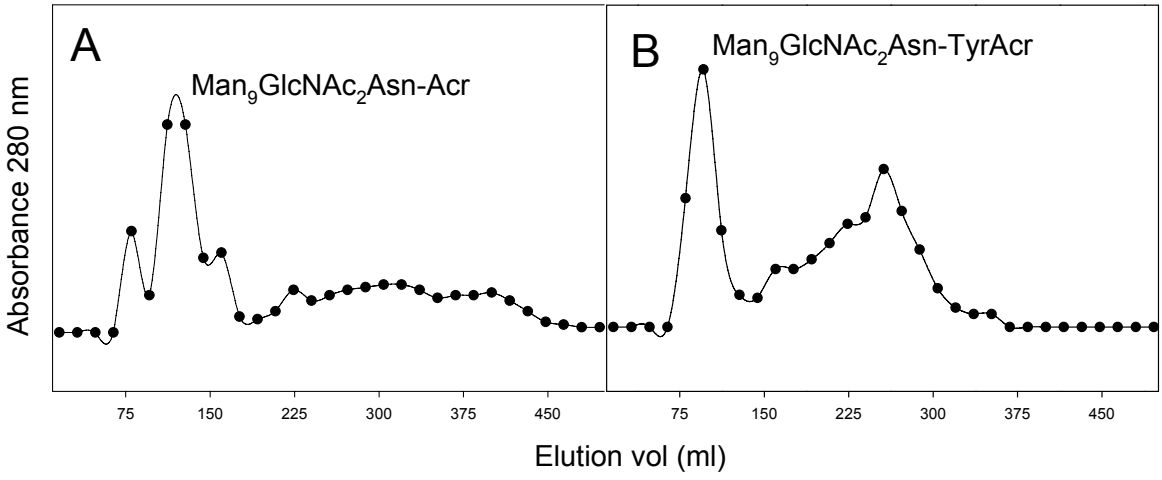

Figure 3-12. *Gel Filtration Purification of $Man_9GlcNAc_2Asn$-Acr and $Man_9GlcNAc_2Asn$-TyrAcr*. For each analog, the reaction mixture was loaded onto a gel filration column containing sephadex G-25 resin and eluted with 0.1% acetic acid. The derivatized glycan is separated from excess Acr-NHS reagent. **A.** The $Man_9GlcNAc_2Asn$-Acr had an unusal elution profile, however the entire 100 ml elution volume was collected. **B**. The $Man_9GlcNAc_2Asn$-TyrAcr eluted from the column in 50 ml.

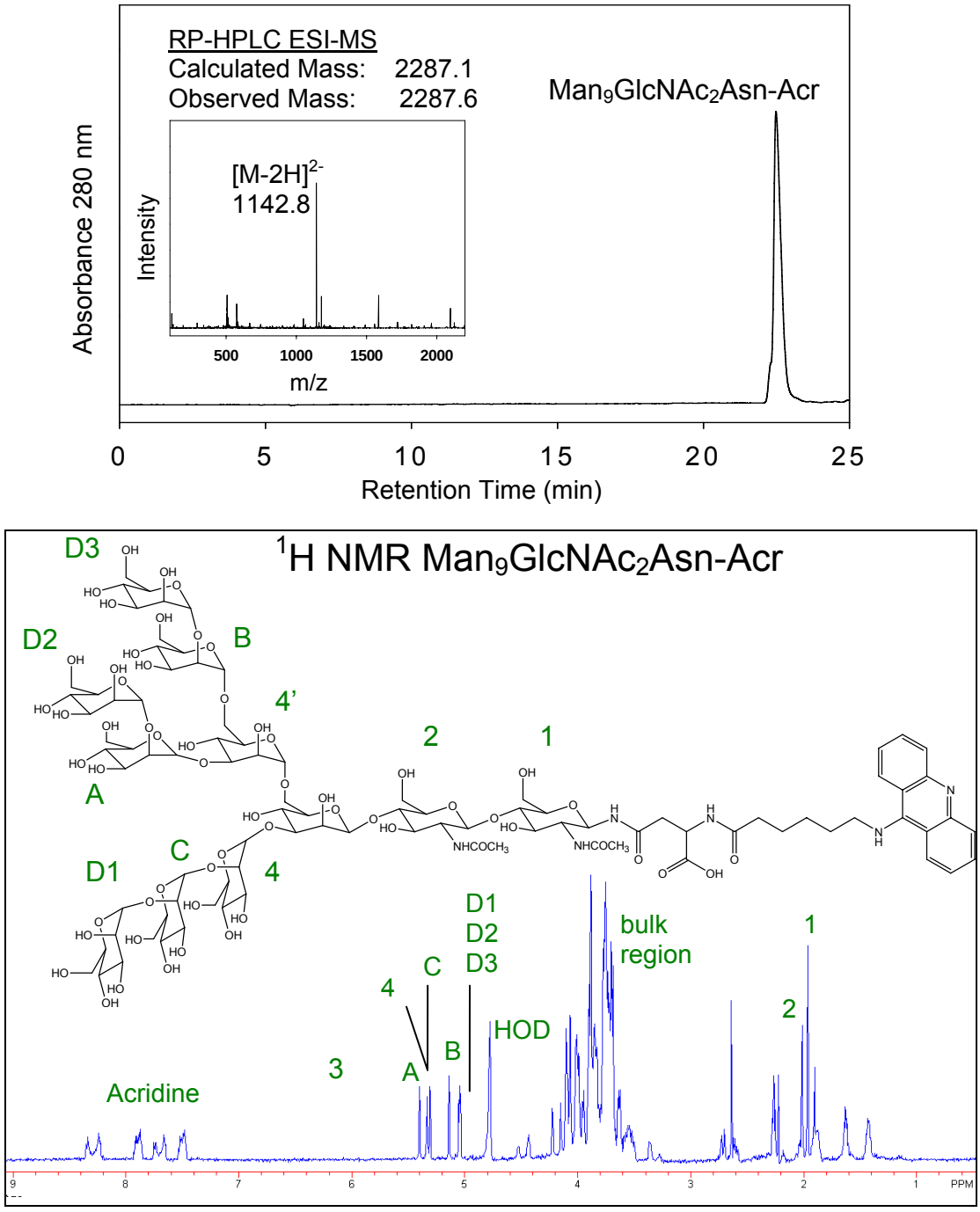

Figure 3-13. *RP-HPLC ESI-MS and 600 MHz ^{1}H NMR Characterization of Man$_9$GlcNAc$_2$Asn-Acr.* Man$_9$GlcNAc$_2$Asn-Acr (2 nmol) was injected on a 30 min 1-30% acetonitrile in 0.1% TFA gradient and analyzed by ESI-MS in the negative mode. A 0.8 mM sample in D_2O was analyzed by NMR. The aromatic signals from the acridine moiety appear downfield between 7.4 and 8.4 ppm. The distortion which appears is likely due to the anisotropic effect of the interaction between the rings and the neighboring methylene protons.

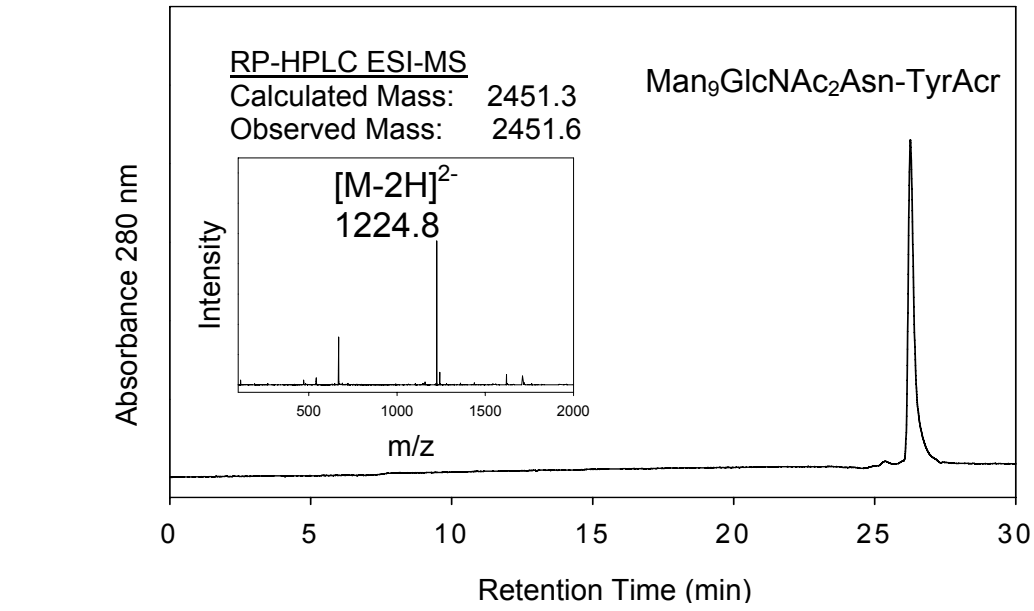

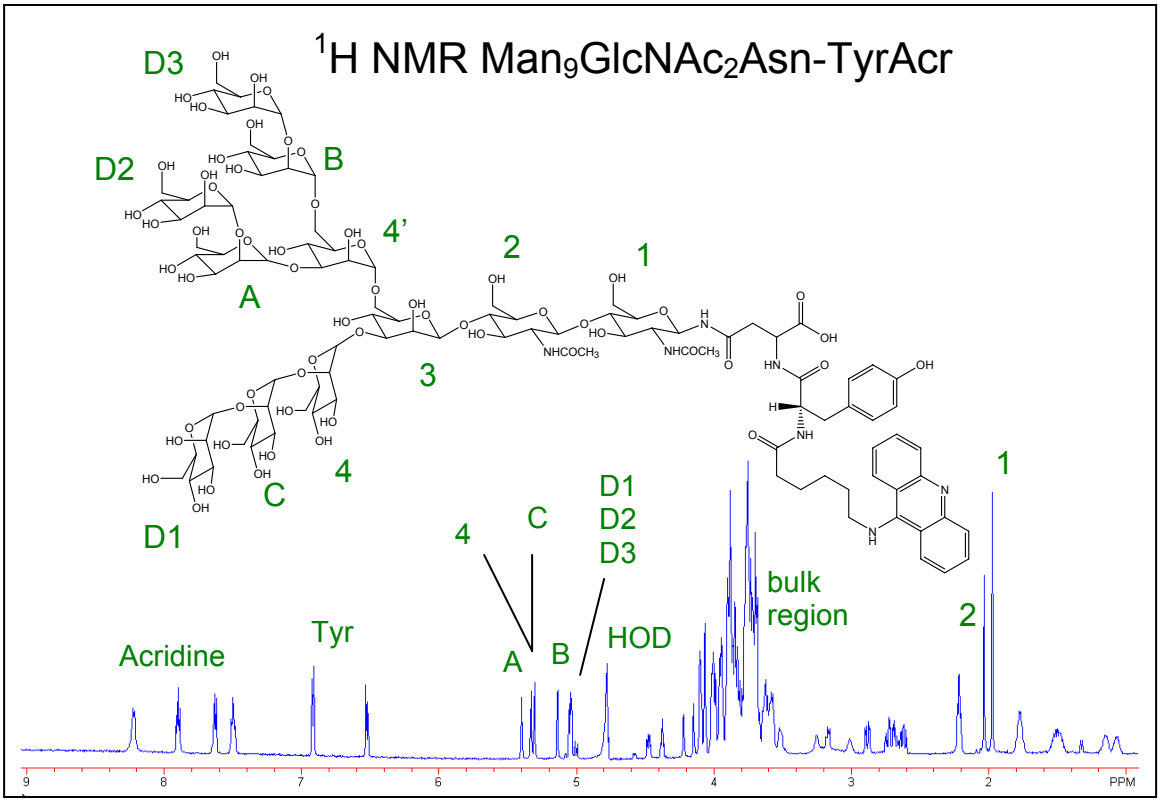

Figure 3-14. *RP-HPLC ESI and 600 MHz ^{1}H NMR Characterization of Man$_9$GlcNAc$_2$Asn-TyrAcr.* Man$_9$GlcNAc$_2$Asn-Acr (2 nmol) was injected on a 30 min 1-30% acetonitrile in 0.1% TFA gradient and analyzed by ESI-MS in the negative mode. A 0.8 mM sample in D_2O was analyzed by NMR. The aromatic signals arising from tyrosine and acridine are seen downfield.

Man_9 Bioconjugate–Plasmid DNA Binding: The Band Shift Assay

The affinity of $Man_9GlcNAc_2Asn$-Acr for plasmid DNA was assayed by a band retardation assay on 0.1% agarose gel (Figure 3-15). The migration of plasmid DNA was compared with DNA containing $Man_9GlcNAc_2Asn$-Acr. Intercalated $Man_9GlcNAc_2Asn$-Acr inhibits plasmid migration. The samples are analyzed after electrophoresis by soaking the gel in an Ethidium bromide solution. Ethidium bromide intercalates into DNA and can be visualized under a UV lightsource. In the control sample, (lane 7), the supercoiled and circular forms of the plasmid are visible as the lowest two bands. Minor impurities are also visible as faint bands. The migration of the bioconjugate-DNA polyplex through the gel was never totally retarded, even at the highest stoichiometry tested. This result led to the development of a second generation of bioconjugate with higher affinity for DNA.

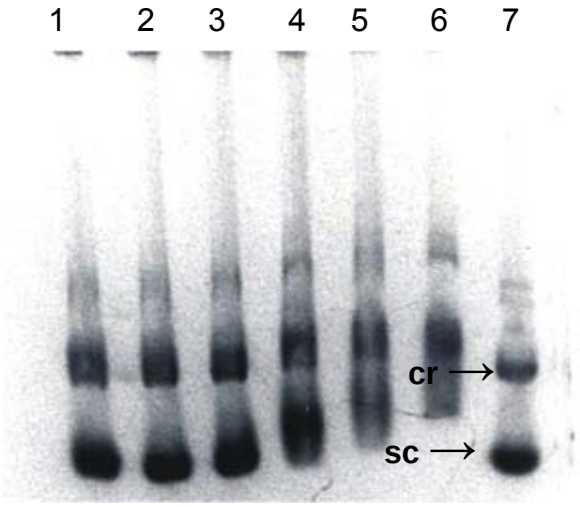

Figure 3-15. *$Man_9GlcNAc_2Asn$-Acr – Plasmid DNA Band Shift Assay*. 0.6 µg of SEAP plasmid was incubated with the Man_9 bioconjugate and assayed at the following levels: Lane 1:0.03 nmol, 2: 0.32 nmol, 3: 3 nmol, 4: 8 nmol, 5: 16 nmol, 6: 32 nmol, 7: no bioconjugate. cr: circular plasmid, sc: supercoiled plasmid

Discussion

Two novel $Man_9GlcNAc_2Asn$-Acridine analogs were prepared through the application of literature procedure and classical medicinal chemistry synthetic strategy. Affinity purified soybean agglutinin was digested with Pronase, and the $Man_9GlcNAc_2Asn$ glycan of interest was separated from contaminating digested amino acids by gel filtration and ion exchange chromatography. This particular strategy for isolating the glycan is currently the most efficient by far, as organic synthetic strategies have been unsuccessful in producing glycans with the correct structure, and hydrazinoysis of the purified glycan requires re-N-acetylation and additional purification.

We investigated acridine with the intent of replacing lysine as the DNA binding agent in our non-viral gene delivery systems. Acridine contains the planar, aromatic fused ring system common to nucleic acid intercalators. 9-Chloracridine starting material was available from commercial sources, and the chemistry to make 6-(Acridin-9-ylamino)-hexanoic acid was straightforward. The NHS ester of the acid was made through traditional DCC coupling, providing a facile reagent for nucleophilic addition.

$Man_9GlcNAc_2Asn$ could be directly coupled to the acridine ester through the N-terminal amine of asparagine; this was the first compound made. An analog was made by derivatizing the $Man_9GlcNAc_2Asn$ with a Boc-tyrosine-NHS, and removing the boc group with TFA. The limiting feature of this strategy was the additional derivatization reaction and gel filtration procedure, and the precarious acid deprotection. Excess water or reaction time hydrolyzed mannose monomer from the glycan.

$Man_9GlcNAc_2Asn$-Acr was a promising compound, requiring relatively simple purification and synthesis to produce it. However, it showed weak affinity for plasmid DNA, based on the stoichiometry required to produce plasmid retardation in an agarose gel band shift assay. This result prompted the development of a bioconjugate with higher affinity for DNA, the Man_9 glycopeptide described in the following chapter.

CHAPTER 4
SYNTHESIS OF AN ACRIDINYLATED HIGH MANNOSE TARGETING LIGAND

Introduction

Our investigation into the synthesis of an acridinylated high mannose targeting ligand began with experimentation on a model compound, triantennary-cysteine-lysine$_4$. We knew that a glycan derivatized with a single acridine had weak affinity for DNA, so our plan was to derivatize the four lysines on our model compound with four acridines. The derivatization proved problematic however; the reaction was often incomplete, and purification, recovery, and analysis of the compound was difficult.

One possible solution lay in the acridinylation of the epsilon amine of lysine and the synthesis of a cysteine-bearing acridine-lysine peptide for conjugation to the glycan. This would allow for versatility and control over peptide length, spacing between acridinylated lysine residues, and other variables which can be manipulated via solid-phase peptide synthesis. A literature search revealed the work Ueyama et. al.[55], who synthesized a series of similar polyacridinylated-lysine peptides in 2001. The short supplement that was submitted did not contain any information pertaining to the synthesis of the acridinylated-lysine amino acid, but molar absorptivity and binding constant data for polyacridinylated lysine peptides of varying length were included in the paper.

In 1992, Tung et al. published the synthesis of a polyacridinylated-lysine peptide for analyzing protease activity. [122] This report did contain a synthetic procedure for the acridinylation of lysine, which was similar to our method for the derivatization of 6-aminohexanoic acid (Scheme 3-1). Based on this, Tung's procedure was adapted and modified slightly to improve the reaction yield, and a polyacridinylated lysine peptide was synthesized on solid phase. A Man$_9$ analog containing a tyrosine and a Maleimide

group was then synthesized, and the analog was then coupled to the peptide to create the Man_9Ac-Lys glycopeptide.

Materials and Methods

Solid phenol was a Riedel-de-Haën product through Sigma-Aldrich. The sodium hydroxide pellets were a Mallinckrodt product through Fisher Scientific. The anhydrous ethyl ether was a Fisher product. Fmoc-Lys-OH was from Novabiochem. NMR spectra were taken with a 300 MHz Bruker NMR. All reagents were certified ACS grade, molecular biology grade, or an equivalent.

Fmoc-Lys(Boc)-Wang resin, Fmoc-Lys(Boc)-OH, Fmoc-Cys(Trt)-OH, N-Methyl-2-pyrrolidinone (NMP), O-Benzotriazole-N,N,N',N'-tetramethl-uronium-hexafluoro-phosphate (HBTU) and Hydroxybenzotriazole hydrate (HOBt) were from Advanced ChemTech. The synthesized N- α-Fmoc-N-ε-9-Acridinyl-Lysine (K_{Ac}) was used as the third amino acid monomer. Diisopropylethylamine, piperidine, triisopropylsilane (TIS), and acetic anhydride were from Sigma-Aldrich. N',N-Dimethylformamide (DMF) was from Amresco. The APEX 396 solid phase peptide synthesizer was an Advanced Chemtech product, the preparatory HPLC system consisted of a model 2350 gradient programmer, pump, and V^4 wavelength detector from ISCO Inc., with a semipreparative C_{18} column (2 x 25 cm) from GraceVydac. The analytical HPLC system was an Agilent 1100 series with a GraceVydac C_{18} column (0.46 x 25 cm) and an inline 1100 series LC/MSD trap.

3-Maleimidoproprionic acid N-hydroxysuccinimide ester was from ABD Bioquest, Inc. The Boc-$Man_9GlcNAc_2$Asn-Tyr was synthesized previously (Chapter 4), N,N-Dimethylformamide (DMF) was from Amresco, Inc, and the sodium bicarbonate was a Fisher Scientific product. An ISCO UA-6 UV/VIS detector and Type 12 optical unit were used to monitor the eluate during gel filtration chromatography. An ISCO HPLC system with a Vydac C_{18} column (0.46 x 25 cm), model 2360 gradient

programmer, model 2350 pump, V^4 absorbance detector was used for additional purification. The freeze dry system was a Labconco Freezone 4.5 with a centrivap concentration accessory.

The 0.1% agarose gel was made with agarose from GIBCO, Tris and Boric acid from Fisher Scientific, and EDTA from Sigma-Aldrich. pGL3 plasmid was obtained from the Promega corporation. The Ethidium bromide stock solution was from Bio-Rad.

Thiazole Orange and HEPES were from Sigma Aldrich, pGL3 plasmid was from the Promega corp., and the fluorimeter was a Perkin Elmer model LS50B.

Synthesis of N-α-Fmoc-N-ε-9-Acridinyl-Lysine

9-phenoxyacridine (3.0 g)(synthesis described in Chapter 3) was added to 6.78 g of phenol and liquefied with stirring under argon at 50°C. Fmoc-Lys-OH (2.18 g) was added, and the reaction was run at 50-60°C for 4 hr. Heating was discontinued, and 80 ml of diethyl ether was added with vigorous stirring. The yellow precipitate that formed was recovered by filtration and washed thoroughly with diethyl ether. The product was then dried overnight under vacuum. The reaction yielded 2.90 g (90%) N- α-Fmoc-N-ε-9-Acridinyl-Lysine which had a m.p. of 135-136°C. (300 MHz, DMSO-d_6): δ = 6.70 – 8.70 (17H, m, Har), 3.60 - 3.95 (2H, m), 3.25 – 3.55 (3H, br), 2.06 (1H, m), 0.80 – 1.50 (6H, m).

Synthesis of Polyacridine-Lysine Peptide

The nine amino acid peptide C-K_{Ac}-K-K_{Ac}-K-K_{Ac}-K-K_{Ac}-K was synthesized using standard Fmoc chemistry with HOBt and HBTU double coupling on 30 μmol scale with an APEX 396 Advanced ChemTech solid phase peptide synthesizer. The peptide was removed from the resin and deprotected with a 2 ml cleavage cocktail consisting of TFA/TIS/H_2O (95:2.5:2.5 v/v/v) for 3 hr followed by precipitation in 40 ml cold ether. The precipitate was collected by centrifugation at 4 000 rpm for 10 min, then reconstituted in 0.1 v/v % TFA and purified by preparatory HPLC with a 16-30% ACN in

0.1% TFA 45 min gradient. The peptide was quantified by UV/VIS with an $\varepsilon_{409\ nm}$ = 37, 064 M^{-1} cm^{-1} for a 17% (2.0 μmol) yield. Purity and identity were verified by RP-HPLC MS with a 15-30% ACN in 0.1% TFA 30 min gradient detecting in positive mode.

Synthesis of $Man_9GlcNAc_2Asn$-Tyrosine Maleimide

Boc-$Man_9GlcNAc_2Asn$-Tyr (250 nmol) was dried by centrivap concentration and the boc group was removed by the addition of 100 μl of 95% TFA for 5 min The reaction was frozen on dry ice and the product was dried by centrivap concentration. The glycan was then brought into 300 μl of 100 mM sodium bicarbonate. 3-maleimidoproprionic acid NHS ester (2.5 μmol) was brought into 125 μl DMF and added to the $Man_9GlcNAc_2Asn$. The reaction continued for 1 hr followed by separation from excess derivatizing reagent on a Sephadex G-25 column (1.5 x 50 cm), eluting with 0.1% acetic acid. The reaction yield was determined by absorbance by monitoring tyrosine ($\varepsilon_{274\ nm}$ = 1 400 M^{-1} cm^{-1}). RP-HPLC analysis showed minor impurities, so the derivatized glycan was purified with the same system on a 1-15% ACN in 0.1% TFA 30 min gradient. The Man_9Asn-Tyr Mal was assayed for purity and identity by RP-HPLC ESI-MS, on a 30 min 1-30% acetonitrile gradient in 0.1% TFA with ESI-MS detection in the negative mode. The recovery of $Man_9GlcNAc_2Asn$-Tyr Mal was 57 nmol, a 23% yield.

Synthesis of the Man_9-AcrLys Glycopeptide

$Man_9GlcNAc_2Asn$-Tyr Mal (435 nmol) and polyacridine lysine peptide (539 nmol) were dried by centrivap. The derivatized glycan was prepared in 435 μl of 5 mM HEPES pH 7.0 and added to the dry peptide. The reaction continued for 2 hr and was purified from excess dimeric peptide by RP-HPLC with a 30 min 15-30% acetonitrile gradient in 0.1% TFA. The purity and identity were verified by analytical RP-HPLC ESI-MS in positive mode. A secondary analysis was performed by MALDI-TOF. The recovery of Man_9-AcrLys Glycopeptide was 102 nmol, for a 23% yield.

Man_9-AcrLys Glycopeptide : DNA Binding: The Band Shift Assay

Four experimental samples were made by mixing 1 μg of the plasmid with 0.054, 0.216, 0.532, and 1.064 nmol Man_9-AcrLys Glycopeptide. Each sample was incubated for 30 min before loading into the agarose gel. A plasmid control was run beside the experimental compounds. The samples were run under an 80V electric field for 60 min. The gel was stained overnight with 200 ml 0.1 μg/μl ethidium bromide.

Acridine : DNA Binding: The Thiazole Orange Displacement Assay

A 40 nM thiazole orange solution containing 1 μg plasmid was made with 5 mM HEPES buffer, pH 7.4. Man_9-Ac was titrated into solution and thiazole orange fluorescence was recorded after 30 min of incubation. The final volume of the samples for analysis was 500 μl. Triplicate measurements were taken with 0.2, 0.3, 0.4, 1, 5 and 10 nmol compound, with excitation at 500 nm and emission at 530 nm. Man_9-AcrLys was assayed by the same procedure; triplicate measurements were made with 0.2, 0.3, 0.4, 0.5, 1 and 2 nmol of the bioconjugate.

Results

Synthesis of N-α-Fmoc-N-ε-9-Acridinyl-Lysine

An acridinylated lysine derivative for use in peptide chemistry was made, as in Tung et. al. (Scheme 4-1).[122] 9-phenoxyacridine was added to solid phenol and liquefied with stirring at 50°C. Fmoc-Lys-OH was then added and the reaction continued for 4 hr. The heat source was removed and diethyl ether was added with vigorous stirring. The derivatized amino acid precipitated out of solution and was recovered by filtration. The N-α-Fmoc-N-ε-9-Acridinyl-lysine was then washed thoroughly with diethyl ether and dried under vacuum.

The amino acid was analyzed for purity and structural identity by NMR, HPLC, and ESI-MS. The signals in the ^{1}H NMR spectra were in agreement with the literature (Table 4-1).[122] The N-α-Fmoc-N-ε-9-Acridinyl-Lysine was prepared in 1:1 methanol : 1 N HCl and analyzed by RP-HPLC with a 30 min 30-60% acetonitrile in 0.1% TFA gradient with detection in the negative mode. The compound was 94% pure, and the observed mass was within one mass unit of the calculated mass. Interestingly, the dimeric anionic species was also detected (Figure 4-1).

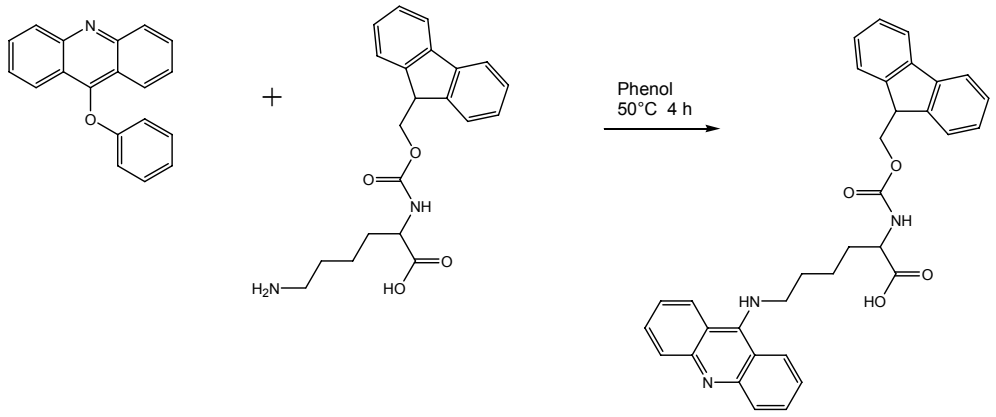

Scheme 4-1. *Synthesis of N-α-Fmoc-N-ε-9-Acridinyl-Lysine*. An acridinylated lysine derivatve was made for solid phase peptide synthesis with Fmoc chemistry.

	^{1}H NMR δ
N-α-Fmoc-N-ε-9-Acridinyl-Lysine	6.70 – 7.80 (17H, m, Har), 3.60 – 3.95 (2H, m), 3.25 – 3.55 (3H, br), 2.06 (1H, m), 0.80 – 1.50 (6H, m)

Table 4-1. *300 MHz ^{1}H NMR Chemical Shift Data for N-α-Fmoc-N-ε-9-Acridinyl-Lysine*

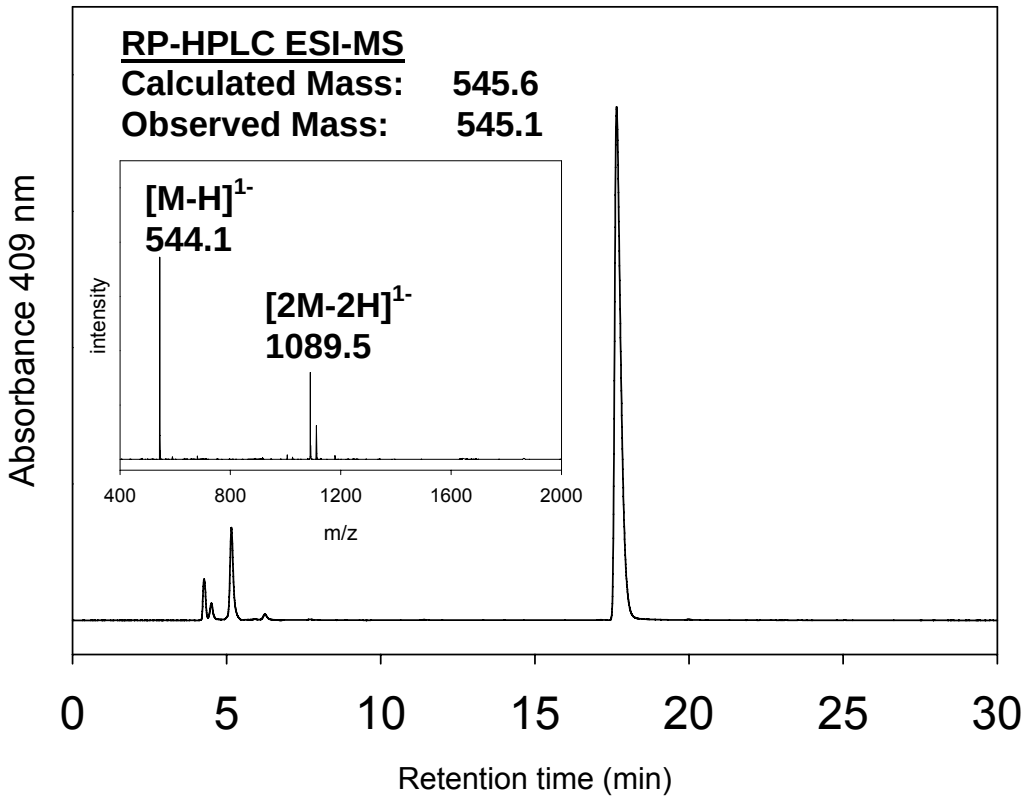

Figure 4-1. *RP-HPLC ESI-MS of N-α-Fmoc-N-ε-9-Acridinyl-Lysine.* A 2 nmol sample of N-α-Fmoc-N-ε-9-Acridinyl lysine in MeOH/1 N HCl was injected on a 30 minute 30-60% acetonitrile in 0.1% TFA. The singly charged species was detected by ESI-MS in the negative mode. The amino acid also ionized as a dimer and was detected.

Synthesis of Polyacridine Lysine Peptide

A nine amino acid peptide C-K_{Ac}-K-K_{Ac}-K-K_{Ac}-K-K_{Ac}-K was synthesized with a cysteine residue to conjugate to $Man_9GlcNAc_2$Asn-Tyr Mal (Scheme 4-2). This particular peptide was designed to have high affinity for DNA (four lysine-acridines amino acids) and to be synthesized efficiently (nine amino acids total). Lysine was selected as a spacing amino acid because it is cationic, and produces higher yields after work-up than do arginine-containing peptides. The derivatized lysine analog N-α-Fmoc-N-ε-9-Acridinyl lysine was used directly in solid phase peptide synthesis of the

polyacridine lysine peptide. The peptide was prepared on a 30 μmol scale with a crude yield of 11.7 μmol (40%) and a 2.0 μmol (17%) purified yield. It had a tendency to form a disulfide bond, and as a result had to be stored at low concentration in 0.1% TFA (-20°C), or in a crude mixture with an excess of TCEP (tris(2-carboxyethyl)phosphine). The Ac-Lys peptide was analyzed for purity and identity by RP-HPLC ESI-MS. The compound was prepared in 0.1% TFA and injected on a 30 min 15-30% acetonitrile in 0.1% TFA gradient with detection in the positive mode (Figure 4-2). It was 97% pure, and the observed mass was within 1 mass unit of the calculated mass.

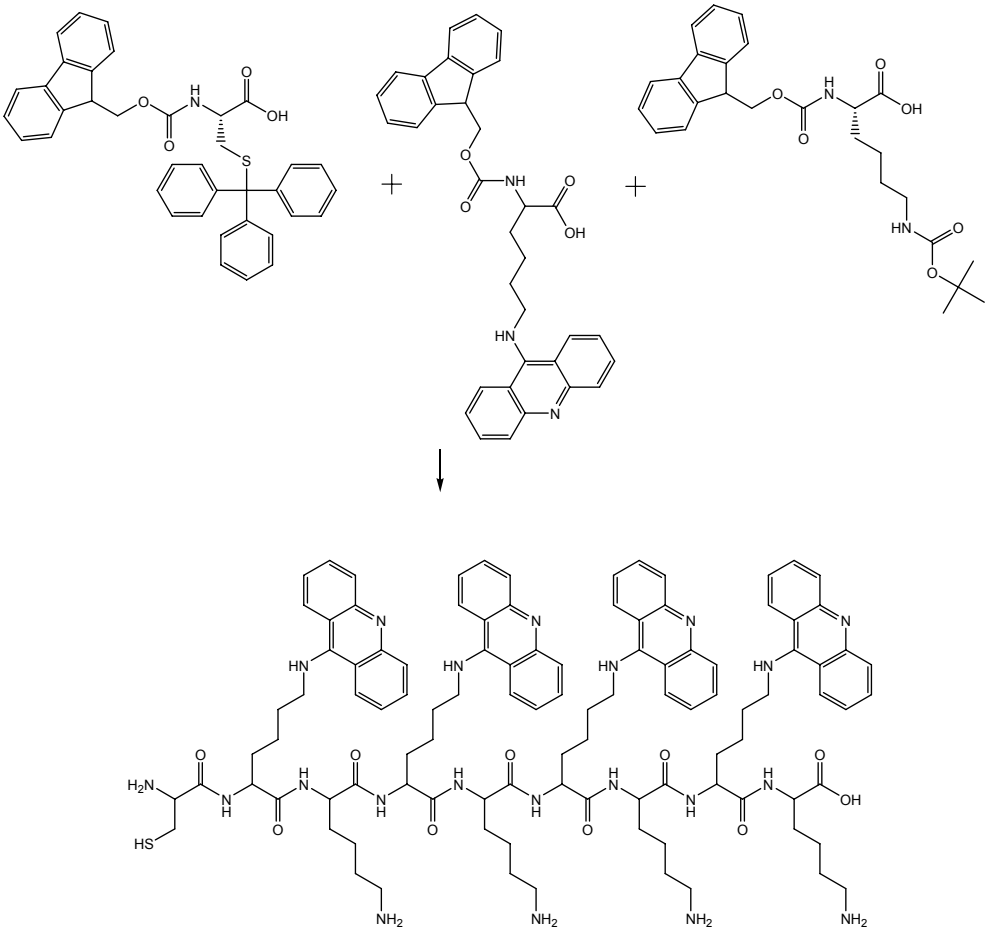

Scheme 4-2. *Polyacridine Lysine Peptide*. The peptide was synthesized on Wang resin using Fmoc chemistry with an automated synthesizer

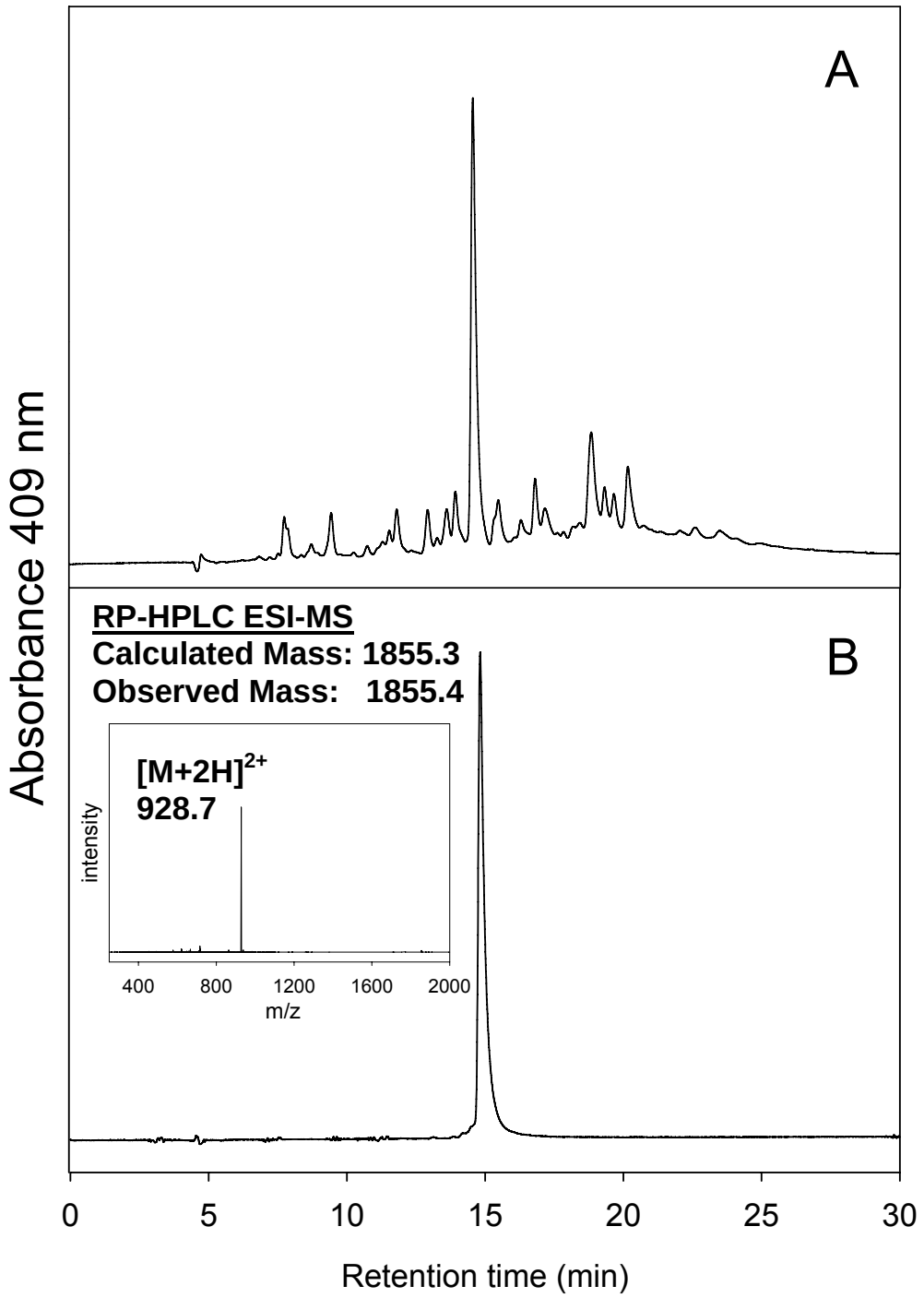

Figure 4-2. *Preparative Purification of Polyacridine-Lysine Peptide*. **A**. The 30 μmol synthesis yielded 11.7 μmol (40%) crude peptide 2 μmol (17%) purified peptide. **B.** 1 nmol of the purified compound was injected on a 30 min 15-30% acetonitrile in 0.1% TFA gradient with detection in the positive mode.

Synthesis of $Man_9GlcNAc_2Asn$-Tyrosine Maleimide

Removal of the Boc group from Boc-$Man_9GlcNAc_2Asn$-Tyr proceeded smoothly and to 100% completion with 95% TFA as evidenced by change in retention time on RP-HPLC from 19 min to 6 min The TFA was removed by evacuation and the amine terminus of the tyrosine was derivatized by the addition of an active ester (Scheme 4-3). The high molecular weight glycopeptide product was easily resolved from the excess reagent (Figure 4-3), and this reaction also proceeded to completion as determined by a shift in retention time to 13 min (Figure 4-4). The $Man_9GlcNAc_2Asn$-Tyr Mal was analyzed with a 30 min 1-30% acetonitrile in 0.1% TFA gradient with ESI-MS detection in the negative mode. The observed mass of the major product was approximately 2 mass units greater than the calculated mass of $Man_9GlcNAc_2Asn$-Tyr Mal.

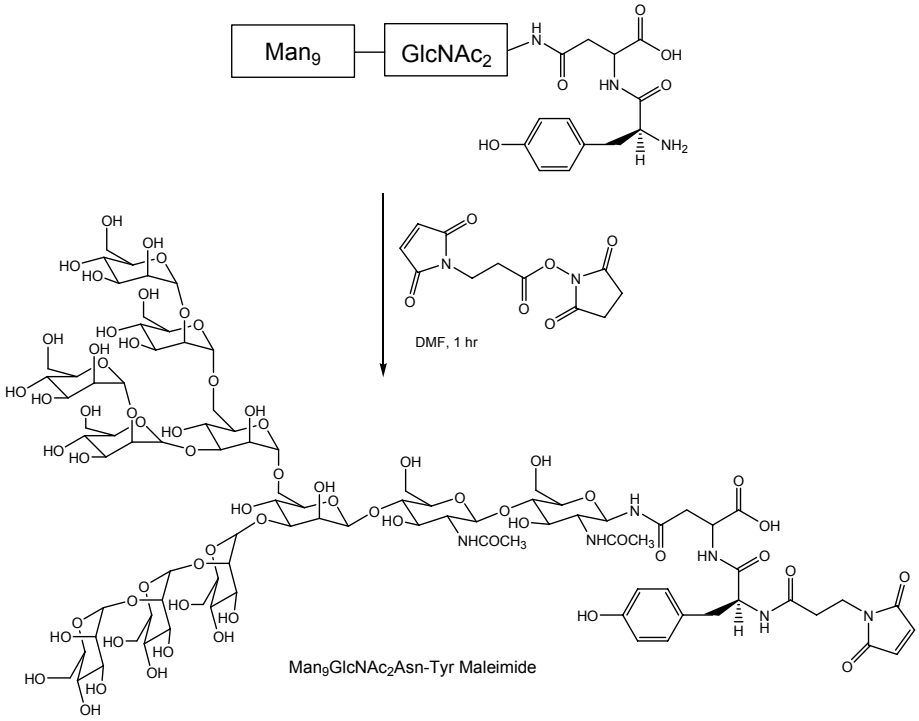

Scheme 4-3. *$Man_9GlcNAc_2Asn$-Tyr Maleimide*. Boc-$Man_9GlcNAc_2Asn$-Tyr was deprotected, dried, and directly derivatized with an NHS ester-maleimido derivative of proprionic acid.

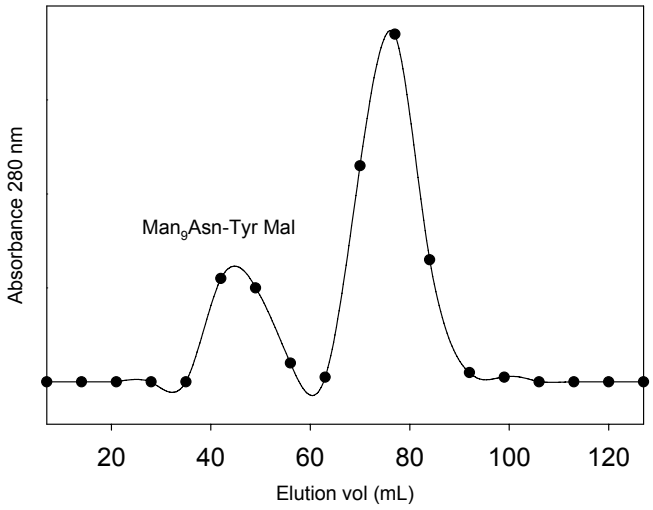

Figure 4-3. *Gel Filtration Purification of $Man_9GlcNAc_2$Asn-Tyr Mal*. The reaction mixture was loaded onto a gel filtration column containing Sephadex G-25 resin and eluted with 0.1% acetic acid. The derivatized glycan was separated from excess 3-maleimidoproprionic acid NHS reagent.

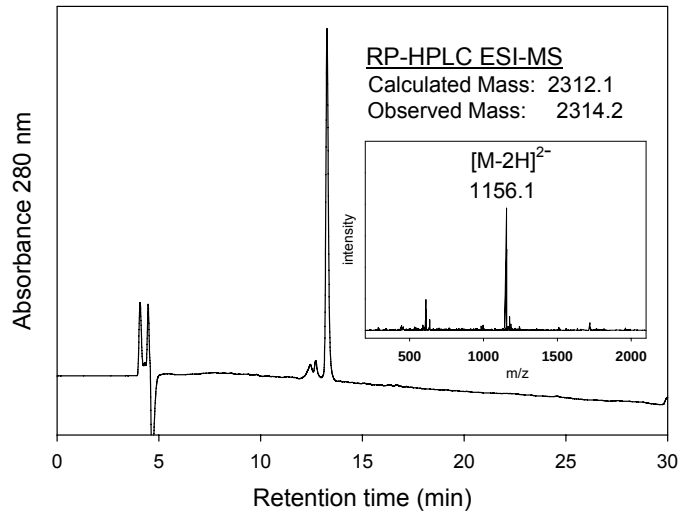

Figure 4-4. *RP-HPLC ESI-MS of $Man_9GlcNAc_2$Asn-Tyr Mal*. 4 nmol of the prepped sample was analyzed with a 1-30% acetonitrile in 0.1% TFA gradient with ESI-MS detection in the negative mode.

Synthesis of the Man_9-AcrLys Glycopeptide

The reaction of Man_9Asn Tyr-Mal with the polyacridine lysine peptide was optimized by varying the pH and stoichiometry of the reactants. The optimal pH (7.0) and reaction stoichiometry of 1.2:1 mol equivalents of peptide : Man_9Asn Tyr-Mal resulted in complete consumption of Man_9Asn Tyr-Mal and formation of the desired product (Scheme 4-4). Excess peptide formed a disulfide and eluted later during RP-HPLC. The purified products rechromatographed as a single product peak of > 95% purity with a mass of 4167 g/mol as determined by ESI-MS (Figure 4-5).

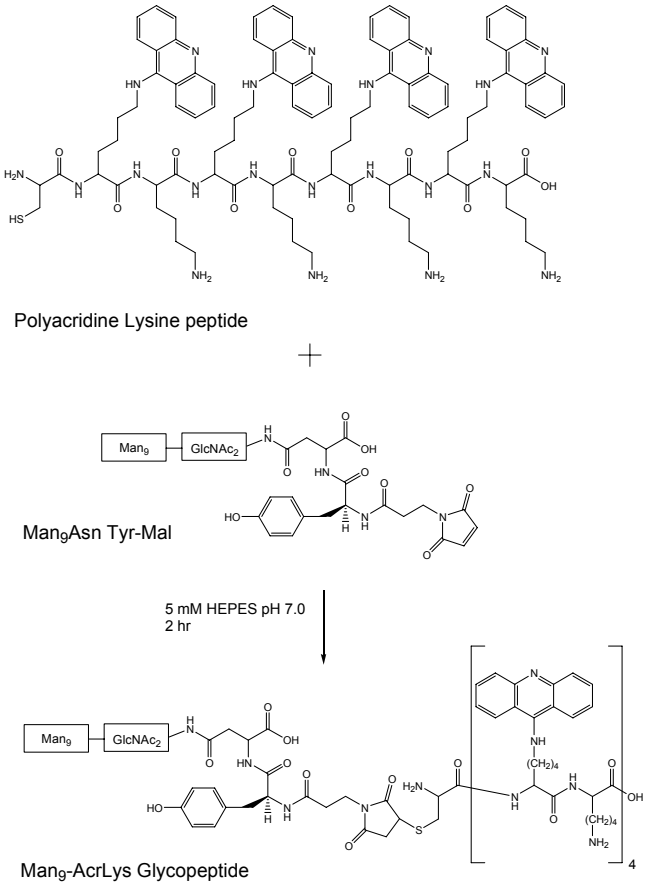

Scheme 4-4. *Synthesis of the Man_9-AcrLys Glycopeptide*. Polyacridine lysine peptide was reacted with Man_9Asn Tyr-Mal at a 1.2:1 ratio in 5 mM HEPES at pH 7.0 for 2 hrs.

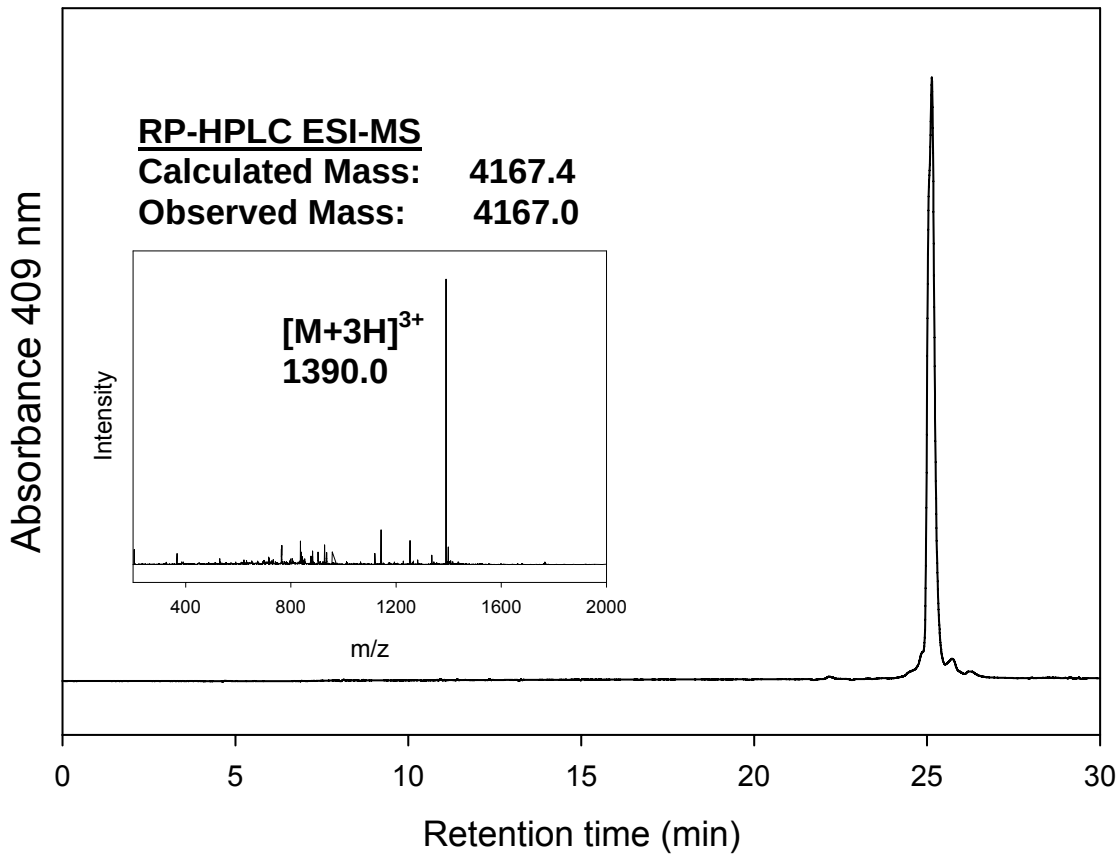

Figure 4-5. *RP-HPLC ESI-MS Analysis of Man_9-AcrLys Glycopeptide*. 400 pmol of Man_9-AcrLys Glycopeptide was analyzed with a 30 min 1-30% ACN gradient in 0.1% TFA. The compound was observed in the triply-charged state by ESI-MS, with detection in the positive mode.

Man_9-AcrLys Glycopeptide : DNA Binding Band Shift Assay

The affinity of the Man_9-AcrLys Glycopeptide for plasmid DNA was assayed by a band retardation assay on 0.1% agarose gel. In the control sample, (lane 1), the supercoiled and circular forms of the plasmid are visible as the lowest two bands. Minor impurities are also visible as faint bands. Four samples were analyzed with an increasing bioconjugate : plasmid ratio. At a ratio of 1 nmol bioconjugate : 1 μg plasmid, migration of the polyplex was completely arrested at the origin (Figure 4-6). The binding affinity of this glycopeptide for DNA was found to be significantly higher than the glycopeptide possessing a single acridine (Figure 3-15).

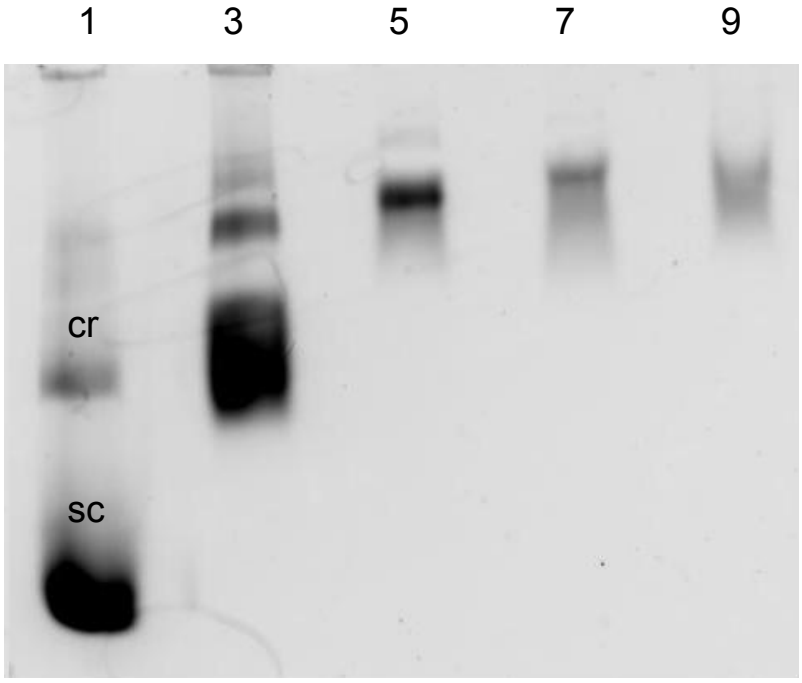

Figure 4-6. *Man_9-AcrLys Glycopeptide:DNA Binding: The Band Shift Assay*. 1 μg pGL3 plasmid was incubated with Man_9-AcrLys Glycopeptide and assayed at the following levels: Lane 3: 0.054 nmol, 5: 0.216 nmol, 7: 0.532 nmol, 9: 1.064 nmol. Lane 1 : 1 μg pGL3. cr: circular plasmid, sc: supercoiled plasmid

Acridine-DNA Binding: Thiazole Orange Displacement Assay

The thiazole orange displacement assay was conducted to determine the relative affinities of the acridine-containing compounds for plasmid DNA (Figure 4-7). In the control sample, 20 pmol thiazole orange was incubated with 1 μg plasmid for 30 min The fluorescence of the control sample Ex $_{500\ nm}$: Em $_{530\ nm}$ was the 0% quench standard. Increasing Man_9-AcrLys Glycopeptide (Scheme 4-17) was titrated in, displacing the thiazole and quenching fluorescence. $ManGlcNAc_2$Asn-Ac (Figure 3-13) was assayed by the same method. The results of this experiment mirrors the result of the band shift assays conducted with the glycopeptides. $ManGlcNAc_2$Asn-Acr cannot displace thiazole from the plasmid, even at the highest stoichiometry tested, and as a result the fluorescence of thiazole is not reduced. However, the Man_9-AcrLys Glycopeptide displaces thiazole at 400 pmol per microgram plasmid, resulting in a complete quench of fluorescence.

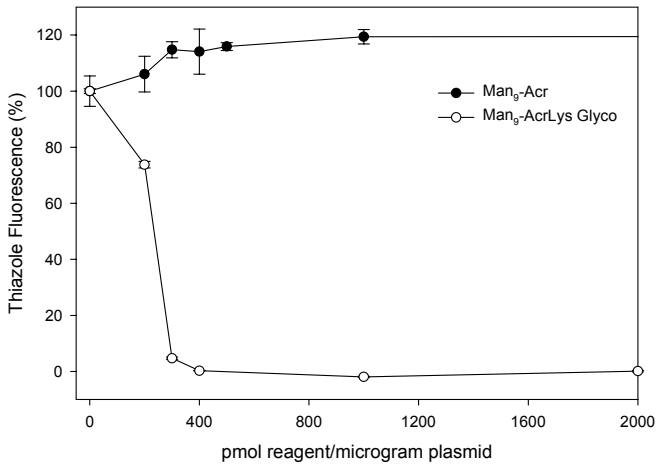

Figure 4-7. *Thiazole Orange Displacement Assay.* The affinities of the Man_9-AcrLys Glycopeptide and Man_9-Acr for plasmid DNA were assayed by the fluorescence-based thiazole orange displacement assay.

Discussion

The high mannose targeting ligand described in the current chapter is a significant improvement over the high mannose ligand presented in the previous chapter due to its higher affinity for plasmid DNA. The poly-acridinylated peptide anchor intercalates between DNA's base pairs, and the lysine-spacer amino acids provide additional electrostatic binding force. This is a much stronger interaction than that provided by the single acridine heterocycle of the $Man_9GlcNAc_2Asn$-Acr.

The comparative binding affinities of the two compounds were demonstrated by agarose gel band-shift assay and by the thiazole orange displacement assay. The band shift assay showed strong plasmid to Man_9-AcrLys Glycopeptide binding at less than 1 nmol per microgram plasmid (Figure 4-6). Whereas at 32 nmol $Man_9GlcNAc_2Asn$-Acr to 1 microgram plasmid, the derivatized glycan was still only weakly bound, as evidenced by the very slight band shift (Figure 3-15). The thiazole orange displacement assay revealed a similar result: thiazole orange was displaced from plasmid DNA at less than 1 nmol per microgram plasmid, quenching thiazole's fluorescence, whereas 10 nmol $Man_9GlcNAc_2Asn$-Acr was not sufficient to displace 1 microgram of plasmid (Figure 4-5).

It is also important to consider whether the synthesis of the compound is efficient and practical. The source of glycan, soy flour is inexpensive and available in large quantity, and the glycoprotein can be isolated easily and in reproducible fashion through a reusable affinity column. The most expensive component of the purification is the pronase enzyme, which is not prohibitively costly. The tyrosine label and proprionic acid maleimido NHS ester are inexpensive small molecules. The acridine-lysine peptide 9-mer is only slightly more expensive to synthesize than an ordinary nine amino acid peptide, due to the four acridinylated lysines. However, the phenoxyacridine and resulting acridinylated lysine can be produced relatively cheaply and loaded directly into the peptide synthesizer without additional purification. The glycopeptide is quickly

formed as the thiol of the peptide attacks the maleimide of the derivatized glycan, and the product is purified by RP-HPLC.

CHAPTER 5
IN VITRO TESTING AND ANALYSIS OF THE HIGH MANNOSE TARGETING LIGAND WITH DC-SIGN CHO CELLS

Introduction

Perhaps the most important phase of this research project was the biological evaluation of the high mannose targeting ligand. A relevant and practical system was required for testing, and positive results were needed to validate the synthetic effort to produce the ligand. We obtained a cell line from Dr. Chae Gyu Park, a member of the Laboratory of Cellular Immunology and Physiology at the Rockefeller University. The cells were immortal Chinese hamster ovary cells (CHO) engineered to stably express recombinant human DC-SIGN receptor. We also received control CHO cells which did not express receptor. The laboratory is well renowned for dendritic cell research; the principal investigator, Dr. Ralph Steinman, co-discovered dendritic cells in 1973.

With the cells in hand, the next task was to show selective targeting and preferential gene delivery to the DC-SIGN using the glycopeptide ligand. We have routine gene delivery assays in our laboratory which employ quantification of expressed luciferase reporter gene, however our supply of ligand was somewhat limited. To compensate we scaled the amount of plasmid used in the assay down to one tenth of the typical quantity, and were still able to elicit significant gene expression.

In order to further establish that selective gene delivery was a receptor dependent phenomenon, I employed FACS analysis. I transfected the CHO cells with pGL3 which had been covalently labeled with a fluorophore, and confirmed preferential endocytosis into the DC-SIGN positive cells.

Materials and Methods

Human DC-SIGN (+) and DC-SIGN (-) CHO cells were a gift from Dr. Chae Gyu Park of the Laboratory of Cellular Immunology and Physiology at The Rockefeller

University. Cy™5 *Label*IT was from Mirus Biotechnology. The Becton Dickson LSR II with DiVA 6.01 software was used for analyzing CHO cell populations. Cy5 data was obtained with 488 nm excitation and 575 nm emission. Phycoerythrin data was obtained with 633 nm excitation and 670 nm emission. FACS data was prepared with WinMDI 2.8. The Hoechst 33258 stain was an Invitrogen product.

pGL3 control vector, a 5.3 kb luciferase plasmid containing an SV40 promoter and enhancer, was was obtained from the Promega corporation, amplified in DH5α *E coli* from Invitrogen, and purified with a Giga kit from Qiagen. D-Luciferin was from Gold Biotechnology, Adenosine 5'-triphosphate was from Roche, and BCA Protein Assay reagents were Pierce protein research products of Thermo Scientific. Polyethylenimine (PEI) was from Aldrich, Dulbecco's Modified Eagle Medium (DMEM), MEM non-essential amino acids, Dulbecco's phosphate buffered saline (DPBS) and fetal bovine serum (FBS) were from Invitrogen. All other reagents were reagent grade or higher. The luminometer was a Lumat LB 9501. The plate reader was a Biotek model EL808.

The DC-SIGN – phycoerythrin conjugate antibody (mouse monoclonal IgG_1 raised against immature myeloid monocyte-derived dendritic cells of human origin) was from Santa Cruz Biotechnology. $Man_9GlcNAc_2Asn$ was obtained through the procedure described in Chapter 3.

FACS Analysis

DC-SIGN (+) CHO cells (1×10^6) in 434 µL PBS, 554 µL DMEM, and 2.4 µg antibody in 12 µL PBS were combined in a polysterene vial. A control sample containing 1×10^6 DC-SIGN (-) CHO cells in 301 µL PBS, 687 DMEM, and 2.4 µg antibody in 12 µL PBS was also made. Prior to analysis, the suspensions stood at RT for 30 min, and 15 µL Hoeschst 33258 stain was added to each sample. Two 1 mL samples containing 1×10^6 unlabeled (+) and (-) CHO cells were prepared and analyzed as additional controls.

pGL3 plasmid (5 μg) was labeled with 5 μL *Label* IT reagent according to the manufacturers instructions. A 66 μL solution containing 0.5 nmoL Man_9-AcrLys Glycopeptide (56 μL) and 1 μg Cy5 labeled pGL3 was made and allowed to stand at RT for 30 min

DC-SIGN (+) CHO cells (1 x 10^6) were plated and transfected with the condensate described above. DC-SIGN (-) CHO cells (1 x 10^6) were also plated and transfected with the condensate. The cells were lifted with 1 mM EDTA in PBS and collected by centrifugation. The EDTA solution was removed and the cells were suspended in 1 mL PBS. The transfected cells were analyzed by FACS, and compared to (+) and (-) untransfected CHO cells.

In Vitro Transfection of CHO Cells

DC-SIGN (+) CHO cells (1 x 10^5) were plated in standard 6 well plates in triplicate in 1 mL DMEM high glucose supplemented with 7% FBS and 1% MEM non-essential amino acids. After incubation for 24 hrs at 37°C and 5% CO_2, the media was removed, the cells were washed with 1 mL DPBS, and the media was replaced with 1 mL DMEM high glucose media supplemented with 2% FBS and 0.3% MEM non-essential amino acids.

DNA polyplexes were prepared at a DNA concentration of 30 μg/mL and were dosed in 30 μL aliquots containing 1 μg DNA. For PEI-DNA gene delivery, 4.3 μL of a 1 mg/mL PEI stock solution was added to 3.5 μg pGL3 DNA in 2.2 μL buffer TE. The PEI : DNA polyplex (9:1 N:P charge ratio) was then diluted to 105 μL with HEPES buffered mannitol, pH 7.4. For WK_{18}, 3.3 μL (1.8 nmoL) of a 0.54 nmoL/μL WK_{18} stock solution was added to 3.5 μg pGL3. The WK_{18} : DNA polyplex (3:1 charge ratio) was then dilued to 105 μL with HBM. Polyacridine-Lysine control peptide (synthesis described in Chapter 4), (1.75 nmoL) peptide was prepared in 69 μL water. 3.5 μg pGL3 and 34 μL HBM were added for a final peptide concentration of 0.5 nmoL/μL. Man_9-

AcrLys Glycopeptide (1.75 nmoL) in water (68.8 µl) was added to 3.5 µg pGL3. The sample was diluted with 34 µl HBM for a final concentration of 0.5 nmol/µl. Each polyplex was given 30 min to form at RT.

DC-SIGN (+) CHO cells were treated with 30 µL of each polyplex in triplicate, and returned to the incubator. After incubation for 24 hr, the transfection media was removed, the cells were washed with 2 mL DPBS and lysed with 0.5 mL lysis buffer (25 mM tris chloride, pH 7.8, 1 mM EDTA, 8 mM magnesium chloride, and 1% Triton X-100) for 10 min at 4°C. Cell lysates were scraped, transferred to 1.5 mL microcentrifuge tubes, and centrifuged for 10 min at 13,000 g (at 4°C) to pellet cell debris. Lysis buffer (400 µL), ATP (4.3 µL of a 165 mM solution at pH 7) were combined in a test tube, mixed briefly, and placed in the luminometer. The relative light units from the activity of Luciferase were determined with 10 sec integration after automatic injection of 100 µL of 0.43 mM D-luciferin. Protein concentration was measured by BCA assay with bovine serum albumin as a standard.[123] The amount of luciferase recovered in each sample was normalized to mg of protein and reported as the mean with standard deviation obtained from triplicate transfections. DC-SIGN (-) control cells were treated simultaneously with identical polyplex formulations.

In Vitro Inhibition of Gene Transfer

DC-SIGN (+) CHO cells (1×10^4) were plated, and transfected by the procedure described above. The PEI : pGL3 and the Man_9-AcrLys Glycopeptide polyplexes were formed and dosed as above. The $Man_9GlcNAc_2Asn$ knockdown sample was prepared by combining 175 nmol of the glycan with 1.75 nmol Man_9-AcrLys Glycopeptide and 3.5 µg DNA in a 2:1 water : HBM solution. The cells were then dosed in triplicate with 30 µL containing 0.5 nmoL Man_9-AcrLys Glycopeptide, 50 nmoL $Man_9GlcNAc_2Asn$, and 1 µg DNA. For antibody knockdown, 1.75 nmol Man_9-AcrLys Glycopeptide was added to 17.5 µg antibody and 3.5 µg DNA in a 5.8 : 1 PBS : HBM solution. The cells were then

dosed in triplicate with 30 μL aliquots containing 0.5 nmoL Man_9-AcrLys Glycopeptide, 5 μg antibody, and 1 μg DNA.

Results

FACS Analysis

An anti-DC-SIGN antibody-phycoerythrin conjugate was procured to verify stable expression of the DC-SIGN receptor on the CHO cells. 1 x 10^6 DC-SIGN (+) CHO cells were incubated with 2.4 μg antibody conjugate in 1 mL isotonic solution, with additional Hoechst stain to identify dead cells. 1 x 10^6 (-) CHO cells were incubated simultaneously with the same preparation. LSR analysis of the samples revealed receptor-mediated binding of the antibody conjugate as indicated by the shift in fluorescence associated with the DC-SIGN (+) CHO cells (Figure 5-1). The overlap between the cell populations suggests that a percentage of the CHO (+) cells did not express receptor.

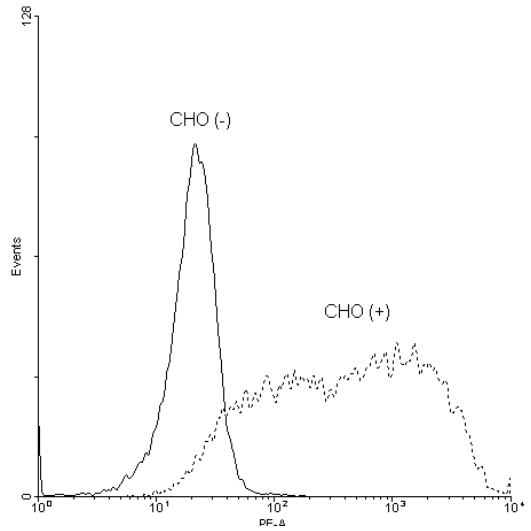

Figure 5-1. *Phycoerythrin FACS Analysis of DC-SIGN (+) and (-) CHO cells.* Both cell types were incubated with 2.4 μg of antibody-phycoerythrin conjugate and subsequently analyzed.

We developed a FACS assay to demonstrate selective receptor binding which utilized the Man_9-AcrLys Glycopeptide. pGL3 plasmid (5 µg) was covalently labeled with 5 µL *Label* IT reagent. A particle containing 0.5 nmoL Man_9-AcrLys Glycopeptide and 1 µg Cy5 labeled pGL3 was made and allowed to stand at room temp. for half an hour (Figure 5-2).

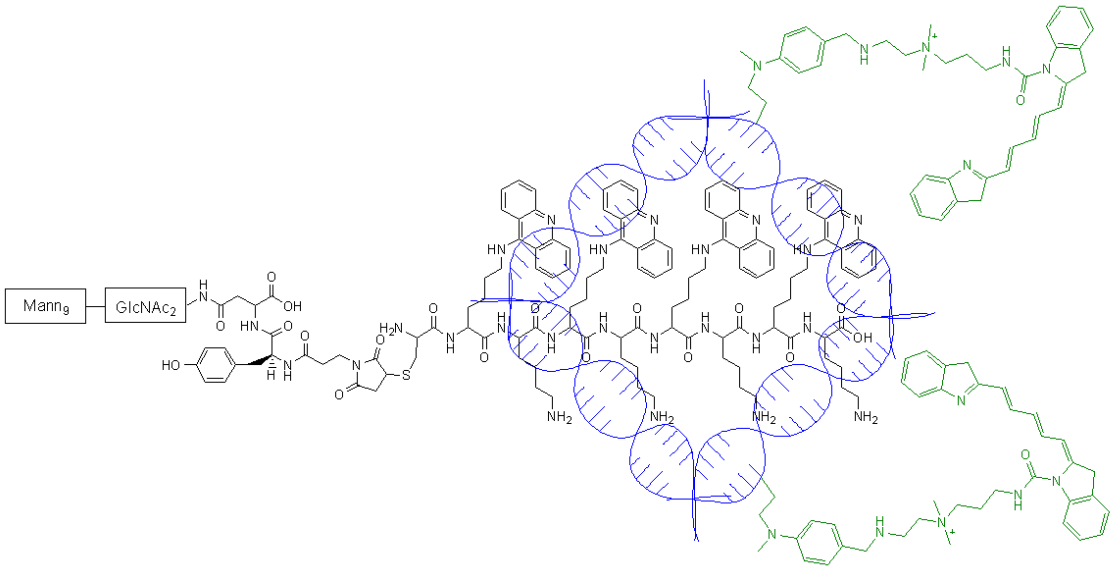

Figure 5-2. *Representation of Cy5 labeled glycopeptide condensate*. A Cy5 labeled polyplex was made at 0.5 nmoL per microgram DNA, consistent with the stoichiometry used for transfection. Transfected CHO cells were imaged by FACS.

DC-SIGN (+) CHO cells (1×10^6) were plated and transfected with labeled condensate. CHO (-) cells (1×10^6) were treated in the same way. After overnight transfection the cells were lifted with 1 mM EDTA in PBS. A two minute centrifugation was used to pellet the cells and remove the EDTA. Each cell population was then brought into a milliliter of PBS and analyzed by FACS (Figure 5-3). The histogram shows higher fluorescence in the (+) CHO cell population due to higher receptor mediated-uptake of

the labeled condensate. An overlap between the cell populations treated with ligand is seen; this suggests that a fraction of the CHO (+) cells did not express receptor.

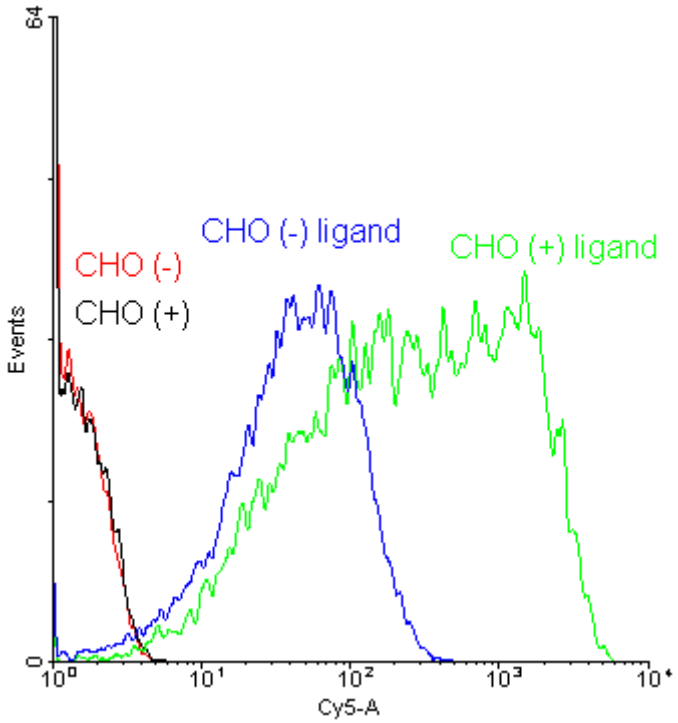

Figure 5-3. *Cy5 FACS Analysis of DC-SIGN (+) and (-) CHO cells.* Both cell types were transfected with 0.5 nmol of Man_9-AcrLys Glycopeptide and 1 µg of Cy5 labeled pGL3 plasmid. After incubation overnight, the cells were lifted and imaged.

In vitro transfection of CHO Cells

hDC-SIGN (+) CHO cells (1 x 10^5) were plated in triplicate for four treatment groups. After incubation for 24 hrs, the media was removed, the cells were washed with PBS and fresh transfection media was added to the cells. Particles containing pGL3 plasmid and PEI, Trp-Lys_{18}, Acridine-Lysine peptide, or Man_9-AcrLys Glycopeptide were made and dosed in polyplex containing 1 µg DNA and 1.2 µg PEI (9:1 N:P), 1.3 µg

WK_{18} (3:1 K:P), 0.5 nmoL AcLys pep, or 0.5 nmoL Man_9-AcrLys Glycopeptide. The cells were returned to the incubator and kept at 37°C for 24 hr. On the following day the cells were lysed and centrifuged to separate the cytosolic solution containing expressed luciferase from cell debris. The solution was combined with a small volume of 165 mM ATP and placed in a luminometer, where a 0.4 mM solution of luciferin was combined with the sample to produce a light response proportional to the amount of luciferase expressed. The experiment was conducted with hDC-SIGN (-) CHO cells simultaneously. Selective targeting to the DC-SIGN expressing CHO-cells was observed by the Man_9-AcrLys Glycopeptide polyplex, as exhibited by a two log increase in relative light unit luminescence over control cell levels (Figure 5-4). The PEI positive controls displayed the highest transfection levels. Transfection with WK_{18} provided a negative control. The polyacridine lysine peptide (AcKPep) lacked the glycan which the bioconjugate (Biocon) contained. Protein levels post-transfection were normalized and quantified with the BCA assay using bovine serum albumin as a standard (Figure 5-5). This assay provided a relative measure of toxicity of the compound in the two cell types.

In Vitro Inhibition of Gene Transfer

DC-SIGN (+) CHO cells (1×10^4) were plated in triplicate for four treatment groups. After incubation for 24 hrs, the media was removed, the cells were washed with PBS and fresh transfection media was added to the cells. PEI and Man_9-AcrLys Glycopeptide control transfections were conducted as in the gene transfer experiment. In order to establish receptor-mediated endocytosis as the mechanism for gene transfer, we tried to reduce endocytosis by including Man_9 and antibody to DC-SIGN into the formulations for transfection. For the Man_9 treatment, 175 nmoL of $Man_9GlcNAc_2Asn$

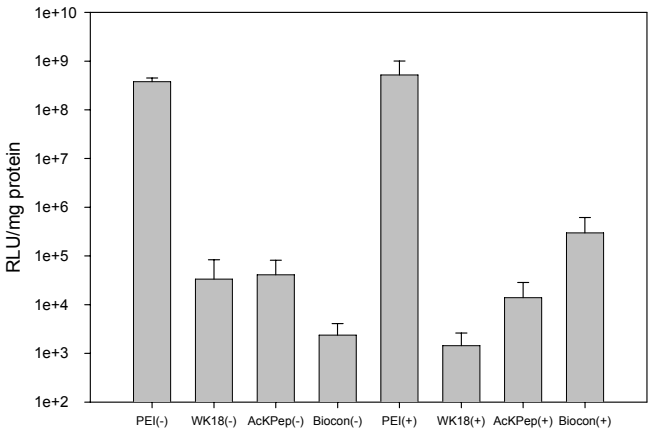

Figure 5-4. *Luciferase Assay of CHO cell transfection.* pGL3 condensates were made with 1 μg plasmid DNA and the follwing transfection reagents: PEI (poly(ethylenimine)), WK_{18} (tryptophan-$lysine_{18}$), AcKPep (C-K_{Ac}-K-K_{Ac}-K-K_{Ac}-K- K_{Ac}-K), Biocon (Man_9-AcrLys Glycopeptide). After transfection and incubation for 24 hr, the cells were lysed and RLU levels were recorded. Luciferase expression from the bioconjugate condensate was 100 fold greater in the DC-SIGN (+) CHO cells than the DC-SIGN (-) CHO cells, indicating receptor mediated uptake.

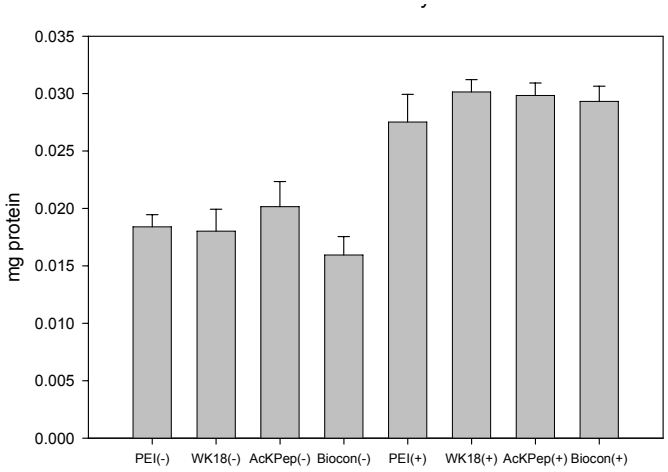

Figure 5-5. *BCA Assay of Protein Levels of PEI, WK_{18}, AcKPep and Bioconjugate.* Protein levels were normalized with the BCA assay using bovine serum albumin as a standard. Total protein levels in the DC-SIGN (-) CHO cells varied between 16 and 20 μg, while levels in the (+) cells were between 28 and 32 μg, reflecting a slight difference. Reagents: PEI (poly(ethylenimine)), WK_{18} (tryptophan-$lysine_{18}$), AcKPep (C-K_{Ac}-K-K_{Ac}-K- K_{Ac}-K- K_{Ac}-K), Biocon (Man_9-AcrLys Glycopeptide).

was mixed with 1.75 nmoL Man_9-AcrLys Glycopeptide. Then 3.5 μg of DNA and HBM were added to bring the solution to volume. The CHO cells were dosed with 0.5 nmoL glycopeptide, 50 nmoL glycan, and 1 μg DNA. For the antibody knockdown dose, 17.5 μg antibody, 1.75 nmoL Man_9-AcrLys Glycopeptide, 3.5 μg DNA and HBM were brought into solution. In this case the CHO cells were dosed with 0.5 nmoL glycopeptide, 5 μg antibody, and 1 μg DNA. We did not observe any reduction in gene transfer with a 10 fold excess of Man_9, and treatment with excess antibody resulted in a two fold reduction in gene transfer (Figure 5-6). These results indicate a strong multivalent enhancement of avidity of the glycopeptide-pGL3 polyplex for the DC-SIGN receptor. Total protein levels were determined by BCA assay and are indicated in Figure 5-7. It may be possible to significantly reduce gene transfer by incubating the CHO cell population with the blocking agent prior to the addition of the pGL3 polyplex, but we felt that simultaneous addition would be more representative of the comparative affinity of the reagents.

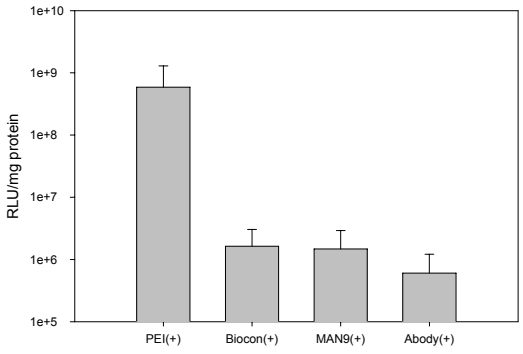

Figure 5-6. *In Vitro Inhibition of Gene Transfer*. An excess of $Man_9GlcNAc_2Asn$ and an excess of antibody to DC-SIGN were included with Man_9-AcrLys Glycopeptide in formulation in order to reduce gene transfer. No knockdown was observed with the glycan and treatment with antibody only resulted in a slight decrease. Reagents: PEI (poly(ethylenimine)), Biocon (Man_9-AcrLys Glycopeptide), Man_9 ($Mannose_9$ $GlcNAc_2$ Asparagine), Abody (antibody to DC-SIGN – phycoerythrin conjugate).

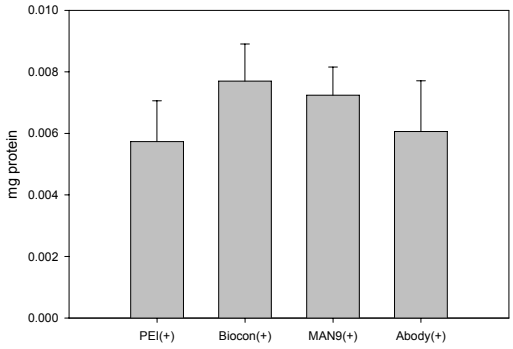

Figure 5-7. *BCA Assay of Protein Levels of PEI, Bioconjugate, Man_9 and Antibody.* Protein levels were normalized with the BCA assay using bovine serum albumin as a standard. Reagents: PEI (poly(ethylenimine)), Biocon (Man_9-AcrLys Glycopeptide), Man_9 ($Mannose_9$ $GlcNAc_2$ Asparagine), Abody (antibody to DC-SIGN – phycoerythrin conjugate).

Discussion

The CHO cell transfection experiments described in this chapter demonstrated that targeted *in-vitro* gene delivery to the DC-SIGN receptor with a novel bioconjugate vector is feasible. Stable polyplex can be formed at a low ligand : plasmid stoichiometry, and avidity for the DC-SIGN receptor is quite high due to the multivalent effect created by glycan clustering. The CHO cell system employed was ideal; the experimental cells stably expressed the DC-SIGN receptor. This was preferable to using commercially available primary human dendritic cells, as DC-SIGN expression was not guaranteed.

Providing evidence of targeted gene delivery can be very challenging. Haensler and Szoka[103] synthesized a vector targeted to the asialoglycoprotein receptor but did not observe gene expression from the pCLUC4 plasmid. Their compound contained two acridines for intercalation into DNA, which it bound with micromolar affinity. It also contained three galactose residues for receptor binding. The authors felt that the bioconjugate did not induce gene expression because it lacked a membrane destabilizing moiety. Our results suggest that this feature may not be necessary for *in vitro* gene expression. Targeting primary hepatocytes in culture is complicated by the down

regulation of the receptor, [103] although Chiu *et al*.[120] targeted ^{125}I labeled biantennary oligosaccharide to hepatocytes *in vivo*, where it must compete with endogenous ligand. This suggests that natural, complex carbohydrates may be the best ligands for ASGP-R binding.

The antibody : phycoerythrin conjugate we employed to establish expression of the DC-SIGN receptor was useful and effective for FACS imaging, however we could not knockdown bioconjugate binding and luciferase expression. This was most likely due to our method of co-administration with Man_9-AcrLys Glycopeptide. If we had pre-treated the DC-SIGN (+) CHO cells with the antibody, it might have been easier to bind and block the receptor.

We transfected CHO cells with Man_9-AcrLys Glycopeptide in triplicate in three separate experiments and consistently saw a two log difference in gene expression which favored the DC-SIGN (+) cells. This is very strong evidence indicating selective receptor mediated of the gene delivery vector. We also know that the glycan, not the polyacridine peptide is essential for binding and transfection because luciferase expression levels for the bioconjugate are ten times higher than with peptide alone.

The Man_9-AcrLys Glycopeptide will be evaluated *in vivo* in a murine system. The experiments would be complicated by the multiplicity of mouse DC-SIGN homologues, and due to the fact the SIGN homologue present on mouse plasmacytoid-pre dendritic cells (CIRE/mDC-SIGN) does not bind pathogens known to interact with human DC-SIGN.[124] Rather, it is mSIGNR1, expressed on macrophage subgroups in the lymph node and in liver sinusoid endothelial cells (LSECs),[125] which shares antigen specificity with hDC-SIGN.[126] However, in 2007, Kretz-Rommel et. al. demonstrated effective targeting to DC-SIGN *in vivo*. [127] The researchers raised Rag2 $^{-/-}\gamma^{-/-}$ mice with human immune cells, and induced a T-cell response by administering anti-DC-SIGN antibody bound to tetanus toxoid peptide or keyhole limpet hemocyanin (KLH). They

were also able to inhibit tumor growth in the same system. This is an indication that targeted gene delivery could be evaluated in a similar type of system.

CHAPTER 6

RESEARCH SUMMARY

The preceding pages have described the development and testing of a novel glycan-targeted gene delivery vector to the dendritic-cell SIGN receptor. These experiments provide evidence that it is possible, in principle, to express foreign protein in cells presenting DC-SIGN receptor. This could be utilized in vaccine development, to prime the immune system against pathogenic protein, which would be transcribed and translated from plasmids delivered to dendritic cells.

The primary focus of my research is to design and synthesize efficient non-viral gene delivery vehicles. Effective gene delivery vectors, whether viral or non-viral, usually contain some type of targeting ligand. As such, my initial research project was to devise a method for the isolation of $Man_9GlcNAc_2$, a high mannose N-glycan we used to target our vectors to the mannose receptor on kupffer cells in mice. A thorough search of the literature revealed two related methods for affinity purification of soybean agglutinin, a natural source of the glycan.[106,111] Allen and Neuberger's method [111] was combined with Bethel and Ayer's, [112] and affinity resin for the purification of soybean agglutinin was made on a large scale.

With multi-gram quantities of pure soybean agglutinin on hand, it was necessary to devise a means of isolating the glycan from the unwanted protein. A mild, enzymatic method was preferable to chemical hydrazinolysis, which would require special safety measures. The glycoprotein proved resistant to digestion with trypsin, and our efforts with PNGase F and pepsin were also met with failure. We soon turned to Lis and Sharon's procedure for pronase digestion, which worked well.[118]

At this point we began to conceptualize a DNA vector which would function as a vaccine. Our target would be the dendritic cell SIGN receptor, found on immature dendritic cells, the primary antigen presenting cell of the immune system. This strategy mirrors that utilized by a variety of pathogens including HIV, which is one of the most

efficient viral vectors in nature.[64] We derivatized $Man_9GlcNAc_2Asn$ on the N-terminus of asparagine with acridine, a polycyclic aromatic hydrocarbon containing three fused benzene rings. The $Man_9GlcNAc_2Asn$-Acr compound (Figure 3-13) could be used to non-covalently glycosylate DNA, a novel approach to gene delivery which we termed Glyco-DNA.

$Man_9GlcNAc_2Asn$-Acr could be made readily in sufficient quantity, but testing revealed that it bound DNA with low affinity (Figure 3-15). The solution to this problem lay in synthesizing a bioconjugate containing one $Man_9GlcNAc_2Asn$ and four acridines. The acridine portion of the compound was made on an automated peptide synthesizer. An fmoc protected lysine with an acridine on the epsilon amine was made and used in the synthesis of peptide C-K_{Ac}-K-K_{Ac}-K-K_{Ac}-K-K_{Ac}-K (Figure 4-17). $Man_9GlcNAc_2Asn$ was derivatized with a maleimido derivative of proprionic acid, and a thioether linkage was formed between the glycan and the peptide. The Man_9-AcrLys Glycopeptide had much higher affinity for plasmid DNA than $Man_9GlcNAc_2Asn$-Acr (Figure 4-5).

I obtained CHO cells stably expressing human DC-SIGN from a collaborator. CHO cells are more robust and easier to work with than primary cells, and they proved to be a valuable resource. An antibody-phycoerythrin conjugate was used in FACS analysis to verify the presence of the receptor (Figure 5-1). The Man_9-AcrLys Glycopeptide was condensed with pGL3 plasmid at a stoichiometry of 0.5 nmol : 1 μg and tested with the CHO cells in a standard 24 hr transfection assay with the appropriate controls (Figure 5-4). Luciferase expression was 100 fold higher in the cells expressing receptor than in control DC-SIGN (-) CHO cells. As an additional experiment to demonstrate receptor mediated uptake, pGL3 was covalently labeled with Cy5 fluorophore. The CHO cells were transfected and analyzed by FACS, and higher levels of fluorescence were clearly seen in the DC-SIGN (+) cell population (Figure 5-3).

As stated earlier, this gene delivery system will be evaluated *in vivo*. Common laboratory mice cannot be used for this type of experiment, because the SIGN homologue

present on mouse plasmacytoid-pre dendritic cells (CIRE/mDC-SIGN) does not bind pathogens known to interact with human DC-SIGN.[124] This includes HIV, and likely precludes Man_9 as a high affinity ligand. Recently, Kretz-Rommel et. al. demonstrated effective targeting to DC-SIGN *in vivo* [127] by raising Rag2 $^{-/-}\gamma^{-/-}$ mice with human immune cells, and inducing a T-cell response by administering anti-DC-SIGN antibody bound to tetanus toxoid peptide or keyhole limpet hemocyanin (KLH). They were also able to inhibit tumor growth in the same system. It is possible that this type of system could be used to measure gene delivery and antibody and T-cell response to foreign protein expression.

REFERENCES

1. Robinson HL, Pertmer TM 2000. DNA vaccines for viral infections: basic studies and applications. Advances in virus research 55:1-74.

2. Banchereau J, Steinman RM 1998. Dendritic cells and the control of immunity. Nature 392(6673):245-252.

3. Kukowska-Kaszuba M, Dzierzbicka K 2007. Synthesis and Structure-Activity Studies of Peptide-Acridine/Acridone Conjugates. Current Medicinal Chemistry 14:3079-3104.

4. Sebestik J, Hlavacek J, Stibor I 2007. A role of the 9-aminoacridines and their conjugates in a life science. Current protein & peptide science 8(5):471-483.

5. Demeunynck M, Charmantray F, Martelli A 2001. Interest of acridine derivatives in the anticancer chemotherapy. Current pharmaceutical design 7(17):1703-1724.

6. Wakelin LP, Bu X, Eleftheriou A, Parmar A, Hayek C, Stewart BW 2003. Bisintercalating threading diacridines: relationships between DNA binding, cytotoxicity, and cell cycle arrest. Journal of medicinal chemistry 46(26):5790-5802.

7. Graebe C, Caro H 1870. Ueber Acridin. Chemische Berichte 3:746.

8. Acheson RM. 1973. Acridines. 2 ed.: John Wiley & Sons.

9. Graebe C, Lagodzinski K 1893. Ueber Oxyderivate des Anthracholinchinons Justus Liebigs Annalen der Chemie 276(35).

10. Albert A, Goldacre R 1946. The Ionisation of Acridine Bases. J Chem Soc:706.

11. Albert A, Rubbo SD, Goldacre R 1941. Correlation of Basicity and Antiseptic Action in an Acridine Series. Nature 147:332-333.

12. Merck. 2001. The Merck Index. 13 ed.: John Wiley & Sons.

13. Bernthsen A 1884. Die Acridine. Justus Liebigs Annalen der Chemie 224:1.

14. Popp FD 1962. Polyphosphoric Acid in the Bernthsen Reaction. The Journal of Organic Chemistry 27(9):2658 - 2659.

15. Huntress EH, Shaw EN 1948. 4-Benzyl-2,6-dimethylpyridine, 1-benzylisoquinoline, 9-benzylacridine, and certain relatives. J Org Chem 13(5):674-681.

16. Dunstan AE, Stubbs JA 1906. Derivate des 9- Phenyl-acridins. III. Mittheilung: Ueber 9- p-Bromphenylacridine. Chemische Berichte 39:2402.

17. Bernthsen A, Traube J 1884. Butylacridin und Acridylbenzoësäure Chemische Berichte 17:1510.

18. Buu-Hoi NP, Lecocq J 1945. Des acridines substituees I. sur quelques 9-alcoyl et 9-aryl-alcoyl-acridines. Recueil des travaux chimiques des Pays-Bas 64:250.

19. Decker H, Hock T 1904. Ueber einige Ammoniumverbindungen: Methylirung der ms-Phenyl-acridin-o-carbonsäure Chemische Berichte 37:1002.

20. Dunstan AE, Hilditch TP 1907. The action of bromine on 5-phenylacridine and its halogen derivatives. J Chem Soc 91:1659.

21. Schmid A, Decker H 1906. Zur Kenntniss der Methylderivate des 9-Phenyl-acridins. Chemische Berichte 39:933.

22. Volpi A 1891. Organische Chemie. Chemische Berichte 24R:912.

23. Volpi A 1892. Organische Chemie. Chemische Berichte 25R:940.

24. Landauer E 1904. Recherches dans le groupe de la phenylacridine. Bulletin de la Société Chimique de France 31:1083.

25. Graef E, Fredericksen JM, Burger A 1946. Antitubercular Studies. Heterocyclic Fatty Acids. The Journal of Organic Chemistry 11(3):257-267.

26. Cook AH, Heilbron IM, Spinks A 1943. New therapeutic agents of the quinoline series. Part V. Pyridylacridines. J Chem Soc:417.

27. Bernthsen A, Hess W 1885. Ueber Amidound Oxyderivate des Phenylacridins. Chemische Berichte 18:689.

28. Kehrmann F, Stepanoff A 1908. Über einige Derivate des 9-Phenyl-acridins Chemische Berichte 41:4133.

29. Besthorn E, Curtman W 1891. Ueber Anilodo- und Oxyacridine. Chemische Berichte 24:2039.

30. Tsuge O, Nishinohara M, Tashiro M 1963. Compounds Related to Acridine. I. Condensation of Acridine Derivatives Having Active Methyl Group and Aromatic Nitroso Compounds. Bulletin of the Chemical Society of Japan 36:1477.

31. Bonna A 1887. V. Ueber Phenylparatoluidin. Justus Liebigs Annalen der Chemie 239(1):55-64.

32. Inagaki S 1938. A study on diphenylisatin and its derivative (the 4th report): regarding the monobromide compound of dianisolisation and its oxidation result. J Pharm Soc Jap 58:961.

33. Kehrmann F, Matusinsky Z 1912. Über ein Analogon des Aposafranons in der Acridin-Reihe. Über Acridin-Derivate. II. Chemische Berichte 45:3498.

34. Horaguchi T, Oyanagi T, Creencia EC, Tanemra K, Suzuki T 2004. Synthesis of Carbazole, Acridine, Phenazine, 4H-Benzo[def]carbazole and Their Derivatives by Thermal Cyclization Reaction of Aromatic Amines. J Heterocyclic Chem 41:1-6.

35. Hodgetts I, Noyce SJ, Storr RC 1984. Catalysis in Flash Vacuum Pyrolysis. Tet Lett 25(47):5435-5438.

36. Baum JS, Condon ME, Shook DA 1987. Nickel-Catalyzed Transformations of 2,1-Benzisoxazoles with Organozinc Reagents. J Org Chem 52:2983-2988.

37. Albert A, Ritchie B 1955. 9-Aminoacridine. Organic Syntheses 3:53.

38. El-Sherief HAH, Abdel-Rahman AE, Mahmoud AM 1983. Synthesis of certain acridine derivatives structurally related to some chemotherapeutic agents. Journal of the Indian Chemical Society 60(1):55-57.

39. Allen CFH, McKee GHW 1943. Acridone. Organic Syntheses 2:15.

40. Peacocke AR, Skerrett JHN 1956. The Interaction of Aminoacridines with Nucleic Acids. Trans Faraday Soc 52:261-279.

41. Lerman LS 1961. Structural considerations in the interactions of deoxyribonucleic acid and acridines. J Mol Biol 3:18-30.

42. Pritchard NJ, Blake A, Peacocke AR 1966. Modified intercalation model for the interaction of amino acridines and DNA. Nature 212(5068):1360-1361.

43. Cohen G, Eisenberg HK 1969. Viscosity and sedimentation study of sonicated DNA-Proflavine complexes. Biopolymers 8:45-55.

44. Wilson WD, Jones RL 1981. Intercalating drugs: DNA binding and molecular pharmacology. Advances in pharmacology and chemotherapy 18:177-222.

45. Saucier JM, Festy B, Le Pecq JB 1971. The change of the torsion of the DNA helix caused by intercalation. II. Measurement of the relative change of torsion induced by various intercalating drugs. Biochimie 53(9):973-980.

46. Gabbay EJ, Scofield RE, Baxter CS 1973. Steric effects on the intercalation of aromatic cations to deoxyribonucleic acid. Journal of the American Chemical Society 95(23):7850-7857.

47. Sobell HM. 1973. The stereochemistry of Actinomycin binding to DNA and its implications in molecular biology. ed.

48. Bauer WR 1978. Structure and reactions of closed duplex DNA. Annual review of biophysics and bioengineering 7:287-313.

49. Waring MJ. 1972. The Molecular Basis of Antibiotic Action. ed.: John Wiley & Sons Ltd

50. Manning GS 1978. The molecular theory of polyelectrolyte solutions with applications to the electrostatic properties of polynucleotides. Quarterly reviews of biophysics 11(2):179-246.

51. Record MT, Jr., Anderson CF, Lohman TM 1978. Thermodynamic analysis of ion effects on the binding and conformational equilibria of proteins and nucleic acids: the roles of ion association or release, screening, and ion effects on water activity. Quarterly reviews of biophysics 11(2):103-178.

52. Lohman TM, Wensley CG, Cina J, Burgess RR, Record MT, Jr. 1980. Use of difference boundary sedimentation velocity to investigate nonspecific protein-nucleic acid interactions. Biochemistry 19(15):3516-3522.

53. Ueyama H, Waki M, Takagi M, Takenaka S 2000. Novel synthesis of a tetra-acridinyl peptide as a new DNA polyintercalator. Nucleic acids symposium series (44):133-134.

54. McGhee JD, von Hippel PH 1974. Theoretical aspects of DNA-protein interactions: co-operative and non-co-operative binding of large ligands to a one-dimensional homogenous lattice. J Mol Biol 86:469-489.

55. Ueyama H, Takagi M, Waki M, Takenaka S 2001. DNA binding behavior of peptides carrying acridinyl units: First example of effective poly-intercalation. NUCLEIC ACIDS SYMP SER (OXF) 1(1):163-164.

56. Curtis BM, Scharnowske S, Watson AJ 1992. Sequence and expression of a membrane-associated C-type lectin that exhibits CD4. ProclNatlAcadSci 89:8356-8360.

57. Curtis BM, Widmer MB, deRoos P, Qwarnstrom EE 1990. IL-1 and its receptor are translocated to the nucleus. J Immunol 144(4):1295-1303.

58. Feinberg H, Mitchell DA, Drickamer K, Weis WI 2001. Structural basis for selective recognition of oligosaccharides by DC-SIGN and DC-SIGNR. Science (New York, NY 294(5549):2163-2166.

59. Soilleux EJ, Barten R, Trowsdale J 2000. DC-SIGN; a related gene, DC-SIGNR; and CD23 form a cluster on 19p13. J Immunol 165(6):2937-2942.

60. Pohlmann S, Soilleux EJ, Baribaud F, Leslie GJ, Morris LS, Trowsdale J, Lee B, Coleman N, Doms RW 2001. DC-SIGNR, a DC-SIGN homologue expressed in endothelial cells, binds to human and simian immunodeficiency viruses and activates infection in trans. Proceedings of the National Academy of Sciences of the United States of America 98(5):2670-2675.

61. Bashirova AA, Geijtenbeek TB, van Duijnhoven GC, van Vliet SJ, Eilering JB, Martin MP, Wu L, Martin TD, Viebig N, Knolle PA, KewalRamani VN, van Kooyk Y, Carrington M 2001. A dendritic cell-specific intercellular adhesion molecule 3-grabbing nonintegrin (DC-SIGN)-related protein is highly expressed on human liver sinusoidal endothelial cells and promotes HIV-1 infection. The Journal of experimental medicine 193(6):671-678.

62. Appelmelk BJ, van Die I, van Vliet SJ, Vandenbroucke-Grauls CM, Geijtenbeek TB, van Kooyk Y 2003. Cutting edge: carbohydrate profiling identifies new pathogens that interact with dendritic cell-specific ICAM-3-grabbing nonintegrin on dendritic cells. J Immunol 170(4):1635-1639.

63. Feinberg H, Castelli R, Drickamer K, Seeberger PH, Weis WI 2007. Multiple modes of binding enhance the affinity of DC-SIGN for high mannose N-linked glycans found on viral glycoproteins. The Journal of biological chemistry 282(6):4202-4209.

64. van Kooyk Y, Geijtenbeek TB 2003. DC-SIGN: escape mechanism for pathogens. Nat Rev Immunol 3(9):697-709.

65. Ratner DM, Plante OJ, Seeberger PH 2002. A Linear Synthesis of Branched High-Mannose Oligosaccharides from the HIV-1 Viral Surface Envelope Glycoprotein gp120. Eur J Org Chem:826-833.

66. Ding X, Wang W, Kong F 1997. Detritylation of mono- and di-saccharide derivatives using ferric chloride hydrate. Carbohydrate Research 303:445-448.

67. Sondheimer SJ, Eby R, Schuerch C 1978. A synthesis of 1,6-anhydro-2,3,4-tri-O-benzyl-β-D-mannopyranose. Carbohydrate Research 60:187-192.

68. Geijtenbeek TB, Torensma R, van Vliet SJ, van Duijnhoven GC, Adema GJ, van Kooyk Y, Figdor CG 2000. Identification of DC-SIGN, a novel dendritic cell-specific ICAM-3 receptor that supports primary immune responses. Cell 100(5):575-585.

69. Steinman RM, Cohn ZA 1973. Identification of a novel cell type in peripheral lymphoid organs of mice. I. Morphology, quantitation, tissue distribution. The Journal of experimental medicine 137(5):1142-1162.

70. Shaw S, Luce GE, Quinones R, Gress RE, Springer TA, Sanders ME 1986. Two antigen-independent adhesion pathways used by human cytotoxic T-cell clones. Nature 323(6085):262-264.

71. Adema GJ, Hartgers F, Verstraten R, de Vries E, Marland G, Menon S, Foster J, Xu Y, Nooyen P, McClanahan T, Bacon KB, Figdor CG 1997. A dendritic-cell-derived C-C chemokine that preferentially attracts naive T cells. Nature 387(6634):713-717.

72. Dustin ML, Springer TA 1989. T-cell receptor cross-linking transiently stimulates adhesiveness through LFA-1. Nature 341(6243):619-624.

73. van Kooyk Y, van de Wiel-van Kemenade P, Weder P, Kuijpers TW, Figdor CG 1989. Enhancement of LFA-1-mediated cell adhesion by triggering through CD2 or CD3 on T lymphocytes. Nature 342(6251):811-813.

74. Binnerts ME, van Kooyk Y, Simmons DL, Figdor CG 1994. Distinct binding of T lymphocytes to ICAM-1, -2 or -3 upon activation of LFA-1. European journal of immunology 24(9):2155-2160.

75. Van der Vieren M, Le Trong H, Wood CL, Moore PF, St John T, Staunton DE, Gallatin WM 1995. A novel leukointegrin, alpha d beta 2, binds preferentially to ICAM-3. Immunity 3(6):683-690.

76. Hernandez-Caselles T, Rubio G, Campanero MR, del Pozo MA, Muro M, Sanchez-Madrid F, Aparicio P 1993. ICAM-3, the third LFA-1 counterreceptor, is a co-stimulatory molecule for both resting and activated T lymphocytes. European journal of immunology 23(11):2799-2806.

77. Juan M, Vinas O, Pino-Otin MR, Places L, Martinez-Caceres E, Barcelo JJ, Miralles A, Vilella R, de la Fuente MA, Vives J, et al. 1994. CD50 (intercellular adhesion molecule 3) stimulation induces calcium mobilization and tyrosine phosphorylation through p59fyn and p56lck in Jurkat T cell line. The Journal of experimental medicine 179(6):1747-1756.

78. Geijtenbeek TB, Krooshoop DJ, Bleijs DA, van Vliet SJ, van Duijnhoven GC, Grabovsky V, Alon R, Figdor CG, van Kooyk Y 2000. DC-SIGN-ICAM-2 interaction mediates dendritic cell trafficking. Nature immunology 1(4):353-357.

79. Vestweber D, Blanks JE 1999. Mechanisms that regulate the function of the selectins and their ligands. Physiological reviews 79(1):181-213.

80. Nortamo P, Li R, Renkonen R, Timonen T, Prieto J, Patarroyo M, Gahmberg CG 1991. The expression of human intercellular adhesion molecule-2 is refractory to inflammatory cytokines. European journal of immunology 21(10):2629-2632.

81. Heisig N 1968. Functional analysis of the microcirculation in the exocrine pancreas. Adv Microcirc 1:89-94.

82. Garcia-Vallejo JJ, van Liempt E, da Costa Martins P, Beckers C, van het Hof B, Gringhuis SI, Zwaginga JJ, van Dijk W, Geijtenbeek TB, van Kooyk Y, van Die I 2008. DC-SIGN mediates adhesion and rolling of dendritic cells on primary human umbilical vein endothelial cells through LewisY antigen expressed on ICAM-2. Molecular immunology 45(8):2359-2369.

83. Geijtenbeek TB, van Duijnhoven GC, van Vliet SJ, Krieger E, Vriend G, Figdor CG, van Kooyk Y 2002. Identification of different binding sites in the dendritic cell-specific receptor DC-SIGN for intercellular adhesion molecule 3 and HIV-1. The Journal of biological chemistry 277(13):11314-11320.

84. Steinman RM 2000. DC-SIGN: a guide to some mysteries of dendritic cells. Cell 100(5):491-494.

85. Geijtenbeek TB, Kwon DS, Torensma R, van Vliet SJ, van Duijnhoven GC, Middel J, Cornelissen IL, Nottet HS, KewalRamani VN, Littman DR, Figdor CG, van Kooyk Y 2000. DC-SIGN, a dendritic cell-specific HIV-1-binding protein that enhances trans-infection of T cells. Cell 100(5):587-597.

86. Engering A, Geijtenbeek TB, van Vliet SJ, Wijers M, van Liempt E, Demaurex N, Lanzavecchia A, Fransen J, Figdor CG, Piguet V, van Kooyk Y 2002. The dendritic cell-specific adhesion receptor DC-SIGN internalizes antigen for presentation to T cells. J Immunol 168(5):2118-2126.

87. Lue J, Hsu M, Yang D, Marx P, Chen Z, Cheng-Mayer C 2002. Addition of a single gp120 glycan confers increased binding to dendritic cell-specific ICAM-3-grabbing nonintegrin and neutralization escape to human immunodeficiency virus type 1. Journal of virology 76(20):10299-10306.

88. Geijtenbeek TBH, van Vliet SJ, Koppel EA, Sanchez-Hernandez M, Vandenbroucke-Grauls CMJE, Appelmelk B, van Kooyk Y 2003. Mycobacteria Target DC-SIGN to Suppress Dendritic Cell Function. The Journal of experimental medicine 197(1):7-17.

89. Maeda N, Nigou J, Herrmann JL, Jackson M, Amara A, Lagrange PH, Puzo G, Gicquel B, Neyrolles O 2003. The cell surface receptor DC-SIGN discriminates between Mycobacterium species through selective recognition of the mannose caps on lipoarabinomannan. The Journal of biological chemistry 278(8):5513-5516.

90. Kaufmann SH, Schaible UE 2003. A dangerous liaison between two major killers: Mycobacterium tuberculosis and HIV target dendritic cells through DC-SIGN. The Journal of experimental medicine 197(1):1-5.

91. Tailleux L, Schwartz O, Herrmann JL, Pivert E, Jackson M, Amara A, Legres L, Dreher D, Nicod LP, Gluckman JC, Lagrange PH, Gicquel B, Neyrolles O 2003. DC-SIGN is the major Mycobacterium tuberculosis receptor on human dendritic cells. The Journal of experimental medicine 197(1):121-127.

92. Chatterjee D, Khoo KH 1998. Mycobacterial lipoarabinomannan: an extraordinary lipoheteroglycan with profound physiological effects. Glycobiology 8(2):113-120.

93. Sada E, Brennan PJ, Herrera T, Torres M 1990. Evaluation of lipoarabinomannan for the serological diagnosis of tuberculosis. Journal of clinical microbiology 28(12):2587-2590.

94. Jonuleit H, Schmitt E, Schuler G, Knop J, Enk AH 2000. Induction of interleukin 10-producing, nonproliferating CD4(+) T cells with regulatory properties by repetitive stimulation with allogeneic immature human dendritic cells. The Journal of experimental medicine 192(9):1213-1222.

95. Okano M, Satoskar AR, Nishizaki K, Abe M, Harn DA, Jr. 1999. Induction of Th2 responses and IgE is largely due to carbohydrates functioning as adjuvants on Schistosoma mansoni egg antigens. J Immunol 163(12):6712-6717.

96. Glover DJ, Lipps HJ, Jans DA 2005. Towards safe, non-viral therapeutic gene expression in humans. Nat Rev Genet 6(4):299-310.

97. Kircheis R, Wightman L, Schreiber A, Robitza B, Rossler V, Kursa M, Wagner E 2001. Polyethylenimine/DNA complexes shielded by transferrin target gene expression to tumors after systemic application. Gene therapy 8(1):28-40.

98. Jans DA, Xiao CY, Lam MH 2000. Nuclear targeting signal recognition: a key control point in nuclear transport? Bioessays 22(6):532-544.

99. Lyman SK, Guan T, Bednenko J, Wodrich H, Gerace L 2002. Influence of cargo size on Ran and energy requirements for nuclear protein import. The Journal of cell biology 159(1):55-67.

100. Paleos CM, Tziveleka LA, Sideratou Z, Tsiourvas D 2009. Gene delivery using functional dendritic polymers. Expert opinion on drug delivery 6(1):27-38.

101. Uherek C, Fominaya J, Wels W 1998. A modular DNA carrier protein based on the structure of diphtheria toxin mediates target cell-specific gene delivery. The Journal of biological chemistry 273(15):8835-8841.

102. Horie K, Masahiro S, Kuramochi K, Hanasaki K, Hamana H, Ito T 1999. Enhanced Accumulation of Sialyl Lewis X-Carboxymethylpullulan Conjugate in Acute Inflammatory Lesion. Pharm Res 16(2):314-320.

103. Haensler J, Szoka JFC 1993. Synthesis and characterization of a trigalactosylated bisacridine compound to target DNA to hepatocytes. Bioconjug Chem 4(1):85-93.

104. Liener IE, Pallansch MJ 1952. Purification of a toxic substance from defatted soy bean flour. The Journal of biological chemistry 197(1):29-36.

105. Dorland L, van Halbeek H, Vleigenthart JF, Lis H, Sharon N 1981. Primary structure of the carbohydrate chain of soybean agglutinin. A reinvestigation by high resolution 1H NMR spectroscopy. The Journal of biological chemistry 256(15):7708-7711.

106. Gordon JA, Blumberg S, Lis H, Sharon N 1972. Purification of Soybean Agglutinin by Affinity Chromatography of Sepharose-N-e-Aminocaproyl-B-D-Galactopyranosylamine. FEBS letters 24(2):193-196.

107. Reisner Y, Itzicovitch L, Meshorer A, Sharon N 1978. Hemopoietic stem cell transplantation using mouse bone marrow and spleen cells fractionated by lectins. Proceedings of the National Academy of Sciences of the United States of America 75(6):2933-2936.

108. Nagler A, Morecki S, Slavin S 1999. The use of soybean agglutinin (SBA) for bone marrow (BM) purging and hematopoietic progenitor cell enrichment in clinical bone-marrow transplantation. Molecular biotechnology 11(2):181-194.

109. Ji X, Chen Y, Faro J, Gewurz H, Bremer J, Spear GT 2006. Interaction of human immunodeficiency virus (HIV) glycans with lectins of the human immune system. Current protein & peptide science 7(4):317-324.

110. Yang Y, Park Y, Man S, Liu Y, Rice KG 2001. Cross-linked low molecular weight glycopeptide-mediated gene delivery: relationship between DNA metabolic stability and the level of transient gene expression in vivo. Journal of pharmaceutical sciences 90(12):2010-2022.

111. Allen AK, Neuberger A 1975. A simple method for the preparation of an affinity absorbent for soybean agglutinin using galactosamine and CH-Sepharose. FEBS letters 50(3):362-364.

112. Bethell GS, Ayers JS, Hancock WS, Hearn MT 1979. A novel method of activation of cross-linked agaroses with 1,1'-carbonyldiimidazole which gives a matrix for affinity chromatography devoid of additional charged groups. The Journal of biological chemistry 254(8):2572-2574.

113. Wilchek M, Miron T, Kohn J 1984. Affinity chromatography. Methods in enzymology 104:3-55.

114. Sihorkar V, Vyas SP 2001. Potential of polysaccharide anchored liposomes in drug delivery, targeting and immunization. J Pharm Pharm Sci 4(2):138-158.

115. Collard WT, Yang Y, Kwok KY, Park Y, Rice KG 2000. Biodistribution, metabolism, and *in vivo* gene expression of low molecular weight glycopeptide polyethylene glycol peptide DNA co-condensates. Journal of pharmaceutical sciences 89(4):499-512.

116. Karup G, Meldal M, Nielsen PE, Buchardt O 1988. 9-Acridinylpeptides and 9-acridinyl-4-nitrophenylsulfonylpeptides. Synthesis, binding to DNA, and photoinduced DNA cleavage. Int J Pept Protein Res 32(5):331-343.

117. Dubois M, Gilles K, Hamilton JK, Rebers PA, Smith F 1951. A Colorimetric Method for the Determination of Sugars. Nature 168(4265):167.

118. Lis H, Sharon N 1978. Soybean Agglutinin--A Plant Glycoprotein. Structure of the Carbohydrate Unit. J Biol Chem 253(10 (25 May)):3468-3476.

119. Evers DL, Hung RL, Thomas VH, Rice KG 1998. Preparative purification of a high-mannose type N-glycan from soy bean agglutinin by hydrazinolysis and tyrosinamide derivatization. Analytical biochemistry 265(2):313-316.

120. Chiu MH, Tamura T, Wadhwa MS, Rice KG 1994. In vivo targeting function of N-linked oligosaccharides with terminating galactose and N-acetylgalactosamine residues. J Biol Chem 269(23):16195-16202.

121. Dupre DJ, Robinson FA 1945. N-Substituted 5-Aminoacridines. Journal of the Chemical Society none:549-551.

122. Tung C, Zhu T, Lackland H, Stein S 1992. An acridine amino acid derivative for use in Fmoc peptide synthesis. Peptide Research 5(2):115-118.

123. Smith PK, Krohn RI, Hermanson GT, Mallia AK, Gartner FH, Provenzano MD, Fujimoto EK, Goeke NM, Olson BJ, Klenk DC 1985. Measurement of protein using bicinchoninic acid. Analytical biochemistry 150(1):76-85.

124. Caminschi I, Corbett AJ, Zahra C, Lahoud M, Lucas KM, Sofi M, Vremec D, Gramberg T, Pohlmann S, Curtis J, Handman E, van Dommelen SL, Fleming P, Degli-Esposti MA, Shortman K, Wright MD 2006. Functional comparison of mouse CIRE/mouse DC-SIGN and human DC-SIGN. International immunology 18(5):741-753.

125. Geijtenbeek TB, Groot PC, Nolte MA, van Vliet SJ, Gangaram-Panday ST, van Duijnhoven GC, Kraal G, van Oosterhout AJ, van Kooyk Y 2002. Marginal zone macrophages express a murine homologue of DC-SIGN that captures blood-borne antigens in vivo. Blood 100(8):2908-2916.

126. Galustian C, Park CG, Chai W, Kiso M, Bruening SA, Kang YS, Steinman RM, Feizi T 2004. High and low affinity carbohydrate ligands revealed for murine SIGN-R1 by carbohydrate array and cell binding approaches, and differing specificities for SIGN-R3 and langerin. International immunology 16(6):853-866.

127. Kretz-Rommel A, Qin F, Dakappagari N, Torensma R, Faas S, Wu D, Bowdish KS 2007. In vivo targeting of antigens to human dendritic cells through DC-SIGN elicits stimulatory immune responses and inhibits tumor growth in grafted mouse models. J Immunother 30(7):715-726.